SANDIA REPORT

SAND2017-12281
Unlimited Release
Printed September 19, 2017

SHDAS Production Seismometer Evaluation

George W. Slad
B. John Merchant

Prepared by
Sandia National Laboratories
Albuquerque, New Mexico 87185 and Livermore, California 94550

Sandia National Laboratories is a multimission laboratory managed and operated by National Technology and Engineering Solutions of Sandia, LLC, a wholly owned subsidiary of Honeywell International, Inc., for the U.S. Department of Energy's National Nuclear Security Administration under contract DE-NA0003525.

Issued by Sandia National Laboratories, operated for the United States Department of Energy by National Technology and Engineering Solutions of Sandia, LLC.

Available to DOE and DOE contractors from
U.S. Department of Energy
Office of Scientific and Technical Information
P.O. Box 62
Oak Ridge, TN 37831

Telephone: (865) 576-8401
Facsimile: (865) 576-5728
E-Mail: reports@osti.gov
Online ordering: http://www.osti.gov/scitech

Available to the public from
U.S. Department of Commerce
National Technical Information Service
5301 Shawnee Rd
Alexandria, VA 22312

Telephone: (800) 553-6847
Facsimile: (703) 605-6900
E-Mail: orders@ntis.gov
Online order: http://www.ntis.gov/search

SAND200X-XXXX
Unlimited Release
September 2017

SHDAS Production Seismometer Evaluation

George W. Slad
B. John Merchant
Ground-Based Monitoring R&E
Sandia National Laboratories
P.O. Box 5800
Albuquerque, New Mexico 87185-MS0404

Abstract

The Seismo-Hydroacoustic Data Acquisition System (SHDAS) is undergoing evaluation in preparation for its engineering, development, and deployment by the U.S Navy as an ocean bottom seismic monitoring system. At the current stage of development, the production seismometers are being evaluated to confirm their performance prior to packaging and assembly for deployment. The testing of the seismometers is being conducted at the Pinon Flats Observatory (PFO), supervised by Sandia National Laboratories, U.S Navy, and RP Kromer Consulting. SNL will conduct evaluation of the collected seismometer data and comment on the performance of the seismometers.

ACKNOWLEDGMENTS

This work was funded by the United States Air Force and was executed in cooperation with the US Air Force, US Navy, Leidos, and RPKromer Consulting.

We are thankful for the opportunity, provided by UC San Diego, to conduct our seismic sensor testing at the Ida and Cecil Green Pinon Flat Observatory.

CONTENTS

FIGURES

TABLES

NOMENCLATURE

dB	decibel
DOE	Department of Energy
NMX	Nanometrics
OBS	Ocean Bottom Seismometer
PFO	Pinon Flats Observatory
PSRF	Pinedale Seismic Research Facility
SHDAS	Seismo-Hydroacoustic Data Acquisition System
SNL	Sandia National Laboratories
UP	Underwater Platform

1 INTRODUCTION

Evaluation of the SHDAS seismometers at PFO was performed to determine the performance characteristics of the production seismometers that are to be used.

The SHDAS will include a total of 18 Underwater Platform packages. Each package will contain two 3-axis seismometers: A Nanometrics Trillium OBS and a custom assembly of GS11D geophones referred to as the Navy OBS. This yields a total of 36 3-axis seismometers to be evaluated.

Evaluation of the SHDAS seismometers will be focused on just production level testing, examining the following characteristics of each sensor:

- Self-Noise
- Dynamic Range
- Sensitivity
- Magnitude and Phase Response
- Passband
- Tilt
- Calibration

2 TEST PLAN

2.1 Objectives

The objectives of this work was to evaluate the overall technical performance and to provide amplitude and phase response curves and sensitivity values of the Leidos short period ocean bottom seismometer (OBS) and the Nanometrics Trillium OBS. Notable features of the Leidos sensor include the utilization of a passive auto-leveling design and passive sensor technology; those of Nanometrics OBS include an active feedback design and a command and control interface allowing one to configure auto-leveling parameters, initiate leveling commands and review sensor state-of-health (SOH) parameters. Seismometer characterization includes determining self-noise, dynamic range, sensitivity, magnitude and phase response, passband, and, in addition for the Nanometrics sensor, calibration and tilt. The results of this evaluation were compared to relevant application requirements or specifications of the seismometer provided by the manufacturer.

2.2 Test and Evaluation Background

Sandia National Laboratories (SNL), Ground-based Monitoring R&E and Geophysics Departments have the long-standing capability of evaluating the performance of seismometers for geophysical applications.

2.3 Standardization and Traceability

Most tests are based on the Institute of Electrical and Electronics Engineers (IEEE) Standard 1057 [Reference 1] for Digitizing Waveform Recorders and Standard 1241 for Analog to Digital Converters [Reference 2]. The analyses based on these standards were performed in the frequency domain or time domain as required. When appropriate, instrumentation calibration was traceable to the National Institute for Standards Technology (NIST).

Prior to testing, the bit weights of the digitizers used in the tests were established by RPKromer Consulting by recording a known reference signal on each of the digitizer channels. The reference signal was simultaneously recorded on an Agilent 3458A high precision meter with a current calibration from Sandia's Primary Standards Laboratory in order to verify the amplitude of the reference signal. Thus, the digitizer bit weights are traceable to NIST.

2.4 Test Bed Configuration and System Specifications

The test configuration was setup consistently with the diagram and descriptions below.

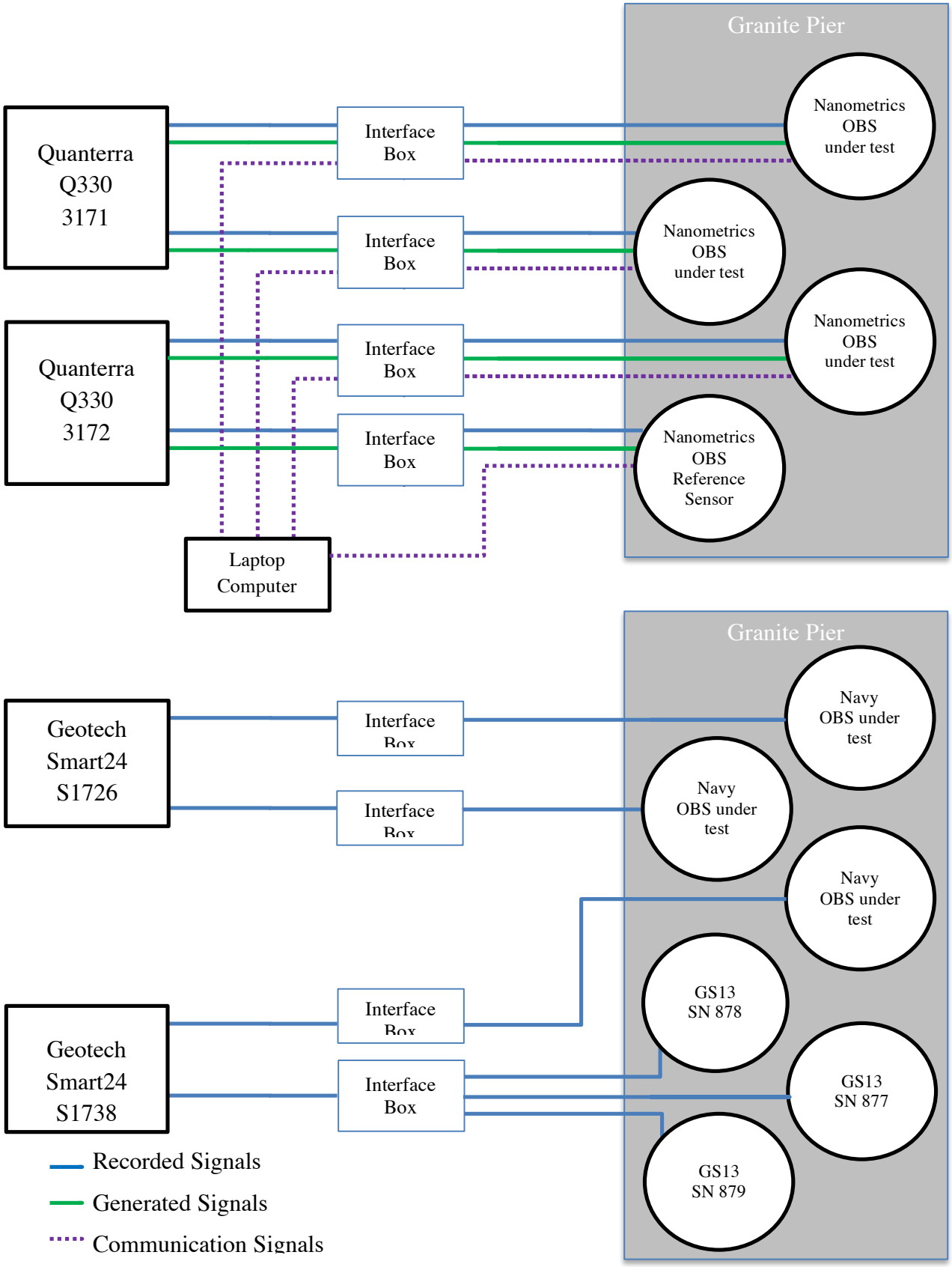

Figure 1 Test Configuration Diagram

2.4.1 Power

The test bed was powered by a Powertek DC Power Supply 3003B.

2.4.2 Data Recording

The data from the sensors used in these tests were recorded on four digitizers: two Geotech Smart24 digitizers, serial numbers S1726 and S1738, recorded the GS-13 and Leidos sensors and two Quanterra Q330 digitizers, serial numbers 3171 and 3172, recorded the Nanometrics sensors. Data were recorded at 100 Hz on both the Smart24 and Q330 digitizers.

2.4.3 Digitizers

The digitizer bit weights were verified by RPKromer Consulting prior to testing using a precision DC source that was verified against an Agilent 3458A that has been calibrated by the SNL Primary Standards Lab to provide traceability. The measured bit weights, shown in the digitizer configuration table below were used for all collected sensor data.

Manufacturer/Model	Serial Number	Application Bitweights	Channel Assignments
Geotech Smart24	S1726	c1p 0.10232 uV/count	Navy Test Sensor 1 (Z)
		c2p 0.10197 uV/count	Navy Test Sensor 1 (N/Y)
		c3p 0.10282 uV/count	Navy Test Sensor 1 (E/X)
		c4p 0.10141 nV/count	Navy Test Sensor 2 (Z)
		c5p 0.10129 nV/count	Navy Test Sensor 2 (N/Y)
		c6p 0.10144 nV/count	Navy Test Sensor 2 (E/X)
Geotech Smart24	S1738	c1p 0.10244 uV/count	Navy Test Sensor 3 (Z)
		c2p 0.10241 uV/count	Navy Test Sensor 3 (N/Y)
		c3p 0.10239 uV/count	Navy Test Sensor 3 (E/X)
		c4p 97.99364 nV/count	SP Reference Sensor (Z)
		c5p 95.22947 nV/count	SP Reference Sensor (N/Y)
		c6p 95.06123 nV/count	SP Reference Sensor (E/X)
Quanterra Q330HR	3171	HHZ00TB 29.75498 nV/count	Nanometrics Test Sensor 1 (Z)
		HHN00TB 29.70997 nV/count	Nanometrics Test Sensor 1 (N/Y)
		HHE00TB 29.75436 nV/count	Nanometrics Test Sensor 1 (E/X)
		HHZ10TB 29.71355 nV/count	Nanometrics Test Sensor 2 (Z)
		HHN10TB 29.7672 nV/count	Nanometrics Test Sensor 2 (N/Y)
		HHE10TB 29.72043 nV/count	Nanometrics Test Sensor 2 (E/X)
Quanterra Q330HR	3172	HHZ00TB 29.76849 nV/count	Nanometrics Test Sensor 3 (Z)
		HHN00TB 29.70822 nV/count	Nanometrics Test Sensor 3 (N/Y)
		HHE00TB 29.75217 nV/count	Nanometrics Test Sensor 3 (E/X)
		HHZ10TB 29.71127 nV/count	BB Reference Sensor 3 (Z)
		HHN10TB 29.76125 nV/count	BB Reference Sensor 3 (N/Y)
		HHE10TB 29.72231 nV/count	BB Reference Sensor 3 (E/X)

2.4.4 Signal Generation

The calibration test signals utilized in Nanometrics OBS testing were generated by the Quanterra Q330 digitizers and were then fed into the seismometer. The generated signals were synchronously recorded on channel 1 or 4 (HHZ00TB or HHZ10TB) of the respective Q330 digitizer, depending upon which Nanometrics sensor was under test.

2.4.5 Reference Sensors

Four reference sensors were utilized for these evaluations: a set of three GS-13 short-period seismometers and a Nanometrics Trillium OBS. GS-13 serial numbers 878, 877 and 879 served as Vertical, North and East, respectively for the Navy OBS sensors. Nanometrics Trillium OBS serial number 2100 served as the reference for the Nanometrics sensors. The sensitivity, amplitude and phase response of the reference sensors utilized are those supplied by the manufacturer, though in the case of the Nanometrics reference, the GS-13 sensors were utilized to compute a refined sensitivity at 10 Hz.

2.4.6 Sensor Configuration

Three sensors of each type were emplaced on a granite pier along with their respective reference sensor; Navy OBS units with the GS-13 references and the Nanometrics sensors under test with the Nanometrics reference, see Figure 1. The Navy OBS units, manufactured by Leidos, were stated to have a nominal output sensitivity of 1050 V/m/s; the Nanometrics OBS units a sensitivity of 750 V/m/s with a maximum output of 20 Volts, zero to peak. The Nanometrics OBS nominal frequency pass band is specified to be 120 s to 100 Hz; the nominal pass band of the Navy OBS is 4.5 Hz to over 100 Hz. The power input voltage range of the Nanometrics sensors is 9 to 29 Volts DC; power consumption varies from as little as 180 mW during normal operations, to as high as 2.4 W at 24 Volts DC during leveling operations. The passive Navy OBS does not require power for operation.

The Nanometrics sensors employ an internal webserver to provide a means for the user to configure the sensor (e.g. XYZ versus UVW mode, 120 second operation, enable calibrations), manually level the sensor, program a leveling schedule, to review and download sensor state-of-health (SOH) and update firmware. The user connects to the sensor with a laptop computer via a SLIP connection to access the webserver.

The Nanometrics sensors were operated in 120 second mode, with XYZ output (except during select calibration operations) and had the auto-leveling schedule disabled at the request of the customer.

2.5 Application Requirements

The SHDAS seismometer requirements drawn from the Systems Requirements Document are:

Table 1 SHDAS Seismometer Requirements

3.2.3.3 Seismic Sensing Capability
Seismic sensing capability shall include the sensing of seismic fluctuations and conversion to electrical signals. Requirements for this capability shall be as follows: • Operating Band: 0.02 – 40 Hz for the broadband, 1 – 40 Hz for the short period • Frequency Response of the Electronics: 3 dB down at 1 Hz and 40 Hz but otherwise flat in the velocity or acceleration passband; ±0.1 dB in amplitude and 5-degrees in phase from calibrated value. • Seismic Directionality: Two, three-single axis seismic sensors installed orthogonally to within ±0.5 degrees. Following installation, the three-axis sensor assembly shall self-adjust to the vertical plane within ±0.5 degrees. • Dynamic Range: 130 dB • Quantization: 24-bit analog-to-digital conversion • Sampling Rate: 100 samples per second All seismic sensors shall be characterized within the operational temperature across the frequency band of interest for the minimum, nominal, and maximum signal levels. The poles-zeros shall be determined through this verification process.

These requirements will be used to compare against the seismometer evaluations.

2.6 Test Facility

The University of California, San Diego (UCSD) maintains the Cecil and Ida Green Pinon Flat Observatory (PFO), which graciously hosted the sensor test bed through duration of testing.

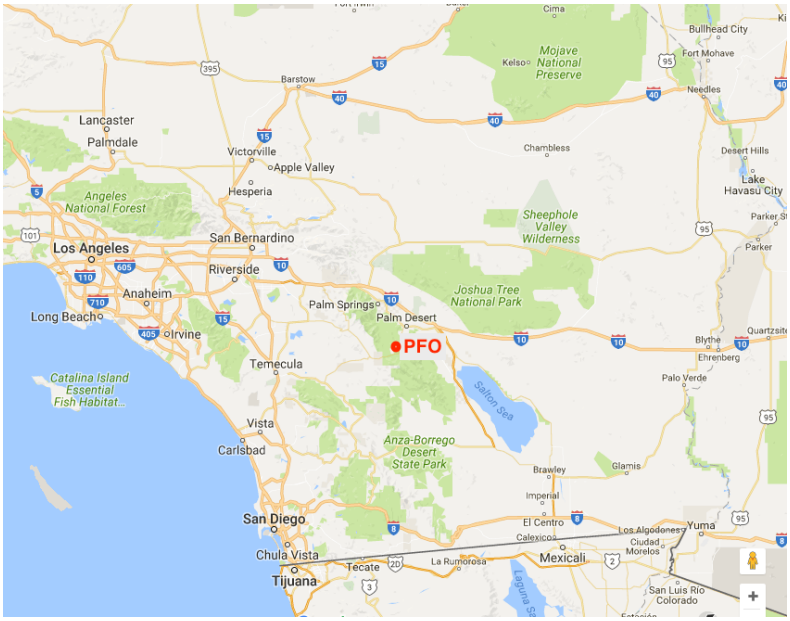

Figure 2 Pinon Flat Observatory (PFO) is approximately 170 km east-southeast of Los Angeles.

UCSD began development of PFO in 1970 on what was at the time USDA Forest Service land; in 1980 the university purchased the property from the Forest Service with a generous support from Cecil and Ida Green. It is composed of a quarter section of land, ½ mile by ½ mile (64.7 hectares) 26 km south-southeast of Palm Springs, California, nestled between the San Jacinto mountains to the north and the Santa Rosa mountains to the south. Tectonically it lies between the San Andreas and San Jacinto faults, one of the more seismically active areas of southern California.

PFO continually hosts various geophysical experiments by way of its 9 surface vaults, 22 boreholes and laser strain meters, including a Global Seismograph Network station.

Figure 3 View from PFO looking south towards the Santa Rosa Mountains. The vault hosting the SHDAS sensor testing lies just behind the dish antenna. The white pipe in the far right of the photo is part of the North-South oriented strain meter in place at PFO.

Figure 4 Nanometrics Trillium OBS broadband sensors on the pier.

Figure 5 Nanometrics sensor resting on the tilt jig

Figure 6 Navy short-period OBS sensors on pier.

In the upper left photo, Figure 4, the author confirms the interface box switch settings for use with the Nanometrics Trillium OBS sensors installed in the PFO vault. The blue plastic unit is the reference sensor, the remaining three are sensors under test. The interface box also provides a serial port for a SLIP connection to a laptop for configuring the Nanometrics sensors and reviewing their state of health. The tilt jig, Figure 5, allows for two rotation angles about the case North-South axis, dipping the case East-West axis, and a variable rotation about the case East-West axis, dipping the case North-South axis as desired. Figure 6 shows three of the Navy OBS manufactured by Leidos, left, and three Geotech GS-13 sensors serving as the references for the short-period sensors under test. All the sensors were installed such that the aluminum extrusion to which they are strapped is glued to the pier, or in the case of the GS-13 sensors, their feet were directly epoxied to the pier.

2.7 Tests

2.7.1 Self-Noise

Purpose: The purpose of the seismic sensor self-noise test is to determine the sensor self-noise in the presence of low seismic background signals.

Configuration: Sensors are installed side-by-side in a seismic vault or stacked vertically in a borehole. The sensor outputs are connected to a data acquisition system that samples the data synchronously. Data are acquired during low seismic backgrounds.

Evaluation: Coherence analysis noise-power computation provides the noise-floor of the sensor pair for low seismic background stimulus. If three or more sensors are available, the use of Three-Channel Coherence Analysis techniques can derive individual sensor self-noise.

2.7.2 Dynamic Range

Purpose: The purpose of the seismic sensor dynamic range test is to quantify the seismic sensor's ability to resolve seismic signals across a range of amplitudes.

Configuration: The seismic sensors test results for self-noise and clip-level are used to estimate dynamic range.

Evaluation: Convert the data from each seismic sensor to relevant ground-motion units using the sensor response mathematical model for each sensor. By using results for the sensor's noise test and the determined full-scale, the sensor's dynamic range is estimated.

2.7.3 Sensitivity

Purpose: The purpose of the seismic sensor sensitivity test is to verify the seismic sensor sensitivity using seismic background signals and a reference seismic sensor.

Configuration: A characterized reference sensor and one or more of the sensors under test, are installed side-by-side in a seismic vault or in an adjacent borehole. The seismic sensor outputs are connected to a data acquisition system that samples the data synchronously. Data are acquired during moderate to high seismic backgrounds and events.

Evaluation: Convert the data from each seismic sensor to ground motion using the sensor response mathematical model for each sensor. If the sensor sensitivity is correct, the amplitude response measurements in earth-motion units will be identical at the calibration frequency.

2.7.4 Response Verification

Purpose: The purpose of the seismic sensor response verification test is to verify the seismic response using seismic background signals and a reference seismic sensor.

Configuration: A characterized reference sensor and one or more of the sensors under test, are installed side-by-side in a seismic vault or in an adjacent borehole. The seismic sensor outputs are connected to a data acquisition system that samples the data synchronously. Data are acquired during moderate to high seismic backgrounds and events.

Evaluation: Convert the data from each seismic sensor to ground motion using the sensor response mathematical model for each sensor. If the sensor response models are correct, the amplitude response measurements in earth-motion units will be identical.

2.7.5 Passband

Purpose: The purpose of the passband test is to verify the seismic sensor passband using seismic background signals and a reference seismic sensor.

Configuration: A characterized reference sensor and one or more of the sensors under test, are installed side-by-side on a common granite pier in a seismic vault or in an adjacent borehole. The seismic sensor outputs are connected to a data acquisition system that samples the data synchronously. Data are acquired during moderate to high seismic backgrounds and events.

Evaluation: Convert the data from each seismic sensor to ground motion using the sensor response mathematical model for each sensor. If the sensor response models are correct, the amplitude response measurements in earth-motion units will be identical.

2.7.6 Tilt

Purpose: To confirm the sensor successfully detects tilt (tilt to be expected during deployment) and is able to perform the commanded leveling sequence, when tilt criteria are met, and brings the internal sensor platform to level.

Configuration: A sensor will be placed in a jig to standardize the physical orientation of the sensor case allowing a large scale tilt about two axes. RPKromer Consulting constructed the tilt jig during prototype testing. The jig provides means for a single sensor to be rotated a fixed amount about the North-South axis and a variable amount about the East-West axis of the case.

Evaluation: The sensor provides measurements of acceleration, in units of “g”, relative to the case, gimbal and internal sensor platform, via a serial-IP connection and internally hosted web page. The sensors are placed in two positions, ranging from approximately “Case East Down” to that which rotates the sensor case about two axes partially inverting it. A leveling command is initiated at these two extremes and a determination on the success of the leveling sequence is made based upon command feedback provided, sensor platform acceleration values, element mass positions and a visual inspection of data quality.

2.7.7 Calibration

Purpose: The purpose of this procedure is to estimate the calibrator constant, better than the +/- 7% value provided by the manufacturer, and to confirm the calibration circuitry continuity.

Configuration: Calibrator constant estimation will make use of the internal calibration signals available within the command structure of the Q330HR dataloggers. Calibrations will be recorded with the sensor in UVW mode and XYZ mode.

Readers are encouraged to refer to the Nanometrics Trillium Compact OBS Users Guide for details regarding the signal transformation from the UVW to the XYZ coordinate system.

Evaluation: Comparison of the calibration input signal with the sensor output of the calibration signal, along with previously determined sensitivity relative to the reference sensor, provides a means to refine the calibrator constants and confirms calibration circuitry continuity.

2.8 Procedures

The following procedures describe, in general terms, how the testing of the 36 3-axis SHDAS seismometers will be performed. The 36 sensors are comprised of 18 broad-band Nanometrics Trillium ocean bottom seismometers (OBS) and 18 Navy short-period OBSs.

For clarity, the tests have been organized into 3 distinct procedures:

A. tests focused on sensor leveling command and control,
B. tests utilized to refine calibrator constant values and confirm calibrator circuitry continuity,
C. tests covering general seismometer characteristics.

The two SHDAS test beds at PFO (Pinon Flat Observatory) provide SNL the capability to simultaneously collect three component data from 3 Nanometrics sensors under test and a broad-band reference and 3 Navy sensors under test and their short period reference. The broadband test bed also utilizes interface boxes allowing direct communication to the sensors for manual leveling command and control and XYZ/UVW mode control via a serial-IP connection and utilizes a jig to tilt a sensor allowing for tests of leveling command and control.

For any given iteration of testing it is critical that there are 3 sensors under test and that these sensors are of the same type. (e.g. all three are either Nanometrics Trillium OBS or Navy OBS). The Three-Channel Coherence method used for evaluating the sensor data requires at least this number of sensors. The more closely matched the sensors are the more useful the results. Testing 36 sensors 6 at a time will require at least 6 iterations of testing, assuming none of the sensor evaluations have to be repeated.

Sandia personnel will travel to PFO to configure and conduct each test. Ideally tests will occur in groups of 6 sensors, 3 broad-band and 3 short-period, to minimize travel requirements. Furthermore, the testing will be organized into two sets: those for broadband sensors only and those for all sensors. The tests unique to the broad-band sensors include A) sensor tilt command and control and B) refinement of calibrator constant values and confirmation of calibration circuitry continuity. All sensors will undergo the second set of tests, C) general seismometer characteristics.

Note the navy OBS, 1) passively self-level without the aid of circuitry or logic, and 2) do not have a calibration circuit, therefore upon completion of the procedure for testing general seismometer characteristics, as outlined below, testing of Navy OBS is considered complete.

A. The procedure for testing Nanometrics sensor leveling command and control is as follows:

1. While under power, each sensor will be placed in the tilt jig such that the sensor will undergo rotations about two axes:
    a. a counter-clockwise rotation about the North-South axis (looking northward) such that the "sensor case east" direction dips downward to the west, in strike/dip terms, dipping downward ~25° (measured from the horizontal).

b. a rotation of the case about the East-West axis such that "sensor case north" dips downward 45°.

2. A leveling command will be issued via the serial-IP connection to the sensor. Upon feedback from the sensor that leveling has completed, the sensor accelerometer values will be recorded and compared against expected values (e.g. after leveling the sensor platform output should indicate the X and Y are horizontal and vertical, pointed upwards).

3. Finally, the sensor will be removed from the tilt jig, while under power, and returned to the granite pier to a nominally level position. A final leveling sequence will be initiated and success confirmed to ensure the sensor is configured for normal operation.

4. The sensor will be allowed to thermally equilibrate under power in preparation of subsequent before advancing to subsequent tests.

B. The procedure for estimation of a sensor's calibrator constant and confirmation of calibration circuit continuity is as follows.

1. Calibrations will be conducted with the sensor providing "XYZ" and "UVW" output. The sensors under test will have been powered for at least 12 hours and leveled for at least 8 hours before starting the calibration procedure. (Sensor tilt command and control tests may be completed during these initial hours of operation prior to the calibration tests.)

2. SNL will initiate a 1 Hz sine calibration signal via the Q330HR with a duration of at least 30 seconds and amplitude sufficient to ensure a reasonable SNR over the nominal background, with the sensor configured "XYZ" mode. Note the mode selected determines whether the sensor provides, as output, the un-transformed signal from the U, V and W elements or the signal after transformation to the vertical and horizontal (X, Y and Z coordinate system). While in "XYZ" mode the calibration signal will be sent individually to each of the 3 elements and separately the cal will also be sent simultaneously to the 3 elements.

3. SNL will initiate a 1 Hz sine calibration via the Q330HR with a duration of at least 30 seconds and amplitude sufficient to ensure a reasonable SNR over the nominal background, while the sensor is configured to record in "UVW" mode.

4. Upon completion of the calibration tests, SNL will confirm data are recording on the server, conduct a "stomp" test, to confirm basic operation of the sensor, allowing the reference and test sensors to collect several days of data for evaluation, as described in Procedure C, Tests Covering General Seismometer Characteristics.

C. The procedure for tests covering general seismometer characteristics is as follows:

1. Sensors will be placed in the PFO vault for a minimum of three days prior to use to allow them to thermally equilibrate. The sensors under test will operate for a period of at least 1 day after being powered to allow them sufficient time to thermally equilibrate. None of the data collected during this initial warm-up period will be considered for use in evaluation as described in this procedure.

2. Like sensors (e.g. broadband reference and Nanometrics sensors or short-period reference and Navy OBS) shall be co-located and co-aligned on a granite slab to ensure that they are all measuring a common input signal.

3. Data will be collected from the sensors under test and the appropriate reference sensor for a sufficient period of time to collect all necessary data to support their evaluation. Determination of when a sufficient amount of data has been collected will be made by SNL with the expectation that each set of 3 sensors under test will be in place for at least 5 days. The general criteria regarding data collection goals for this procedure that SNL will use are defined as follows.

    a. Time periods of low seismic backgrounds will provide at least 5 hours of continuous data that may be used for determining self-noise and dynamic range. SNL will assume that two overnight data collections, preferably over a weekend, will be sufficient for determining self-noise. At the discretion of SNL, additional nights of recording may be included to ensure a sufficient volume of data.

    b. At least one seismic event with sufficient amplitude will be used to provide an observable signal well above site noise across the application passband. These seismic events will provide a common input signal to the seismometers in order to determine sensitivity, response, and passband. SNL will determine whether a sufficiently large seismic event has occurred by monitoring the USGS and/or IRIS earthquake bulletins, looking for events that meet the following criteria:

        - Magnitude ~3.5 or greater within 100 km of PFO

        or

        - Magnitude ~3.0 or greater within 50 km of PFO

        or

        - Magnitude ~2.5 or greater within 25 km of PFO

Post-testing procedure:

1. Space is limited at PFO, therefore, as evaluation of individual sensors is completed, SNL will inform the Navy so arrangements may be made to transport these sensors to and from PFO in a timely manner.

2. When able, the Navy will assist with the physical handling of the sensors into, and out of, the vault.

3. The Navy will transport sensors to PFO such that there are always at least 3 broadband and 3 short-period sensors in the PFO vault thermally equilibrating prior to their testing, in addition to the sensors currently under test, until exhausting the supply of sensors.

4. SNL will collect and evaluate the recorded data and analyze the results while at PFO, prior to the sensors under test being removed by the Navy. Any issues with sensors under test will be identified and discussed with the Navy to determine whether a re-evaluation of a particular sensor is warranted.

3 RESULTS

3.1.1 Self-Noise

Test Description: The purpose of the self-noise test is to provide an evaluation of the sensor's internal noise. The data are generally collected overnight to minimize the cultural noise and noise associated with thermally-induced winds often found in the deserts of southern California. Data and the USGS earthquake catalog are reviewed to ensure a time period with minimal local earthquakes and no large tele-seismic or regional events are in the window of interest. The sensors' electronics and transducer noise are best evaluated under these conditions of minimal excitation.

The 3-Channel Sleeman coherence technique was applied to the power spectra of the sensors to compute their incoherent noise, using a noise model that is able to uniquely identify the noise of each sensor. For comparison purposes the Trillium OBS noise, the Quanterra Q330 noise expressed as Trillium OBS noise and NLNM are plotted along with the PSD and incoherent noise for the broadband sensors. Similarly, the Navy OBS have Leidos (Navy OBS) noise and the NLNM plotted along with the sensors' PSD and incoherent noise levels.

For this test, a 10 to 12 hour time window for the Nanometrics sensors, and a 6 to 10 hour window for the Navy OBS, typically recorded during the night or early morning hours, was used for each subset of the three instruments tested. The exact duration varied due to the need to utilize data with minimal coherent excitation (cultural noise, earthquakes, etc).

Below are example instrument-corrected PSD plots from the Nanometrics sensors.

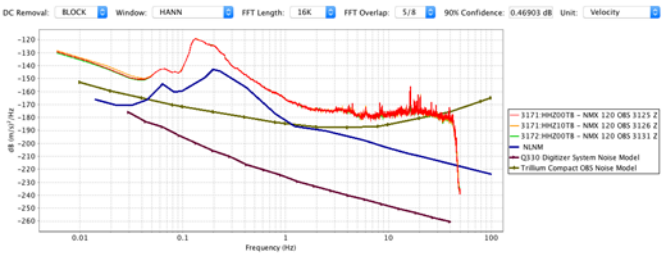

Figure 7 Example Self-Noise PSD, Broadband Vertical Component.

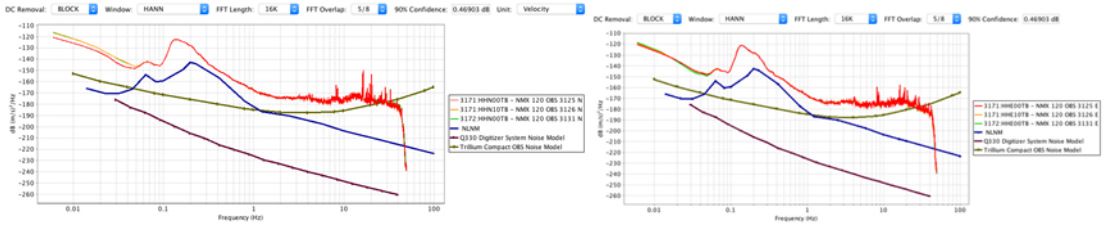

Figure 8 Example Self-Noise PSD, Broadband Horizontal Components.

Sensor self-noise plots are grouped as follows: Nanometrics OBS first, Navy OBS second. Within each sensor-type group, plots are organized by test date and component: Vertical – top, North – middle, East – bottom. Power spectral density was calculated for each sensors' data utilizing: a Hann taper, FFT length of 16384 samples for Nanometrics sensors (4096 samples for Navy OBS) with a 5/8th window overlap. An empirically derived model from a pre-production prototype Navy OBS is used for reference purposes.

All of the Nanometrics self-noise plots exhibit elevated incoherent noise estimates at low frequencies, exceeding the Nanometrics model of self-noise. We suggest this elevated noise may be in part a manifestation of air circulation/convection within the vault. While the PFO vault has a reasonably well-sealed door and a separate insulation baffle, it is likely there was some convection in the vault and intermixing of vault and outside air. It should also be noted that the Nanometrics sensors under test and reference were placed adjacent to the overhead vault entry, perhaps more directly exposing the sensors to what little convection and intermixing of vault and outside air that exists in the vault.

Q-330 noise, shaped by the nominal Trillium response and expressed as earth noise, is significantly lower than the measured incoherent noise for all Nanometrics sensors and Nanometrics-provided noise model.

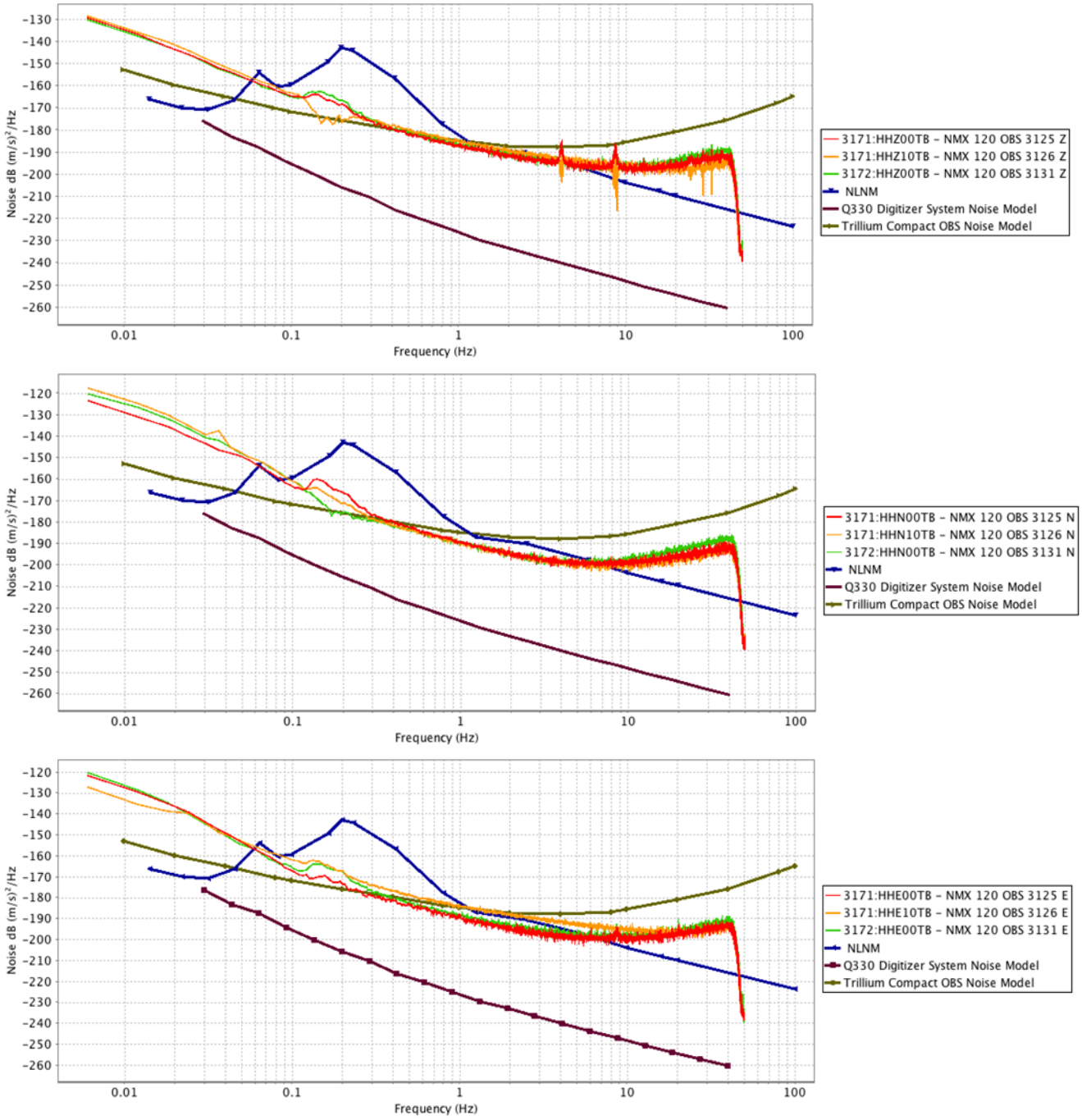

Figure 9 Incoherent Noise, Nanometrics OBS Sensors, Serial Numbers 3125, 3126 and 3131.

Ten hours of data recorded during the early morning hours of October 23, 2015 are used to calculate self-noise estimates, with a 90% confidence level of 0.47 dB, for Nanometrics sensors 3125, 3126 and 3131. The vertical, north and east components exhibit self-noise estimates below that specified by Nanometrics at frequencies above 0.5 Hz to 0.9 Hz, 0.2 Hz to 0.4 Hz and 0.3 to 2 Hz, respectively. The east components' self-noise estimates vary slightly more; sensor 3126's east component is significantly noisier, as much as 6 dB at 4 Hz, than its counterparts.

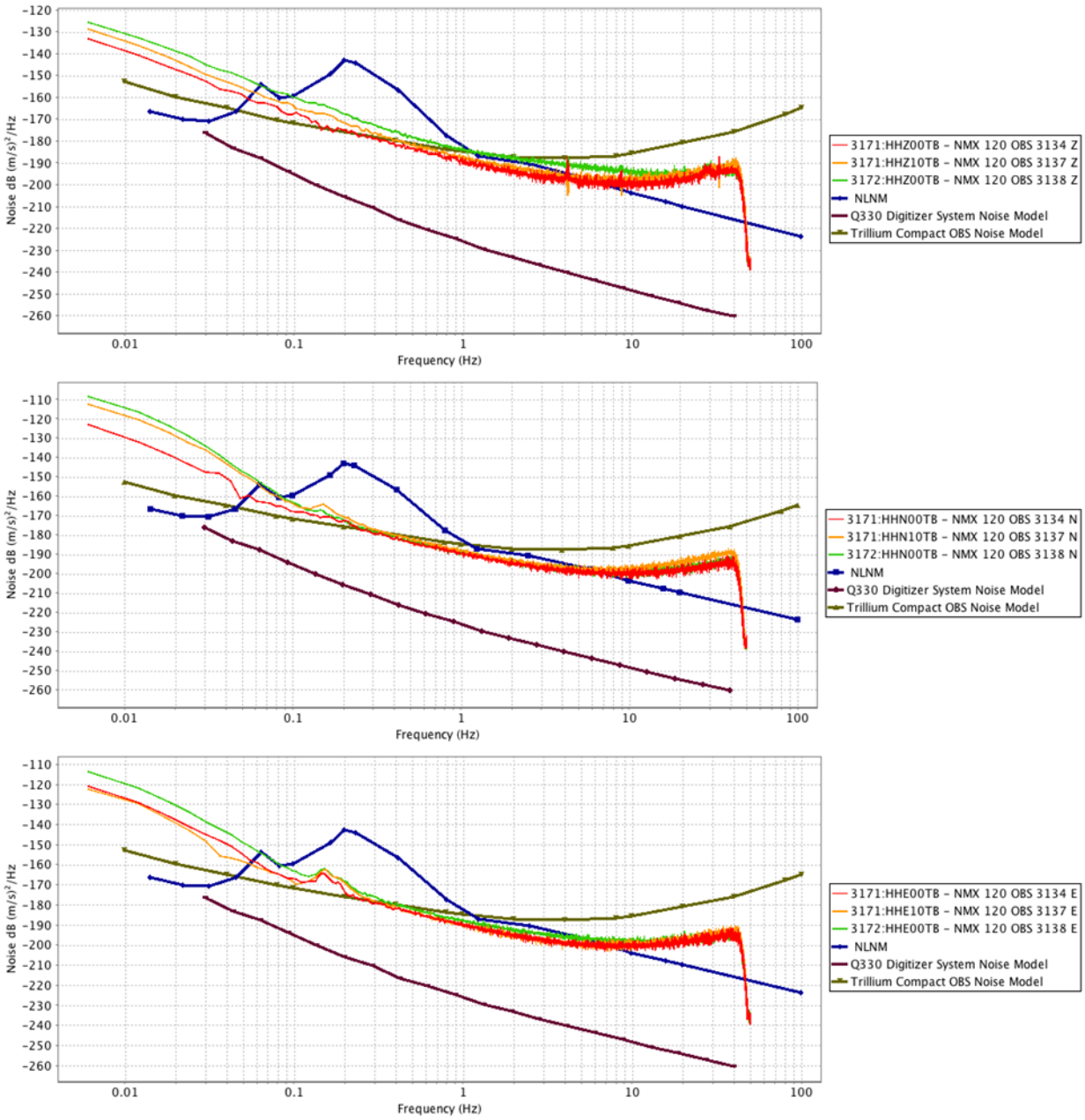

Figure 10 Incoherent Noise, Nanometrics OBS Sensors, Serial Numbers 3134, 3137 and 3138.

Ten hours of data recorded overnight on November 17-18, 2015 were used to calculate the sensor self-noise estimates, with a 90% confidence level of 0.47 dB, for Nanometrics sensors 3134, 3137 and 3138. The vertical, north and east components exhibit self-noise estimates below that specified by Nanometrics at frequencies above 0.25 Hz to 2.0 Hz, 0.28 Hz to 0.44 Hz and 0.28 to 0.45 Hz, respectively. The vertical components' self-noise estimates vary slightly more; 3138's vertical component is significantly noisier (3 dB to 6 dB) than its counterparts up to 6 Hz, then it approaches self-noise estimates of the other two sensors at approximately 20 Hz. Self-noise estimates of 3138's east component increase over that of the other sensors, up to 7 dB to 8 dB, at frequencies below approximately 0.1 Hz.

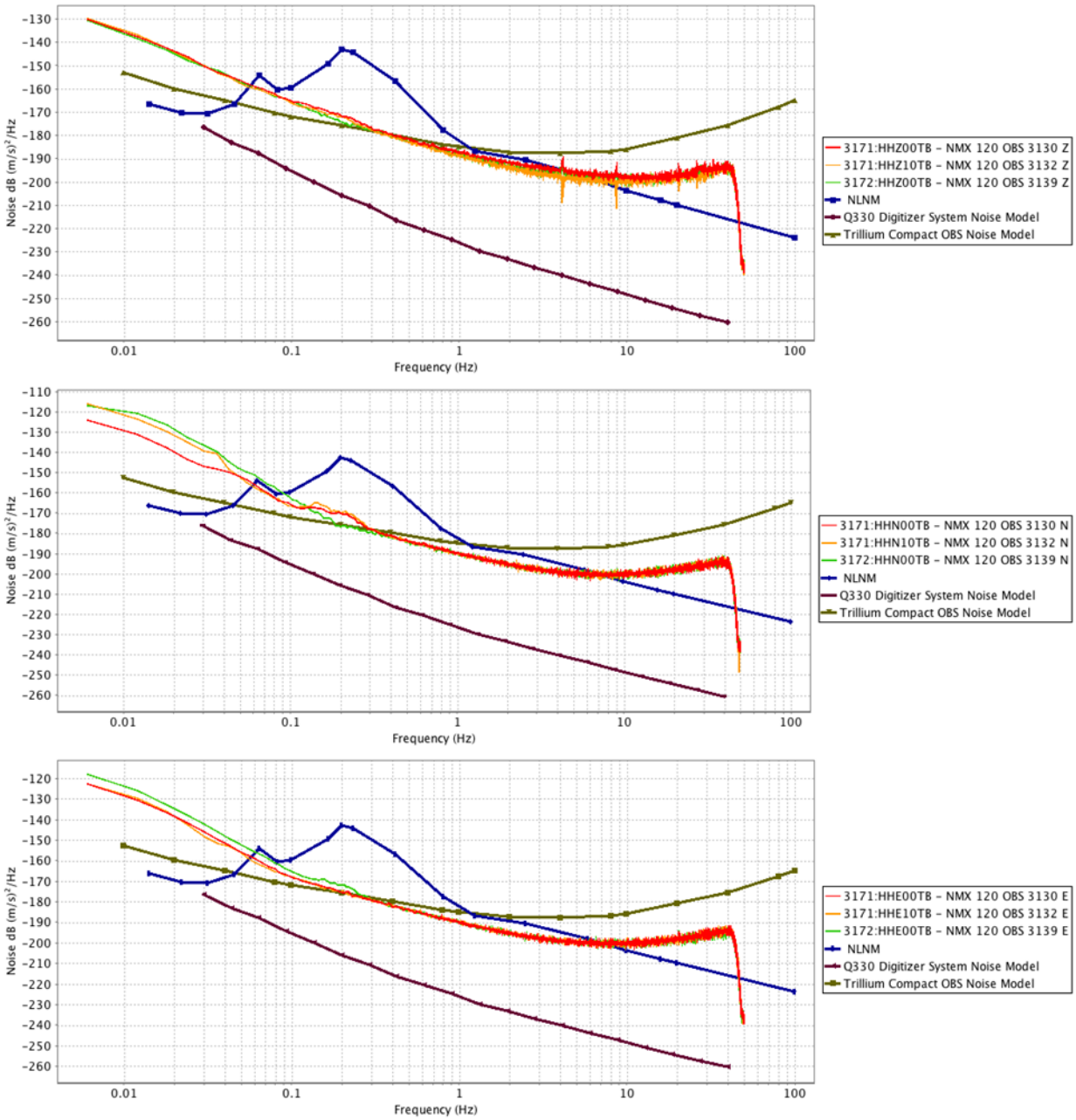

Figure 11 Incoherent Noise, Nanometrics OBS Sensors, Serial Numbers 3130, 3132 and 3139.

Twelve hours of data recorded overnight November 22 - 23, 2015 were used to calculate the sensor self-noise estimates, with a 90% confidence level of 0.43 dB, for Nanometrics sensors 3130, 3132 and 3139. The vertical, north and east components exhibit self-noise estimates below that specified by Nanometrics at frequencies above 0.32 Hz to 0.45 Hz, 0.19 Hz to 0.32 Hz and 0.22 to 0.29 Hz, respectively. The north components of 3132 and 3139 have elevated self-noise estimates (~8 dB) relative to sensor 3130 at frequencies below 0.04 Hz.

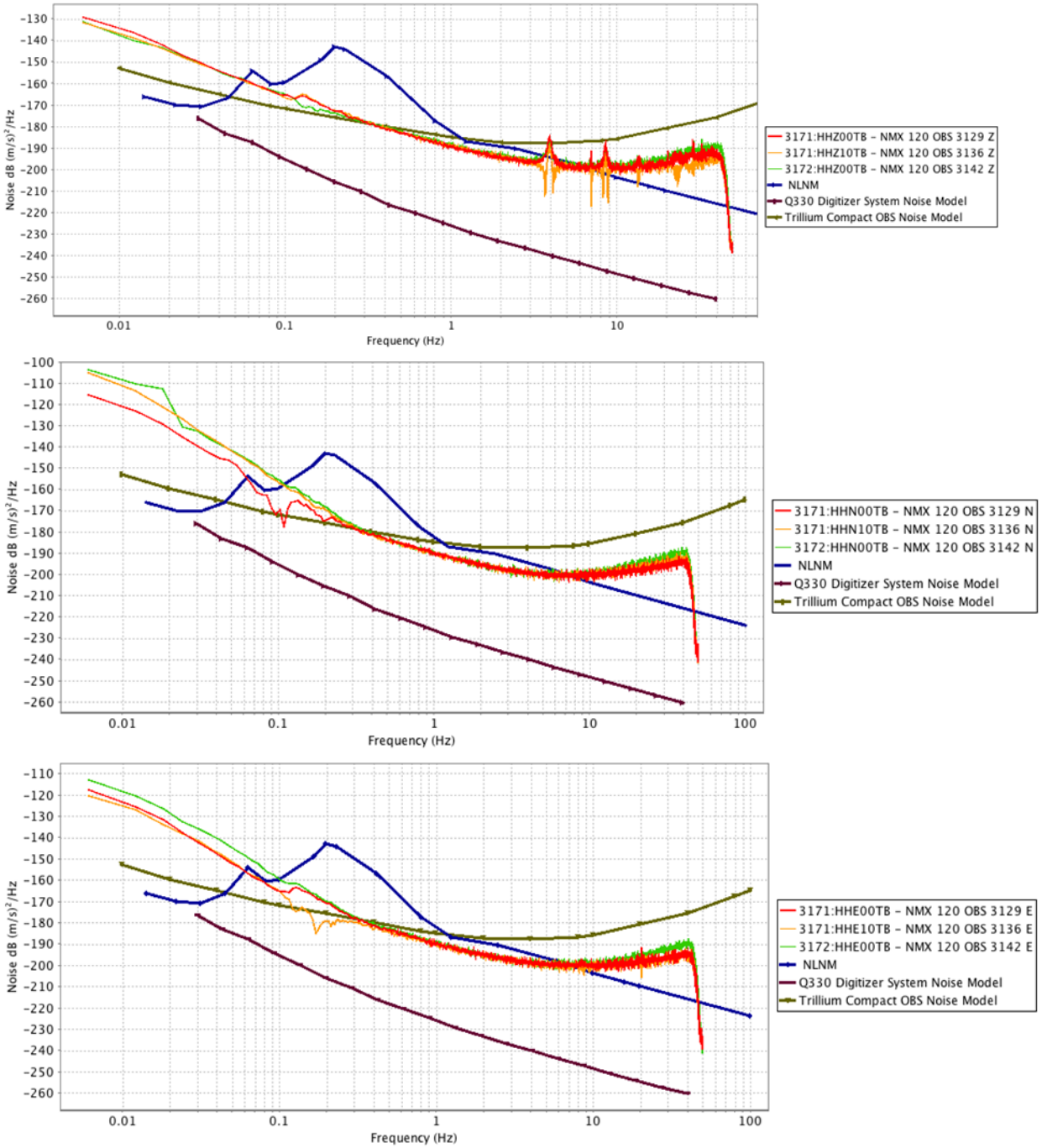

Figure 12 Incoherent Noise, Nanometrics OBS Sensors, Serial Numbers 3129, 3136 and 3142.

Ten hours of data recorded overnight on December 27 – 28, 2015 were used to calculate the sensor self-noise estimates, with a 90% confidence level of 0.47 dB, for Nanometrics sensors 3129, 3136 and 3142. The vertical, north and east components exhibit self-noise estimates below that specified by Nanometrics at frequencies above 0.35 Hz to 0.38 Hz, 0.33 Hz to 0.36 Hz and 0.15 to 0.36 Hz, respectively. The north components of sensors 3136 and 3142 have increased self-noise estimates (~8 dB) relative to 3129, below 0.2 Hz.

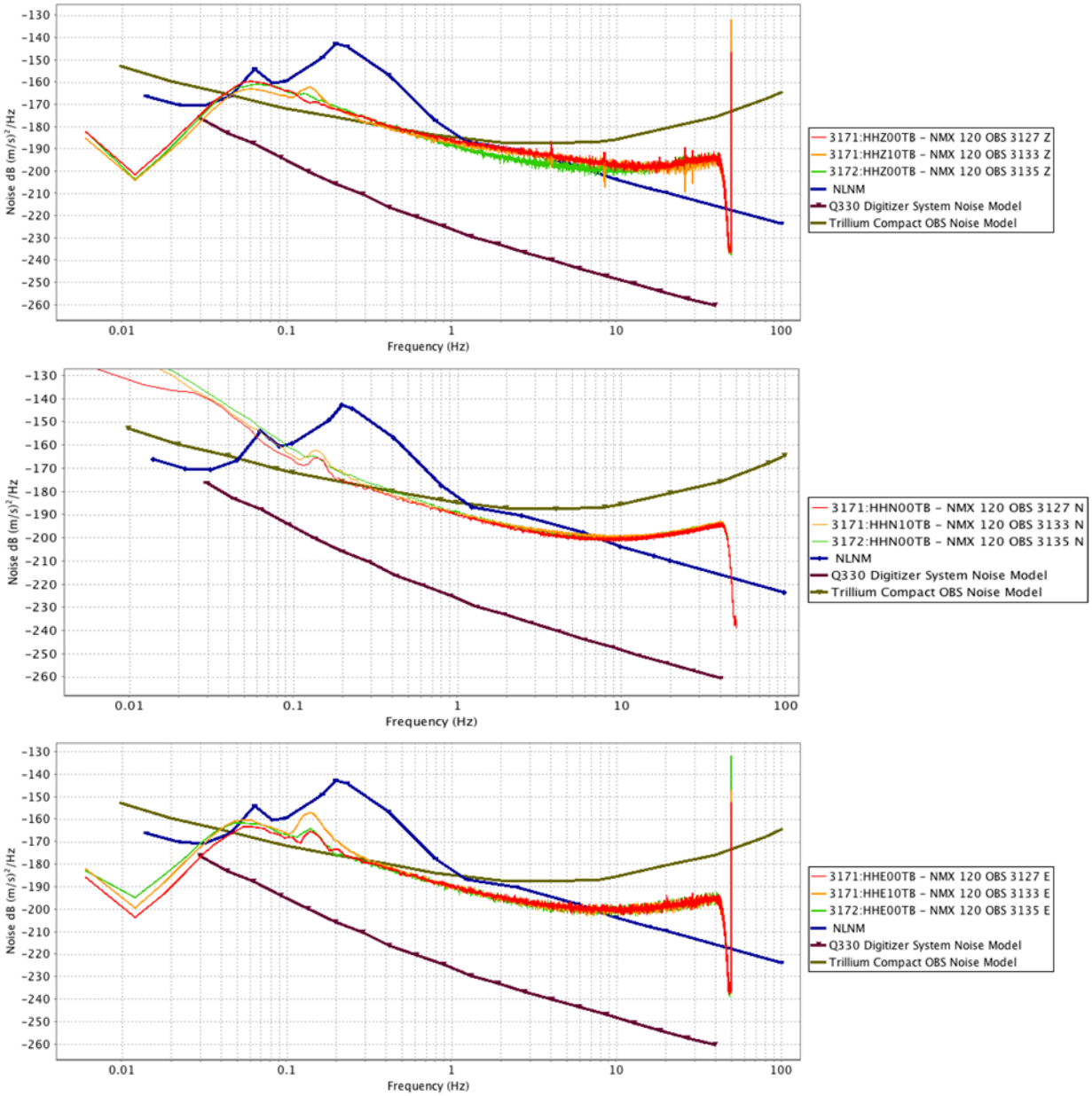

Figure 13 Incoherent Noise, Nanometrics OBS Sensors, Serial Numbers 3127, 3133 and 3135.

Ten hours of data recorded during the morning hours of March 18-19, 2016 were used to calculate the sensor self-noise, with a 90% confidence level of 0.47 dB, for Nanometrics sensors 3127, 3133 and 3135. The vertical, north and east components exhibit self-noise estimates below that specified by Nanometrics at frequencies above 0.38 Hz to 0.38 Hz, 0.24 Hz to 0.41 Hz and 0.25 to 0.31 Hz, respectively. The east component of 3127 has elevated self-noise estimate estimates relative to 3133 and 3135 between approximately 0.1 and 0.3 Hz. Coherence drops off rapidly below 0.5 Hz on all components, therefore the high self-noise estimates of the North components below 0.5 Hz have little meaning in reality.

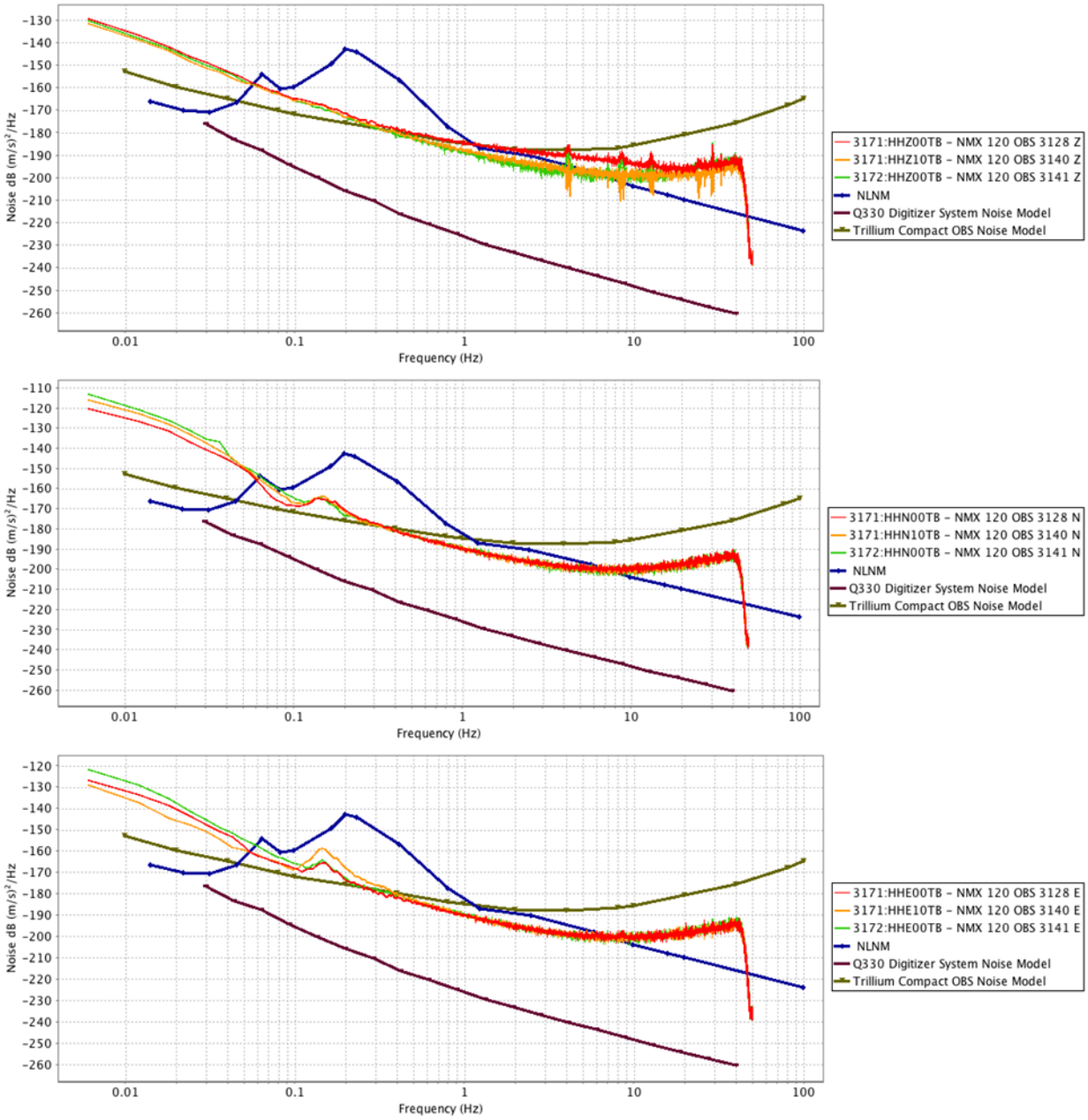

Figure 14 Incoherent Noise, Nanometrics OBS Sensors, Serial Numbers 3128, 3140 and 3141.

Ten hours of data recorded during the early morning hours of May 1, 2016 were used to calculate the sensor self-noise, with a 90% confidence level of 0.47 dB, for Nanometrics sensors 3128, 3140 and 3141. The vertical, north and east components exhibit self-noise estimates below that specified by Nanometrics at frequencies above 0.37 Hz to 1.7 Hz, 0.32 Hz to 0.37 Hz and 0.28 to 0.41 Hz, respectively. The vertical component of sensor 3128 has elevated noise, as much as 6 dB at 5 Hz, relative to the other two sensors and the east component of sensor 3140 has elevated noise of 5 dB over a relatively narrow frequency band centered on 0.15 Hz.

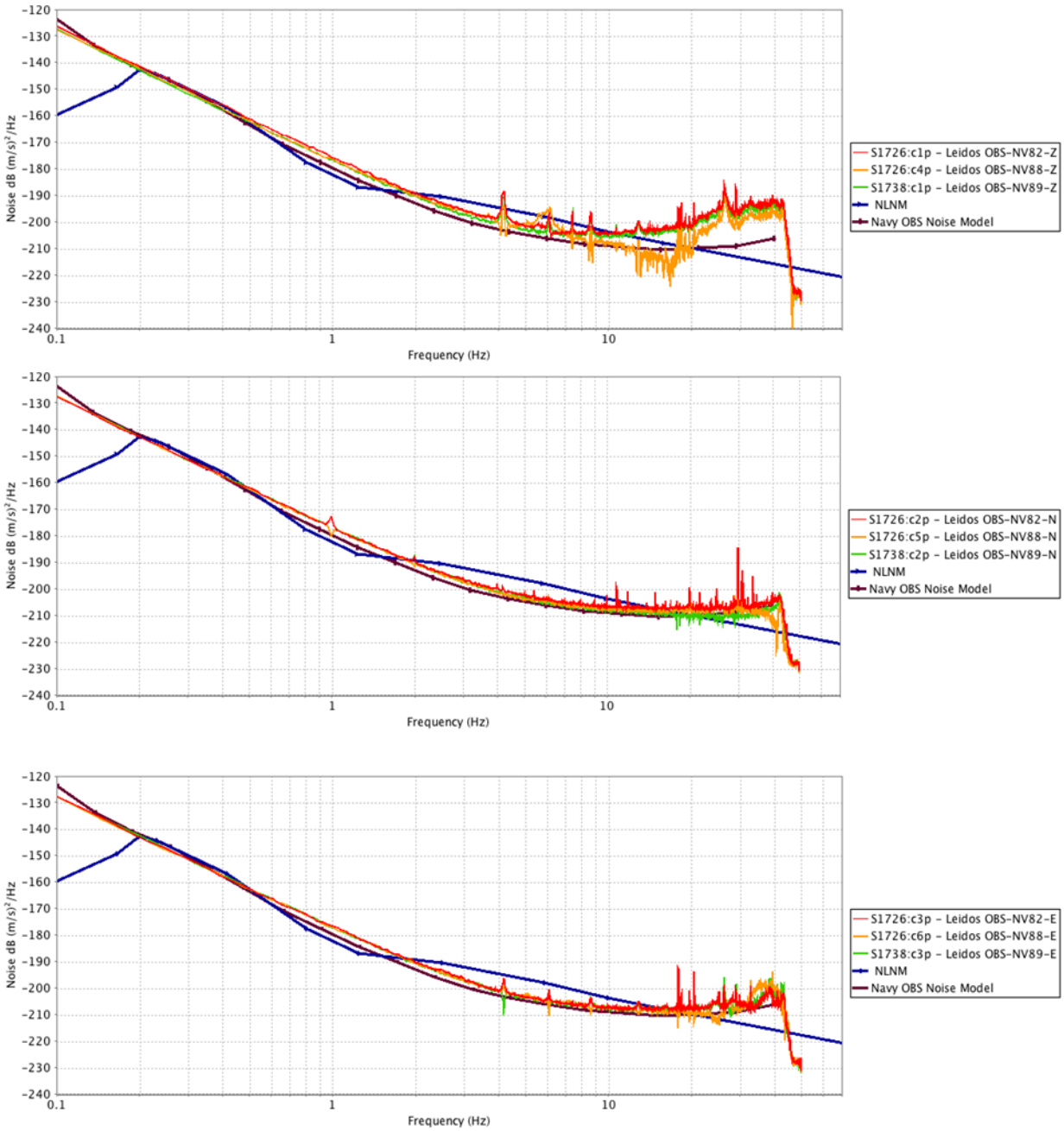

Figure 15 Incoherent Noise, Navy OBS Sensors, Property numbers 82, 88 and 89.

Six hours of data recorded during the early morning of November 18, 2015 were used to calculate the self-noise estimates, with a 90% confidence level of 0.30 dB, for Navy sensors 82, 88 and 89. Sensor noise estimates for vertical of sensor 88, north of sensor 89 and east fall below the empirically derived noise model, between 12 and 21 Hz, above 18 Hz and over a narrow band centered on 28 Hz, respectively.

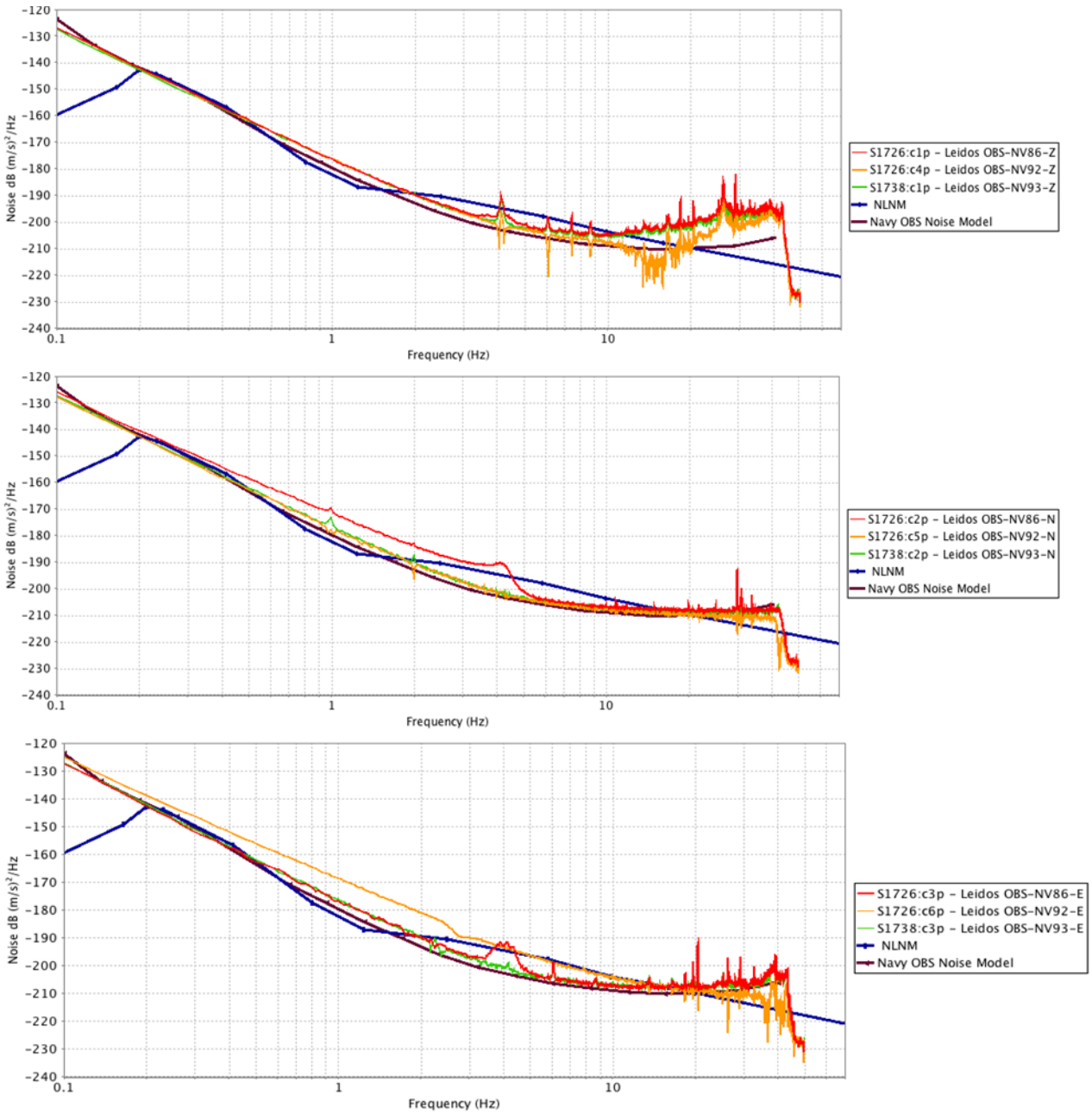

Figure 16 Incoherent Noise, Navy OBS Sensors, Property numbers 86, 92 and 93.

Eight hours of data recorded overnight during November 22 and 23, 2015 were used to calculate the self-noise estimates, with a 90% confidence level of 0.26 dB, for Navy sensors 86, 92 and 93. The north components exhibit self-noise estimates below empirically-derived model at frequencies above 20 to 32 Hz. The vertical and east components of sensor 92 was the only vertical and east component to exhibit self-noise estimates below the model, doing so between 11 and 18 Hz and above 23 Hz, respectively. The north component of sensor 86 and east component of sensor 92 exhibit elevated self-noise below 5 Hz, relative to the Navy OBS noise model. The coherence between East and North components drops off rapidly below 4 Hz,

therefore, the elevated noise levels exhibited the North and East components of sensors 86 and 92 should be discounted by the reader.

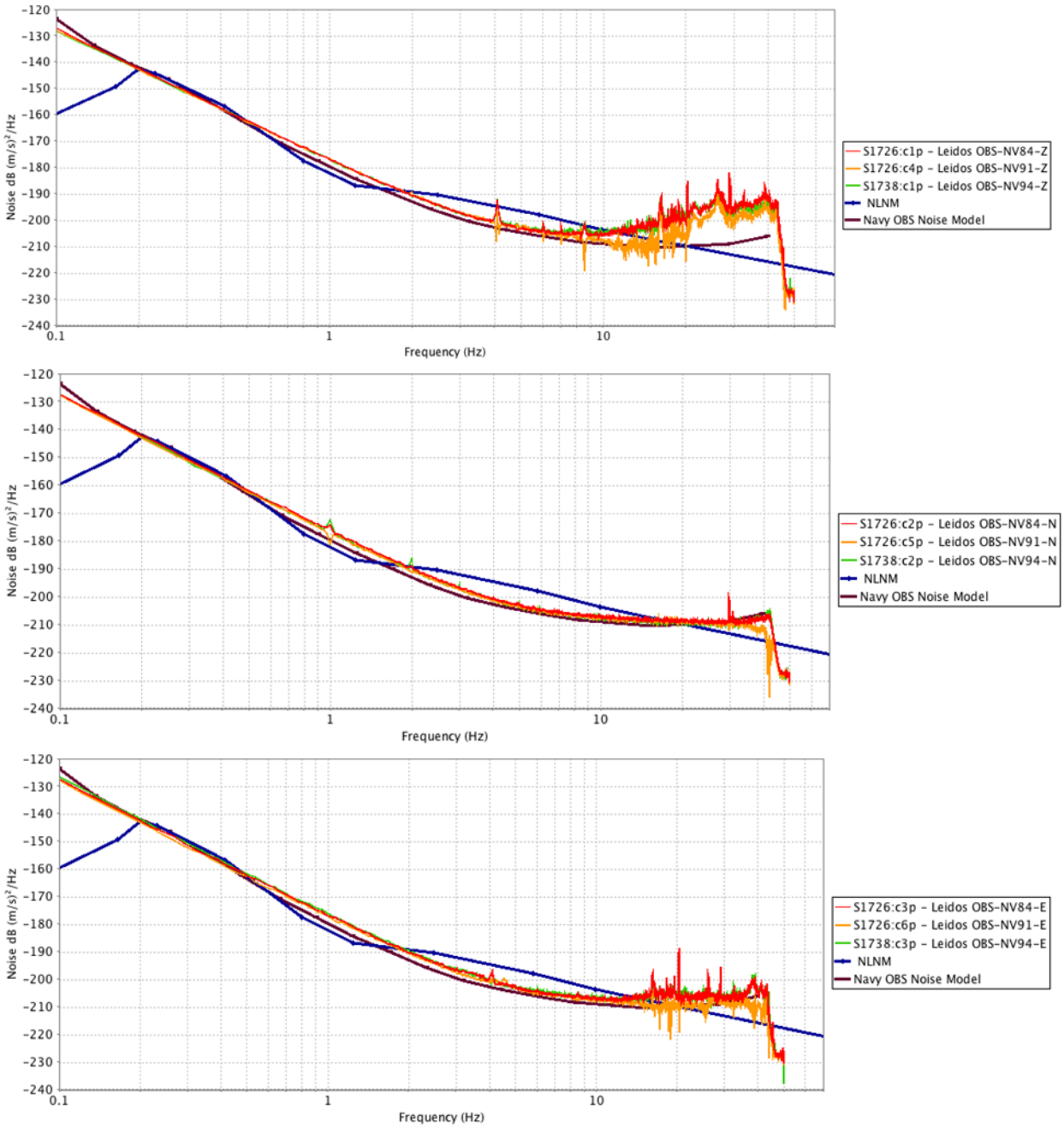

Figure 17 Incoherent Noise, Navy OBS Sensors, property numbers 84, 91 and 94.

Eight hours of data recorded overnight during January 1 - 2, 2016 were used to calculate the self-noise estimates, with a 90% confidence level of 0.26 dB, for Navy sensors 84, 91 and 94. The vertical component of sensor 91 exhibits self-noise estimates below empirically-derived model at frequencies between 11 Hz and 14 Hz. The north components exhibit self-noise estimates below Navy OBS model at frequencies above 24 to 31 Hz. The east component of sensor 91 was the only east component to exhibit self-noise estimates below the model, doing so above 30 Hz.

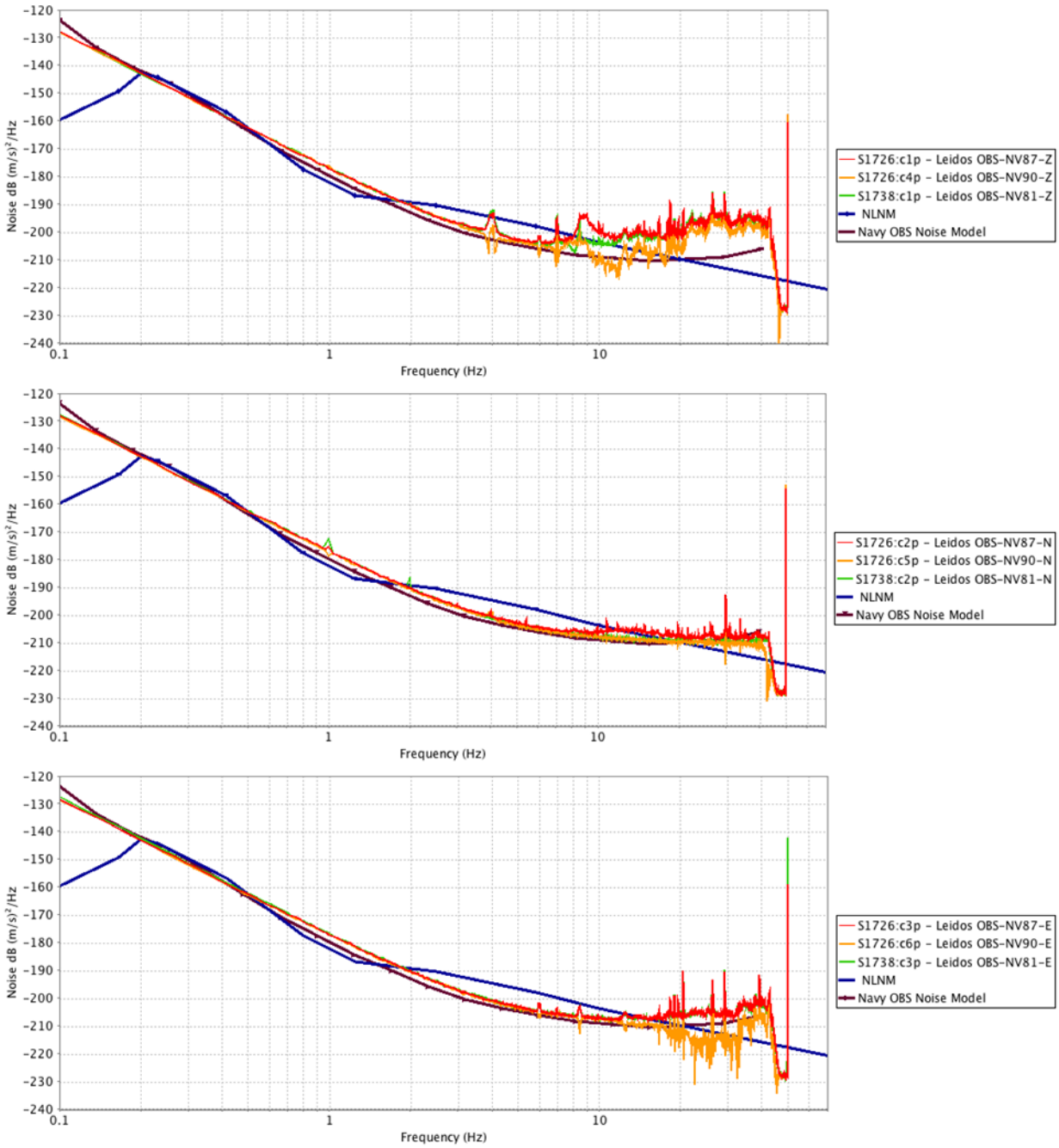

Figure 18 Incoherent Noise, Navy OBS Sensors, property numbers 81, 87 and 90.

Ten hours of data recorded during the early morning of March 20, 2016 were used to calculate the self-noise estimates, with a 90% confidence level of 0.23 dB, for Navy sensors 81, 87 and 90. The vertical component of sensor 90 exhibits self-noise estimates below empirically-derived model at frequencies between 9.0 Hz and 12 Hz, with some narrow banded excursions below the model between 12 Hz and 18 Hz. The north components exhibit self-noise estimates below the Navy OBS model at frequencies above 21 Hz to 31 Hz. The east component of sensor 90 noise estimates fall below the Navy OBS model between 17 and 38 Hz, with a few narrow-banded excursions above the model between these two frequencies.

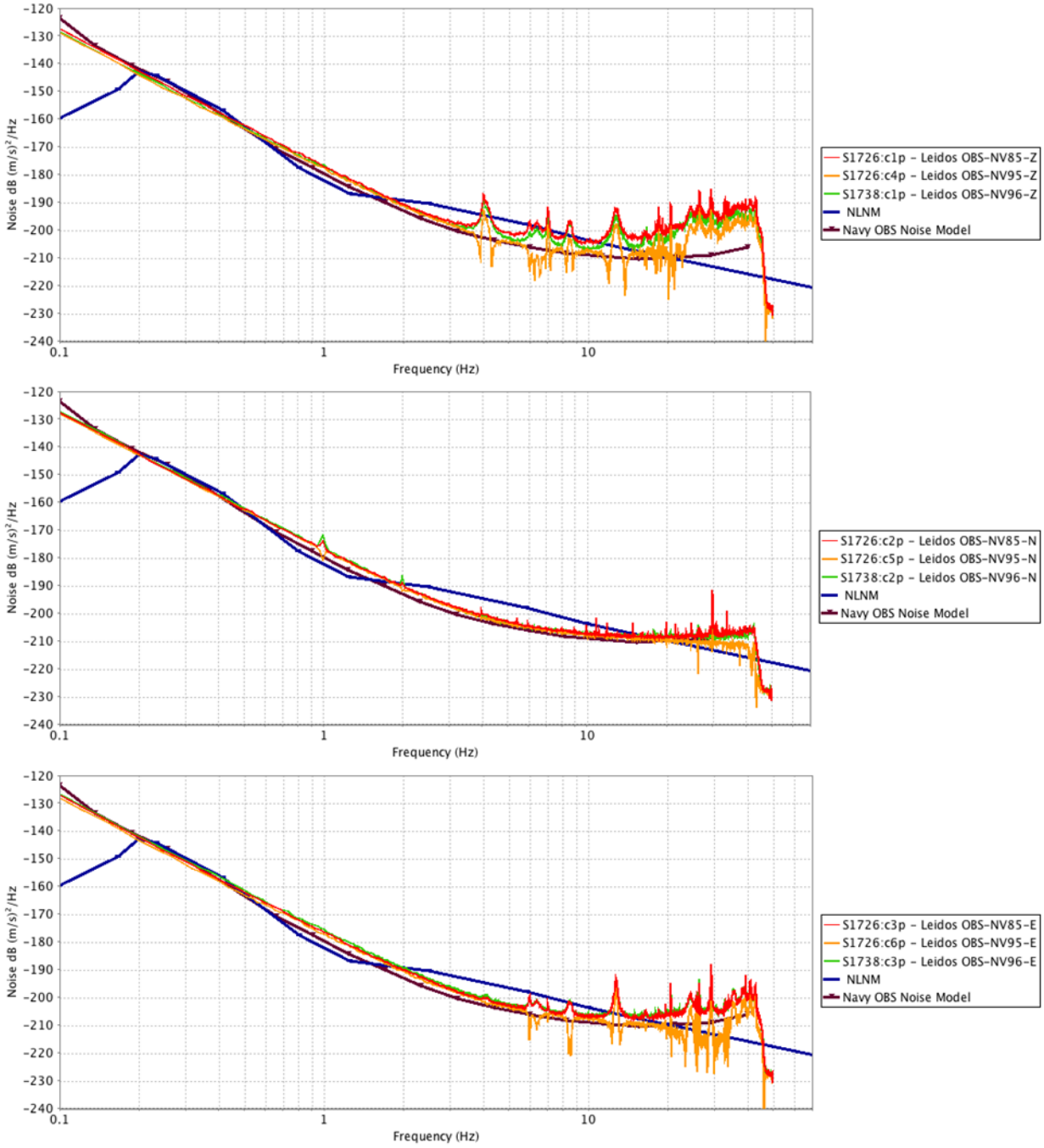

Figure 19 Incoherent Noise, Navy OBS Sensors, property numbers 85, 95 and 96.

Ten hours of data recorded during the early morning of May 1, 2016 were used to calculate the self-noise estimates, with a 90% confidence level of 0.23 dB, for Navy sensors 85, 95 and 96. The vertical component of sensor 95 exhibits self-noise estimates below empirically-derived model in narrow frequency bands between 4 Hz and 21 Hz. The north components exhibit self-noise estimates below the Navy OBS model at frequencies above 21 Hz to 36 Hz. The east component of sensor 95 noise estimates fall below the Navy OBS model between 19 and 35 Hz, with a few narrow-banded excursions above the model between these two frequencies.

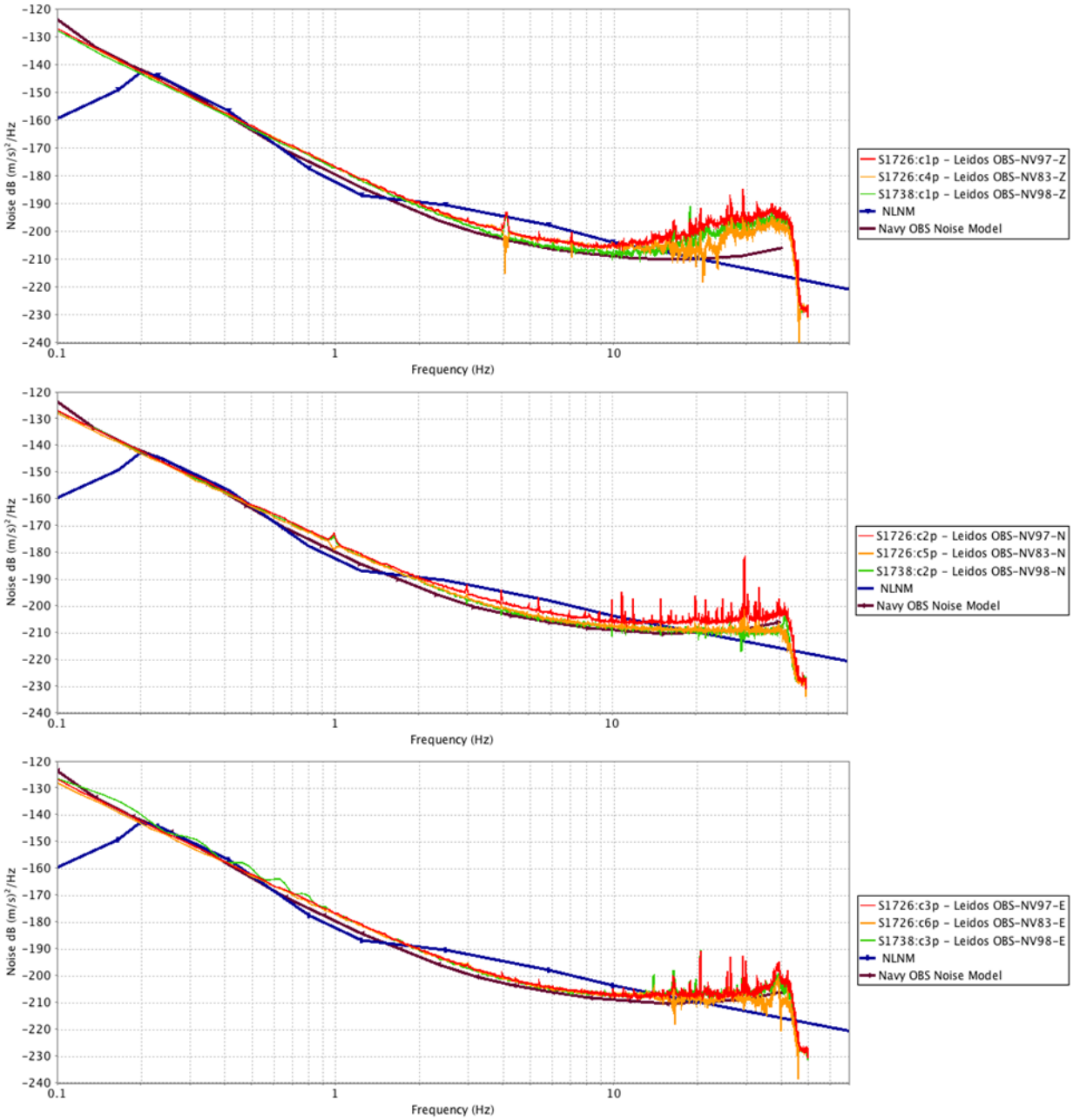

Figure 20 Incoherent Noise, Navy OBS Sensors, property numbers 83, 97 and 98.

Ten hours of data recorded overnight during June 6 - 7, 2016 were used to calculate the self-noise estimates, with a 90% confidence level of 0.23 dB, for Navy sensors 83, 97 and 98. The vertical component of sensor 83 exhibits self-noise estimates below empirically-derived model in a narrow frequency band centered on 21 Hz, though this may be an artifact of processing. The north components of sensors 83 and 98 exhibit self-noise estimates below the Navy OBS model at frequencies above 25 Hz and 22 Hz, respectively. Noise estimates of the east component of sensor 83 fall below the Navy OBS model above 31 Hz.

Table 2 Nanometrics OBS Noise Estimates (0.02 Hz – 40 Hz)

Serial Number	Vertical	North	East
3125	6.269E-9 m/s rms	11.51E-9 m/s rms	10.80E-9 m/s rms
3126	7.249E-9 m/s rms	19.66E-9 m/s rms	10.64E-9 m/s rms
3127	2.752E-9 m/s rms	15.06E-9 m/s rms	2.058E-9 m/s rms
3128	6.098E-9 m/s rms	15.13E-9 m/s rms	6.832E-9 m/s rms
3129	5.533E-9 m/s rms	17.32E-9 m/s rms	12.91E-9 m/s rms
3130	5.649E-9 m/s rms	8.094E-9 m/s rms	8.255E-9 m/s rms
3131	6.375E-9 m/s rms	16.34E-9 m/s rms	9.937E-9 m/s rms
3132	5.308E-9 m/s rms	17.77E-9 m/s rms	7.132E-9 m/s rms
3133	2.495E-9 m/s rms	18.82E-9 m/s rms	3.529E-9 m/s rms
3134	4.075E-9 m/s rms	7.269E-9 m/s rms	9.084E-9 m/s rms
3135	2.689E-9 m/s rms	22.23E-9 m/s rms	2.373E-9 m/s rms
3136	5.154E-9 m/s rms	43.09E-9 m/s rms	13.05E-9 m/s rms
3137	6.059E-9 m/s rms	23.85E-9 m/s rms	6.808E-9 m/s rms
3138	10.17E-9 m/s rms	32.64E-9 m/s rms	19.42E-9 m/s rms
3139	5.188E-9 m/s rms	23.41E-9 m/s rms	12.56E-9 m/s rms
3140	4.889E-9 m/s rms	21.58E-9 m/s rms	5.165E-9 m/s rms
3141	5.446E-9 m/s rms	28.31E-9 m/s rms	8.906E-9 m/s rms
3142	5.395E-9 m/s rms	33.96E-9 m/s rms	25.65E-9 m/s rms

Table 3 Navy OBS Noise Estimates (1 Hz – 40 Hz)

Tag Number	Vertical	North	East
81	1.148 nm/s rms	0.8688 nm/s rms	0.8596 nm/s rms
82	1.312 nm/s rms	0.9034 nm/s rms	0.8607 nm/s rms
83	0.9243 nm/s rms	0.7792 nm/s rms	0.7981 nm/s rms
84	1.331 nm/s rms	0.8743 nm/s rms	0.8689 nm/s rms
85	1.306 nm/s rms	0.8479 nm/s rms	0.9228 nm/s rms
86	1.199 nm/s rms	1.573 nm/s rms	0.8824 nm/s rms
87	1.169 nm/s rms	0.8387 nm/s rms	0.8503 nm/s rms
88	1.000 nm/s rms	0.7845 nm/s rms	0.8451 nm/s rms
89	1.143 nm/s rms	0.8605 nm/s rms	0.8228 nm/s rms
90	0.9687 nm/s rms	0.7675 nm/s rms	0.7785 nm/s rms
91	1.019 nm/s rms	0.7641 nm/s rms	0.7868 nm/s rms
92	0.9762 nm/s rms	0.7506 nm/s rms	2.106 nm/s rms
93	1.081 nm/s rms	0.8633 nm/s rms	0.8640 nm/s rms
94	1.183 nm/s rms	0.8661 nm/s rms	0.8982 nm/s rms
95	0.8655 nm/s rms	0.7526 nm/s rms	0.7891 nm/s rms
96	1.080 nm/s rms	0.8999 nm/s rms	0.9792 nm/s rms
97	1.182 nm/s rms	0.9789 nm/s rms	0.8760 nm/s rms
98	0.9896 nm/s rms	0.8358 nm/s rms	0.8358 nm/s rms

The self-noise estimates (0.02 Hz to 40 Hz) of the Nanometrics sensors were lowest for the verticals with an average estimate 5.378 nm/s rms; the highest vertical component self-noise

value is 10.17 nm/s rms for sensor 3138. The east components rank second, with an average self-noise estimate of 9.73 nm/s rms, with sensor 3142 having the highest calculated self-noise at 25.65 nm/s rms. The north components have the highest calculated self noise averageing 20.7 nm/s rms; the highest rms noise on the north component of 3136 at 43.09 nm/s rms.

Self-noise estimates (1 Hz to 40 Hz) of the passive short-period sensors (Navy OBS) were, not surprisingly, better than those of the active broadband sensors (Nanometrics OBS). The north component self-noise average was the lowest, at 0.878 nm/s rms with the highest self-noise found on sensor 86 (1.573 nm/s rms). The east component follows with an average self-noise is 0.924 nm/s rms; sensor 92 had the highest self-noise of the group (2.106 nm/s rms). Recall the coherence between sensors under test for sensors 86, 92 and 93 had low coherence below 4 Hz and high calculated self noise for sensor 92 below 0.5 Hz, which increased the calculated rms noise over the frequency band of interest. The vertical component average self-noise was the noisiest of self-noise estimates of the components, with an average value of 1.104 nm/s rms and the noisiest sensor being 84 with a self-noise of 1.537 nm/s rms.

3.1.2 Dynamic Range

Test Description: The purpose of the dynamic range test is to determine the ratio between the largest and smallest possible signals that may be observed on the sensor. We define dynamic range as the ratio between the RMS of a full-scale sinusoid at the calibration frequency, typically 1 Hz, and the RMS noise present in the self-noise of the sensor across an application pass band.

Below, in Tables 4 and 5, are provided dynamic range values using the sensor self-noise estimates obtained from 3.1.1 Self-Noise, which is believed to be the best estimate of self-noise available. Two full scale levels are used for each of the Nanometrics and Navy OBS sensors: The sensor full scale and the deployment digitizer channel full scale. For the Nanometrics OBS the full scales are 20 Vp and 1.4 Vp, respectively. For the Navy OBS the full scales are 20 Vp and 0.65 Vp, respectively.

Table 4 Nanometrics Dynamic Range, 0.02 Hz – 40 Hz: 20 V_{peak} and 1.4 V_{peak} Full Scale

Serial Number	Vertical		North		East	
	20 V_p Full Scale	1.4 V_p Full Scale	20 V_p Full Scale	1.4 V_p Full Scale	20 V_p Full Scale	1.4 V_p Full Scale
3125	129.5 dB	106.4 dB	124.3 dB	101.2 dB	124.8 dB	101.7 dB
3126	128.3 dB	105.2 dB	119.7 dB	96.6 dB	125.0 dB	101.9 dB
3127	136.7 dB	113.6 dB	121.9 dB	98.8 dB	139.1 dB	116.0 dB
3128	129.8 dB	106.7 dB	121.9 dB	98.8 dB	128.8 dB	105.7 dB
3129	130.7 dB	107.6 dB	120.7 dB	97.6 dB	123.2 dB	100.1 dB
3130	130.4 dB	107.3 dB	127.3 dB	104.2 dB	127.1 dB	104.0 dB
3131	129.5 dB	106.4 dB	121.4 dB	98.3 dB	125.7 dB	102.6 dB
3132	131.0 dB	107.9 dB	120.4 dB	97.3 dB	128.4 dB	105.3 dB
3133	137.5 dB	114.4 dB	120.9 dB	97.8 dB	134.5 dB	111.4 dB
3134	133.3 dB	110.8 dB	128.3 dB	105.2 dB	126.3 dB	103.8 dB
3135	137.0 dB	113.9 dB	118.5 dB	95.4 dB	137.9 dB	114.8 dB
3136	131.4 dB	108.3 dB	112.7 dB	89.6 dB	123.2 dB	100.1 dB
3137	129.9 dB	107.4 dB	117.9 dB	94.8 dB	128.8 dB	106.3 dB
3138	125.5 dB	103.0 dB	115.3 dB	92.2 dB	119.8 dB	097.3 dB
3139	131.3 dB	108.2 dB	118.1 dB	95.0 dB	123.6 dB	100.5 dB
3140	131.7 dB	108.6 dB	118.8 dB	95.7 dB	131.2 dB	108.1 dB
3141	130.8 dB	107.7 dB	116.4 dB	93.3 dB	126.5 dB	103.4 dB
3142	130.8 dB	107.8 dB	114.7 dB	91.6 dB	117.2 dB	094.1 dB

Over the frequency band of interest for the Nanometrics sensors (0.02 Hz – 40 Hz), the vertical has an average 20 V_{peak} dynamic range of 131.4 dB, with no sensor deviating more than 6.1 dB from the average. The horizontal components had dynamic ranges lower than that of the vertical component; dynamic ranges also spanned a larger range of values. The east component fared better than the north components with a 20 V_{peak} dynamic range average of 127.3 dB and dynamic range values staying within 11.8 dB of the average, whereas the north component average dynamic range is 120.0 dB and values varied as much as 8.3 dB from the average. While the average dynamic range (20 V_{peak}) for the vertical components meets the requirement of 130 dB, 6 individual sensors do not meet the criteria, the lowest being 125.5 dB. Dynamic ranges of 4 sensors' east components meet the 130 dB criterion; their average does not. None of the North component (20 V_{peak}) meets the 130 dB criterion.

Table 5 Navy OBS Dynamic Range, 1 Hz – 40 Hz: 20 V_{peak} and 0.65 V_{peak} Full Scale

Tag Number	Vertical		North		East	
	20 V_p Full Scale	0.65 V_p Full Scale	20 V_p Full Scale	0.65 V_p Full Scale	20 V_p Full Scale	0.65 V_p Full Scale
81	141.6 dB	111.7 dB	143.6 dB	113.8 dB	144.2 dB	114.2 dB
82	141.7 dB	112.0 dB	143.4 dB	113.7 dB	144.0 dB	114.2 dB
83	143.6 dB	113.9 dB	144.4 dB	114.7 dB	144.8 dB	115.0 dB
84	140.5 dB	110.7 dB	144.2 dB	114.4 dB	144.2 dB	114.4 dB
85	140.5 dB	110.7 dB	143.9 dB	114.1 dB	143.7 dB	113.9 dB
86	141.8 dB	112.0 dB	139.2 dB	109.4 dB	143.9 dB	114.2 dB
87	141.4 dB	111.7 dB	144.0 dB	114.2 dB	144.0 dB	114.2 dB
88	143.2 dB	113.5 dB	144.6 dB	114.8 dB	144.4 dB	114.6 dB
89	141.8 dB	112.0 dB	143.7 dB	113.9 dB	144.2 dB	114.4 dB
90	143.2 dB	113.4 dB	144.7 dB	114.9 dB	144.9 dB	115.1 dB
91	142.7 dB	112.9 dB	144.7 dB	114.9 dB	144.8 dB	115.1 dB
92	143.7 dB	114.0 dB	144.7 dB	114.9 dB	137.0 dB	107.2 dB
93	142.2 dB	112.5 dB	143.7 dB	114.0 dB	144.2 dB	114.5 dB
94	141.4 dB	111.6 dB	143.6 dB	113.8 dB	144.3 dB	114.6 dB
95	142.8 dB	113.1 dB	144.8 dB	115.0 dB	144.8 dB	115.0 dB
96	141.5 dB	111.8 dB	143.5 dB	113.7 dB	143.6 dB	113.8 dB
97	141.3 dB	111.6 dB	143.0 dB	113.3 dB	144.0 dB	114.3 dB
98	142.5 dB	112.7 dB	144.0 dB	114.2 dB	144.0 dB	114.2 dB

The Navy OBS' component-specific average 20 V_{peak} full scale dynamic range exceeds the requirement of 130 dB in the band of interest, 1 Hz -40 Hz: 142.1 dB, 143.8 dB and 143.8 dB, for the vertical, north and east components, respectively. The lowest 20 V_{peak} full scale dynamic range across components was Navy OBS 92 at 137.0 dB.

3.1.3 Sensitivity and Response Verification

Test description: The seismic response verification test serves two purposes: first to determine seismic sensitivity, discussed within this section, and second, to verify the seismic sensor frequency/amplitude/phase response over a range of frequencies, using a natural seismic source, an earthquake, and a characterized reference broadband or short period sensor, as applicable. Details regarding the test description and evaluation and results regarding the sensors' response will be addressed following the results of the sensitivity determination.

Sensors with known instrument response models served as references for this test: for the broadband sensors, a Nanometrics Trillium OBS S/N 2100, and for the Navy OBS units, a set of GS-13 seismometers: Vertical S/N 878, North S/N 877, and East S/N 879. Natural seismic sources, local earthquakes, are utilized as a relatively broadband source of seismic excitation of the reference and test sensors. A time-window of sufficient length, to capture the earthquake's P wave through its coda, is defined and the analysis performed; window lengths varied from one to four minutes depending on the source earthquakes. The time-series between the red vertical lines in Figure 21 denote the window used in the analysis.

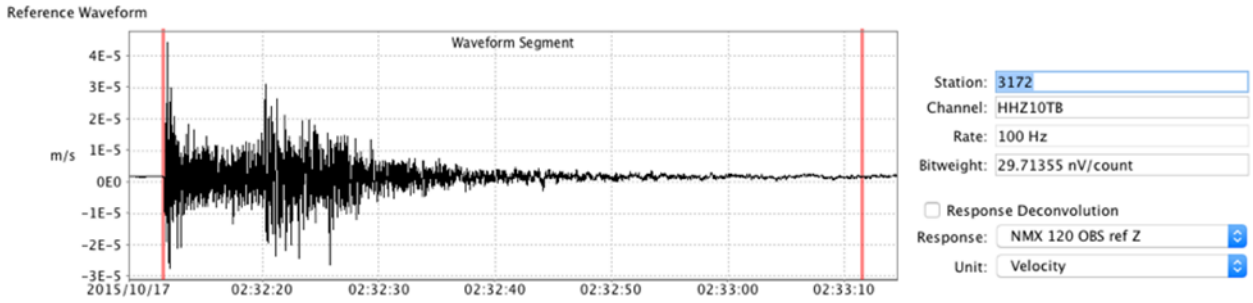

Figure 21 Example time series of an earthquake used to calculate sensitivities of the broadband sensors, vertical component data shown.

The example provided in Figure 21 is the recording of the M=3.31 October 17, 2015 earthquake. The data window, between the two red lines, is 1 minute in duration.

The two PSD plots below in Figure 22 illustrate the significant advantage of utilizing the frequent earthquakes, which occur in the vicinity of PFO, for instrument response verification. The first PSD plot is of ten hours of background seismic noise recorded overnight; the second a PSD of one minute during which a typical earthquake utilized in this exercise occurred. Note the significant increase in signal power across a relatively broad spectrum of frequency of the earthquake over the background noise.

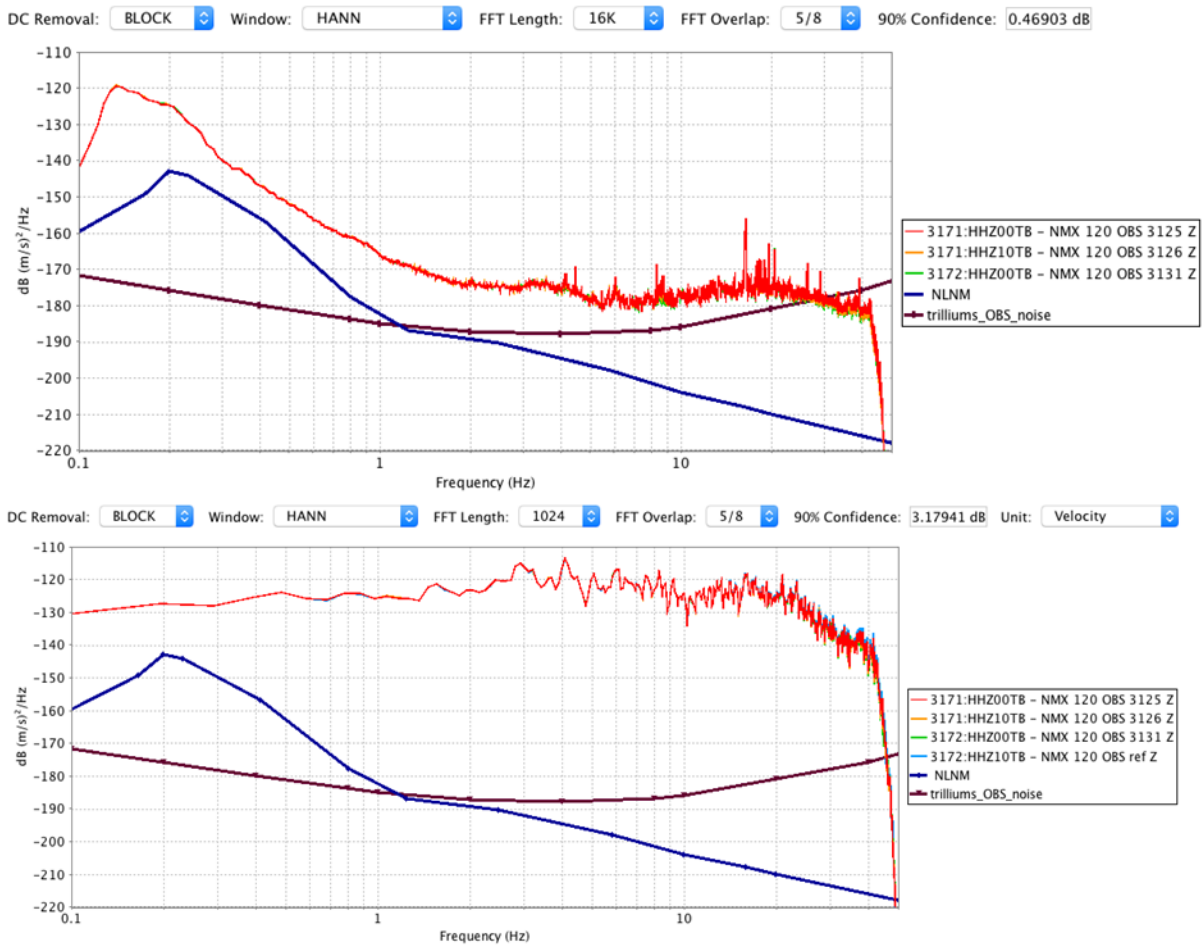

Figure 22 Comparison of Power Spectral Density (PSD) of vertical component seismic background versus the vertical component of a M=3.31 earthquake at 70 km distance, as recorded by the Nanometrics broadband seismometers.

The PSD on the top of Figure 22 is comprised of 10 hours of typical background noise, FFT window length of 16k samples. The plot on the bottom of Figure 22 is comprised of one minute of data, capturing the initial P wave arrival through the duration of the coda, FFT window length of 1024 samples. Data were recorded at 100 Hz. Over the frequencies where valid comparisons may be made, the PSD of the earthquake shows a 30 to 40 dB increase in signal power. At frequencies below ~0.25 Hz, the PSD of background noise shows more power than the earthquake signal. Recall though the background PSD contains 10 hours of data, whereas the earthquake PSD only 1 minute, therefore there are relatively few samples of the lowest frequencies available in the earthquake time-series versus the overnight time-series and comparisons at low frequencies may not be appropriate. Also significant in this comparison is that small, local earthquakes are typically void of low frequency content, therefore PSD results at lower frequencies may be more a sample of the random background noise at that moment than that of the earthquake itself.

The data representing select earthquakes were analyzed in the frequency domain and instrument corrected utilizing the nominal response models and sensitivities as provided by RPKromer Consulting. The deviation of the amplitude response of the sensors under test from the reference

sensors' sensitivity at 10 Hz is noted and used to calculate a unique sensitivity of each component of every sensor under test.

Table 6 Nanometrics OBS Sensitivities at 10 Hz

Sensor	Vertical		North		East	
	Sensitivity (V*s/m)	Difference from nominal	Sensitivity (V*s/m)	Difference from nominal	Sensitivity (V*s/m)	Difference from nominal
3125	752.1	0.277% (0.012 dB)	748.8	-0.162% (-0.007 dB)	751.6	0.212% (0.009 dB)
3126	747.1	-0.384% (-0.017 dB)	748.4	-0.213% (-0.009 dB)	747.0	-0.397% (-0.017 dB)
3127	750.5	0.063% (0.003 dB)	751.5	0.200% (0.009 dB)	758.7	1.166% (0.050 dB)
3128	748.8	-0.157% (-0.007 dB)	750.5	0.067% (0.003 dB)	750.1	0.017% (0.001 dB)
3129	747.3	-0.355% (-0.015 dB)	753.0	0.403% (0.017 dB)	756.2	0.828% (0.036 dB)
3130	754.3	0.569% (0.025 dB)	753.4	0.456% (0.020 dB)	754.6	0.614% (0.027 dB)
3131	741.7	-1.104% (-0.048 dB)	740.1	-1.318% (-0.058 dB)	742.4	-1.017%(-0.044 dB)
3132	750.7	0.092% (0.004 dB)	756.0	0.796% (0.034 dB)	750.5	0.066% (0.003 dB)
3133	751.8	0.238% (0.010 dB)	760.2	1.365% (0.059 dB)	757.5	0.996% (0.043 dB)
3134	752.1	0.275% (0.012 dB)	752.1	0.276% (0.012 dB)	754.6	0.620% (0.027 dB)
3135	747.0	-0.399% (-0.017 dB)	752.7	0.362% (0.016 dB)	755.7	0.763% (0.033 dB)
3136	740.9	-1.208% (-0.053 dB)	757.2	0.961% (0.042 dB)	751.4	0.192% (0.008 dB)
3137	746.7	-0.442% (-0.019 dB)	755.2	0.697% (0.030 dB)	750.2	0.030% (0.001 dB)
3138	740.6	-1.252% (-0.055 dB)	747.4	-0.344% (-0.015 dB)	742.3	-1.031% (-0.045 dB)
3139	742.6	-0.986% (-0.043 dB)	752.1	0.274% (0.012 dB)	747.1	-0.380% (-0.017 dB)
3140	752.6	0.349% (0.015 dB)	754.2	0.562% (0.024 dB)	754.4	0.581% (0.025 dB)
3141	747.9	-0.285% (-0.012 dB)	754.4	0.588% (0.025 dB)	747.4	-0.350% (-0.015 dB)
3142	751.7	0.221% (0.010 dB)	768.3	2.447% (0.105 dB)	758.6	1.152% (0.050 dB)

Table 7 Navy OBS Sensitivities at 10 Hz

Sensor	Vertical		North		East	
	Sensitivity (V*s/m)	Difference from nominal	Sensitivity (V*s/m)	Difference from nominal	Sensitivity (V*s/m)	Difference from nominal
81	1030.0	-1.91% (-0.08 dB)	1080.6	2.91% (0.12 dB)	1019.8	-2.88% (-0.13 dB)
82	882.4	-16.0% (-0.76 dB)	1054.1	0.39% (0.02 dB)	1036.4	-1.30% (-0.06 dB)
83	1005.6	-4.23% (-0.19 dB)	1092.0	4.00% (0.17 dB)	1025.4	-2.34% (-0.10 dB)
84	1004.1	-4.38% (-0.19 dB)	997.5	-5.00% (-0.22 dB)	1004.4	-4.34% (-0.19 dB)
85	1027.0	-2.20% (-0.10 dB)	1066.5	1.57% (0.07 dB)	1000.6	-4.71% (-0.21 dB)
86	959.7	-8.60% (-0.39 dB)	984.8	-6.21% (-0.28 dB)	1021.1	-2.75% (-0.12 dB)
87	1025.2	-2.36% (-0.10 dB)	1064.5	1.38% (0.06 dB)	1053.0	0.28% (0.01 dB)
88	974.0	-7.24% (-0.33 dB)	1065.5	1.48% (0.06 dB)	1009.9	-3.82% (-0.17 dB)
89	1010.1	-3.80% (-0.17 dB)	1073.3	2.22% (0.10 dB)	1060.2	0.97% (0.04 dB)
90	1010.5	-3.76% (-0.17 dB)	1077.9	2.66% (0.11 dB)	1037.0	-1.23% (-0.05 dB)
91	1015.5	-3.29% (-0.15 dB)	1076.7	2.54% (0.11 dB)	1029.8	-1.93% (-0.08 dB)
92	944.6	-10.0% (-0.46 dB)	1095.5	4.33% (0.18 dB)	949.8	-9.54% (-0.44 dB)
93	1012.9	-3.53% (-0.16 dB)	1064.2	1.35% (0.06 dB)	1005.3	-4.26% (-0.19 dB)
94	1018.7	-2.98% (-0.13 dB)	1081.8	3.03% (0.13 dB)	954.3	-9.11% (-0.41 dB)
95	1181.8	12.6% (0.51 dB)	1085.3	3.36% (0.14 dB)	1034.2	-1.50% (-0.07 dB)
96	1097.0	4.48% (0.19 dB)	1050.8	0.078% (0.00 dB)	959.1	-8.66% (-0.39 dB)
97	1025.7	-2.32% (-0.10 dB)	1018.0	-3.05% (-0.13 dB)	1014.6	-3.37% (-0.15 dB)
98	1072.6	2.15% (0.09 dB)	1068.9	1.80% (0.08 dB)	1072.7	2.17% (0.09 dB)

The sensitivities of the Navy OBS varied significantly more than the broadband sensor values, as much as 16% of the nominal value of 1050 V*s/m; the Nanometrics sensors remained tightly clustered around the nominal value of 750 V*s/m, varying no more than 2.45%.

For the Response Verification portion of the test, these data were further analyzed in the frequency domain with the reference sensors' instrument response removed from its data and the data from sensors under test with the appropriate calculated sensitivities applied. For an ideal sensor, the deviation of the sensor under test from the reference sensor, in magnitude and phase, would be 0 dB and 0°, respectively. Provided in this section are refined response curves of magnitude and phase generated by comparison on the sensors' response compared to that of the reference sensor while recording a local earthquake.

The data from the reference sensors and the sensors under test were corrected for their respective instrument response models, scaling the records to velocity (m/s) and correcting for amplitude and phase. If all of the instrument response models perfectly represent the reference sensor and the sensors under test, then the plots of relative magnitude and phase should be perfectly flat lines at 0 dB and 0 degrees, respectively. The extents to which the relative magnitude and phase are zero represent how consistent the sensors are with their responses and serves to validate the pass band of the sensor.

The coherence was computed using the technique described by Holcomb (1989) under the distributed noise model assumption. The spectra (power spectral density estimates or PSDs) were computed using block-by-block DC removal, Hann windowing, 1024-2048 sample FFT lengths and 5/8 window overlap.

The requirement to characterize the Nanometrics sensors' response to frequencies as low as 0.01 Hz could not be met by analysis of local earthquakes alone. A review of teleseisms during the testing periods yielded teleseisms which had sufficient energy to characterize the sensors with a high degree of confidence to frequencies approaching, and sometimes falling below 0.01 Hz.

Note that the plots of amplitude response shown have units of dB relative to signal power $(V/m/s)^2$, and not amplitude, V/m/s. Therefore, the dB values should be reduced by a factor of 2 in order to convert them to be relative to amplitude.

Presented here are two sets of coherence, relative magnitude and phase plots, for each group of sensors under test. The first group of plots is based upon the analysis of data from a local event as the local events provided data with sufficiently high coherence to allow comment at frequencies typically above 0.5 Hz. The second group of coherence, relative magnitude and phase plots are based upon the analysis of teleseisms, which exhibited sufficiently high coherence at the low frequencies, typically from 0.5 Hz and below.

3.1.3.1 Nanometrics OBS 3125, 3126 and 3131

Figure 23 Coherence between the broadband reference sensor and sensors under test, local earthquake source: Vertical (top), North (middle) and East (bottom).

Coherence between the reference sensor and sensors under test is excellent (at least 0.995 gamma^2) between 0.2 Hz and 25 Hz on all components and is sufficient between the sensors under test and the reference sensor to be able to comment on the relative magnitude and phase response over this frequency range.

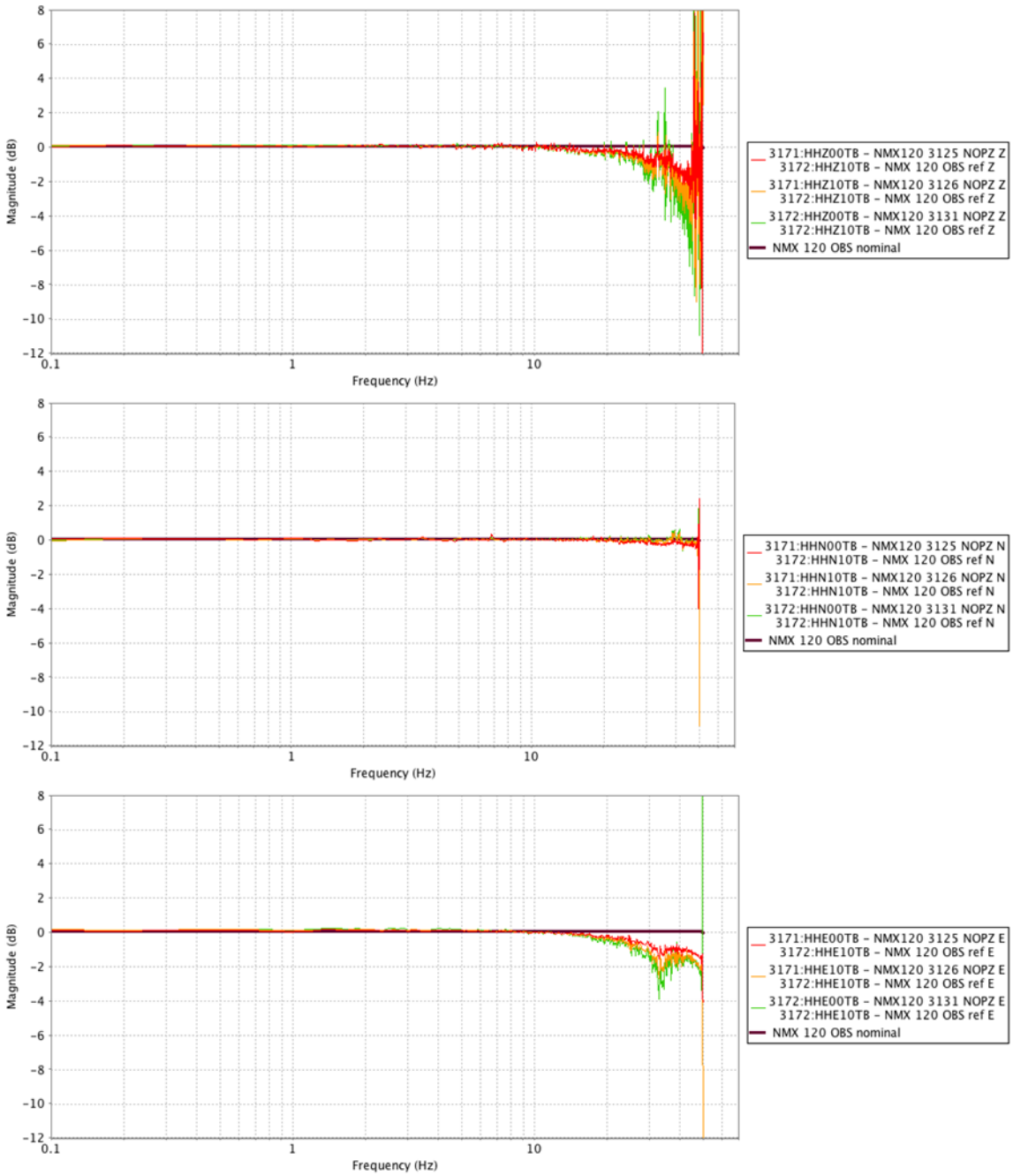

Figure 24 Broadband sensor magnitude response comparisons, local earthquake source, between the reference sensor and sensors under test: Vertical (top), North (middle) and East (bottom).

Relative magnitudes of the north components are relatively flat over the frequency range for all sensors, from 0.1 Hz through 35 Hz. The vertical and east components, however, exhibit a slight roll-off at frequencies above 20-25 Hz, most noteworthy on the sensors 3131 and 3126 vertical and east components. Recall coherence values of the vertical and east components begin to decrease above 25 Hz (Figure 23), perhaps requiring caution regarding the use of the relative magnitudes provided above 25 Hz.

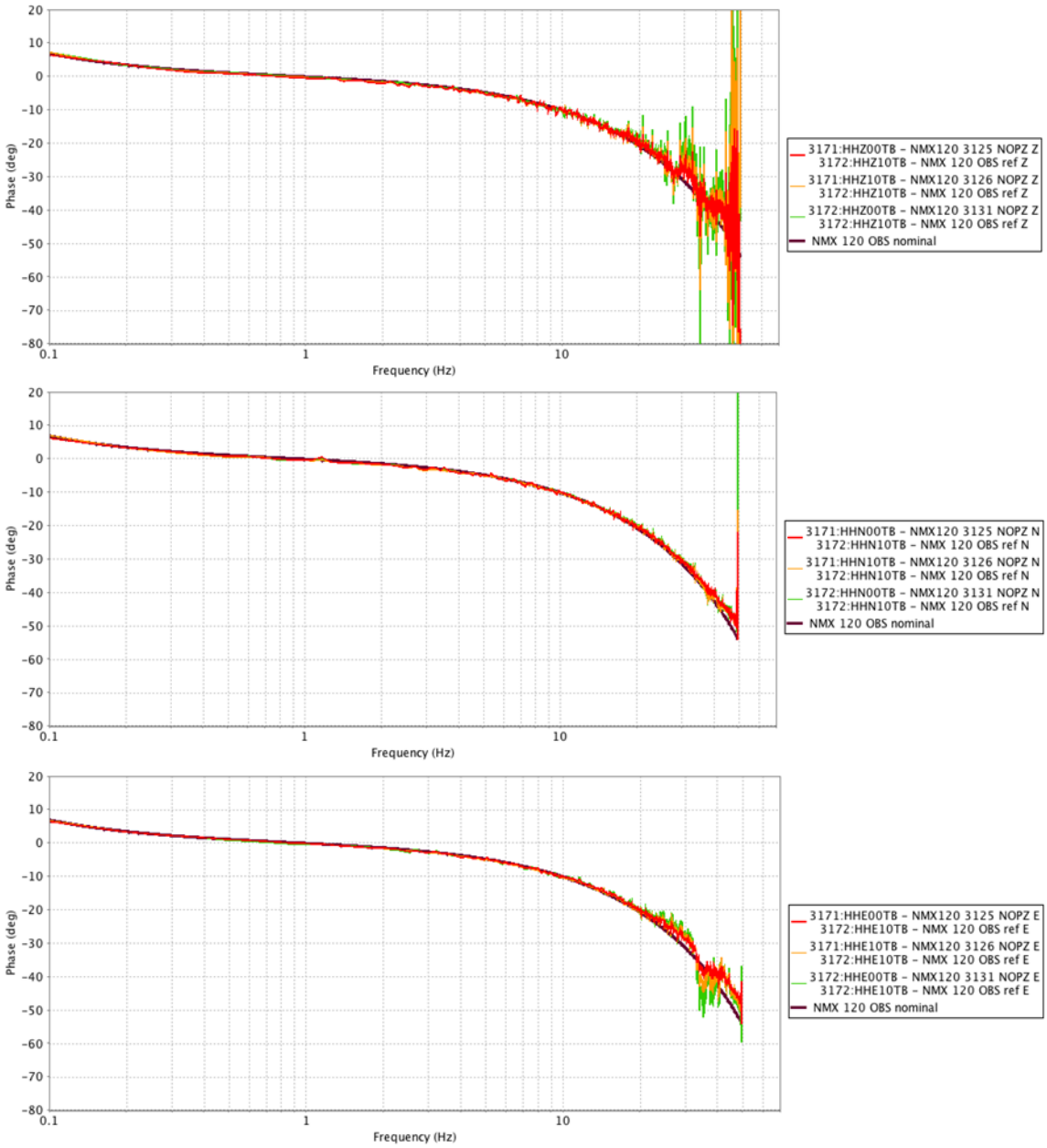

Figure 25 Broadband sensor phase response comparisons, local earthquake source, between the reference sensor and sensors under test: Vertical (top), North (middle) and East (bottom).

Across components and sensors phases are within the 5° maximum of the nominal phase response, as specified in Table 1 SHDAS Seismometer Requirements, over the frequency band with highest coherence 0.2 Hz to 25 Hz. The north components in particular are within the specification for phases up to frequencies approaching the Nyquist.

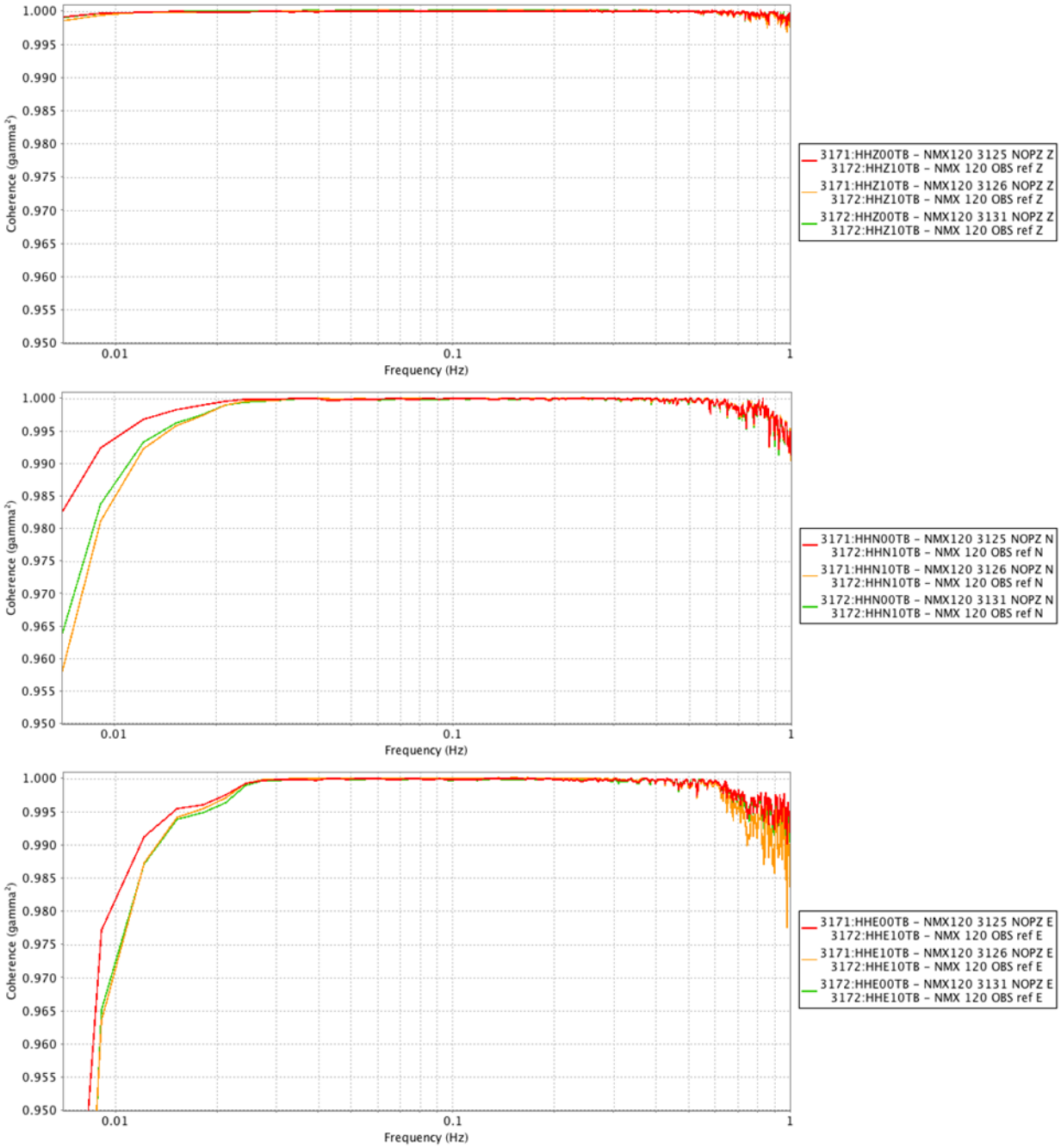

Figure 26 Coherence between the broadband reference sensor and sensors under test, tele-seismic source: Vertical (top), North (middle) and East (bottom).

Coherence between the reference sensor and sensors under test is excellent (at least 0.995 gamma^2) between 0.02 Hz and 0.6 Hz on the horizontal components and even over a broader range, below 0.01 Hz to above 1 Hz, for the vertical component and is sufficient between the sensors under test and the reference sensor to be able to comment on the relative magnitude and phase response over these frequency ranges.

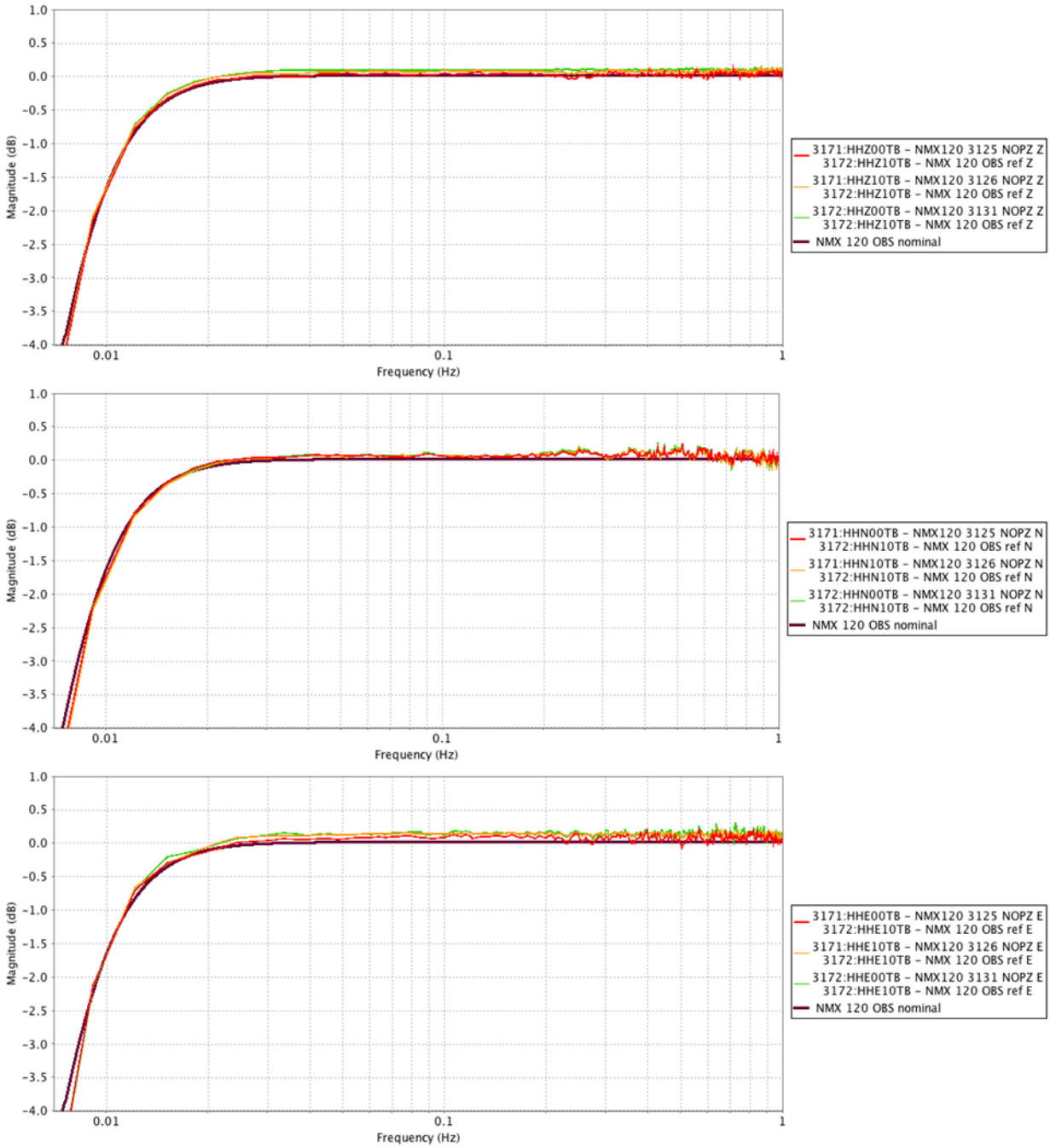

Figure 27 Broadband sensor magnitude response comparisons, tele-seismic source, between the reference sensor and sensors under test: Vertical (top), North (middle) and East (bottom).

Relative magnitudes of all components are in good agreement with the nominal response of the sensor, from 0.01 Hz through 1 Hz. While the agreement is excellent as the frequency approaches the corner, recall the coherence decreased at and below 0.02 Hz on the horizontal components. While the same is true near 1 Hz, the coherence utilizing a local earthquake source, Figure 23, allows use of its analysis and response comparisons down to 0.5 Hz.

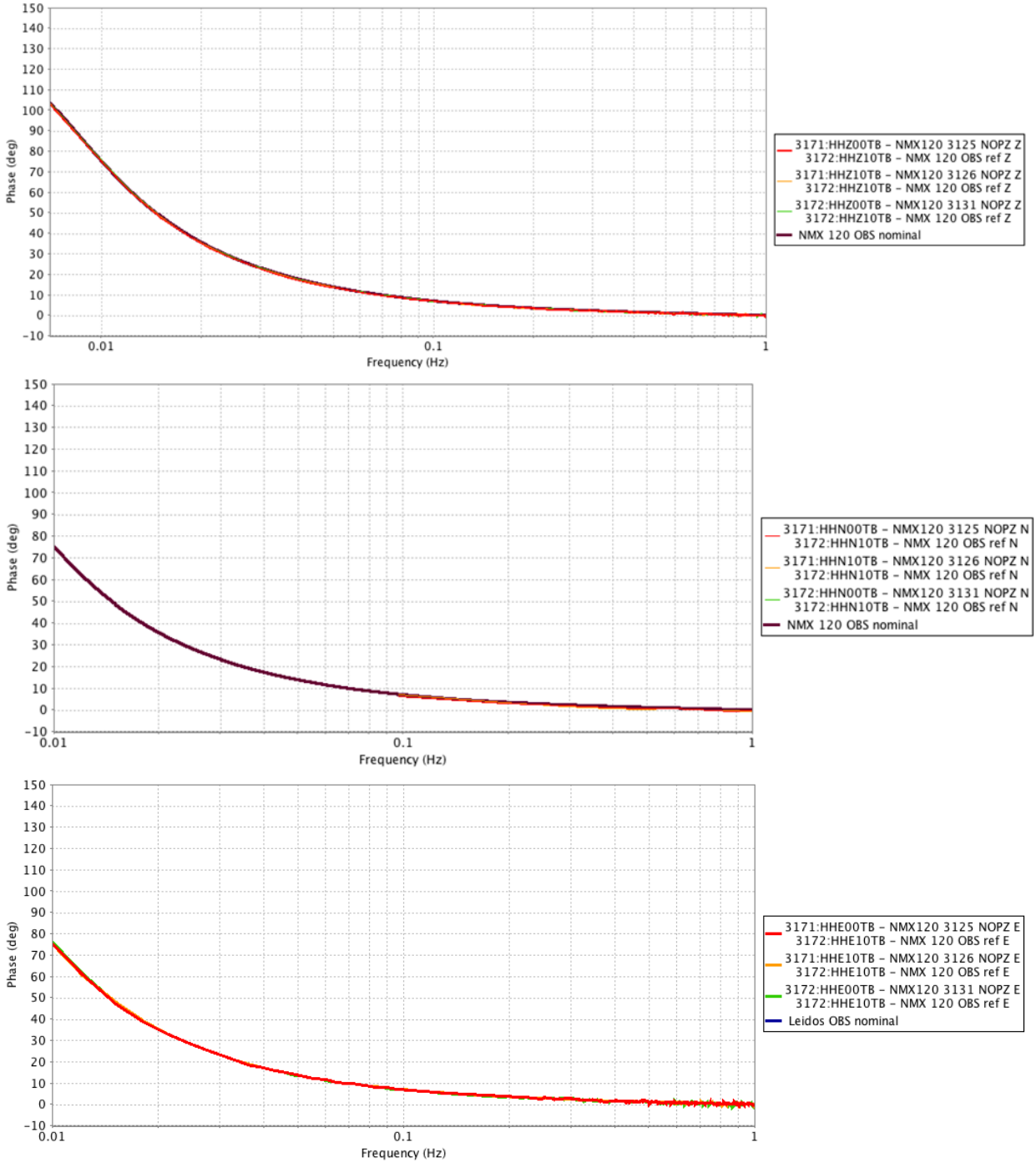

Figure 28 Broadband phase response comparisons, tele-seismic source, between the reference sensor and sensors under test: Vertical (top), North (middle) and East (bottom).

As with the relative magnitude analysis utilizing a teleseism, the relative phase response of all components is in good agreement with the nominal response of the sensor, from 0.01 Hz through 1 Hz. While the agreement is excellent as the frequency approaches the corner, recall the coherence decreased at and below 0.02 Hz on the horizontal components. While the same is true near 1 Hz, the coherence utilizing a local earthquake source, Figure 23, allows use of its analysis and response comparisons down to 0.5 Hz.

3.1.3.2 Nanometrics OBS 3134, 3137 and 3138

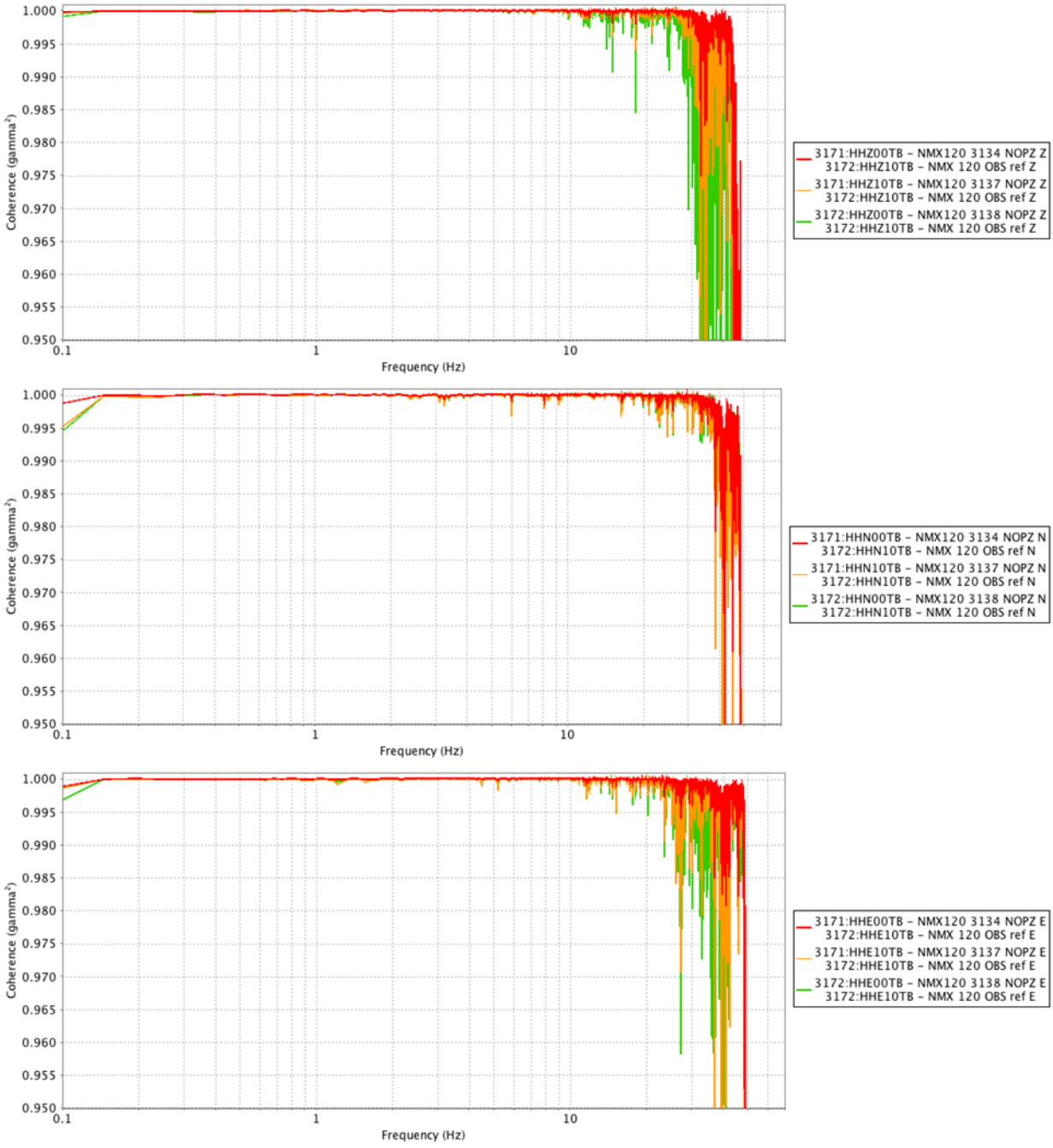

Figure 29 Coherence between the broadband reference sensor and sensors under test, local earthquake source: Vertical (top), North (middle) and East (bottom).

Coherence between the reference sensor and sensors under test is excellent (at least 0.995 gamma^2) between 0.1 Hz and 25 Hz on all components (perhaps even higher on the north components) and is sufficient between the sensors under test and the reference sensor to be able to comment on the relative magnitude and phase response over this frequency range.

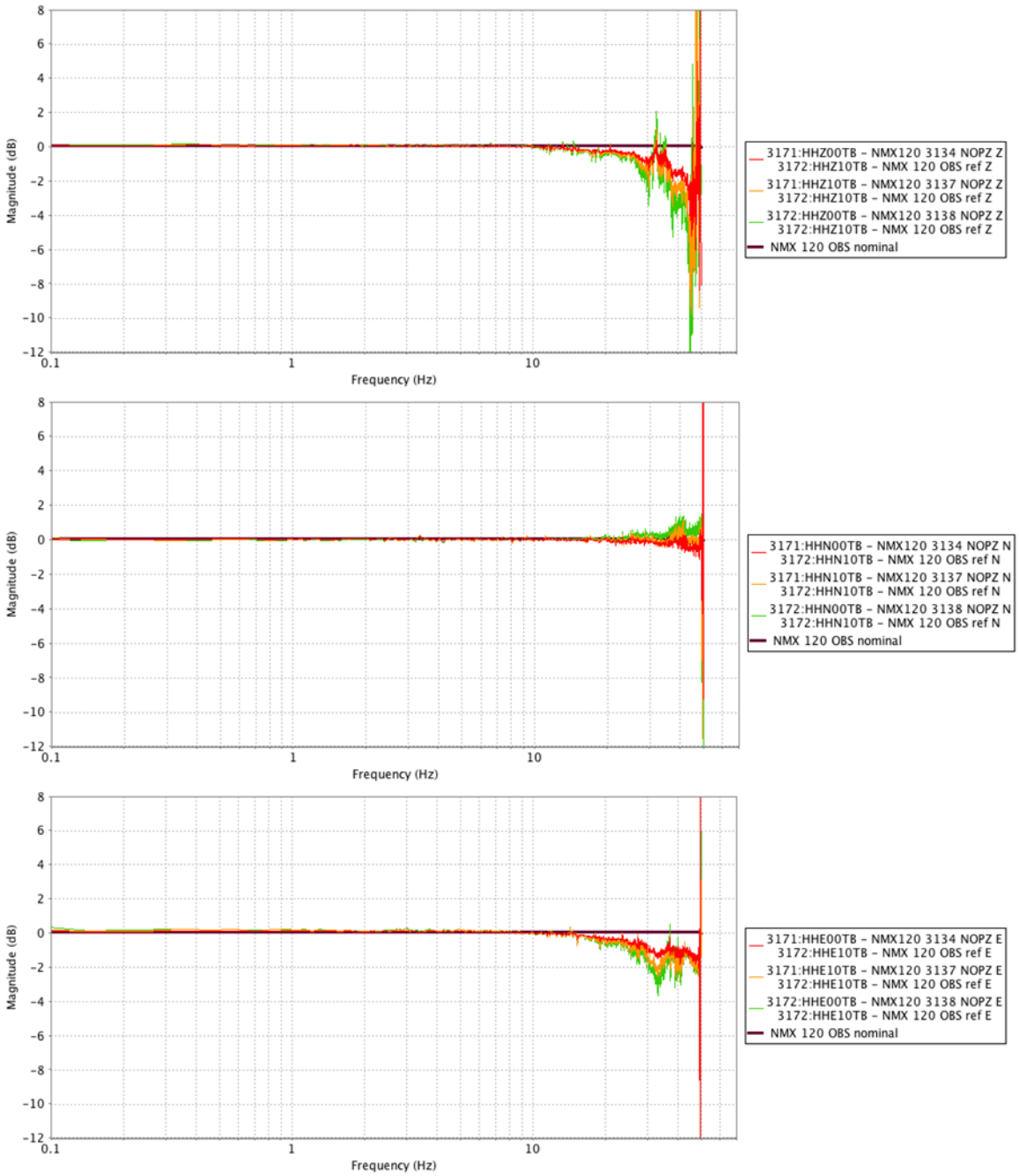

Figure 30 Broadband sensor magnitude response comparisons, local earthquake source, between the reference sensor and sensors under test: Vertical (top), North (middle) and East (bottom).

Relative magnitudes of the north components are relatively flat over the widest frequency range; for sensor 3137 up to 22 Hz. The vertical and east components, however, exhibit a slight roll-off at frequencies above 11 to 13 Hz, sensors 3134 having the least amount of roll-off on both the Vertical and East. Note however, all of the East components are at or above the 0.1 dB deviation limit desired. Coherence over this range is excellent from 0.1 Hz to about 23 Hz allowing one to have high confidence in the measurement.

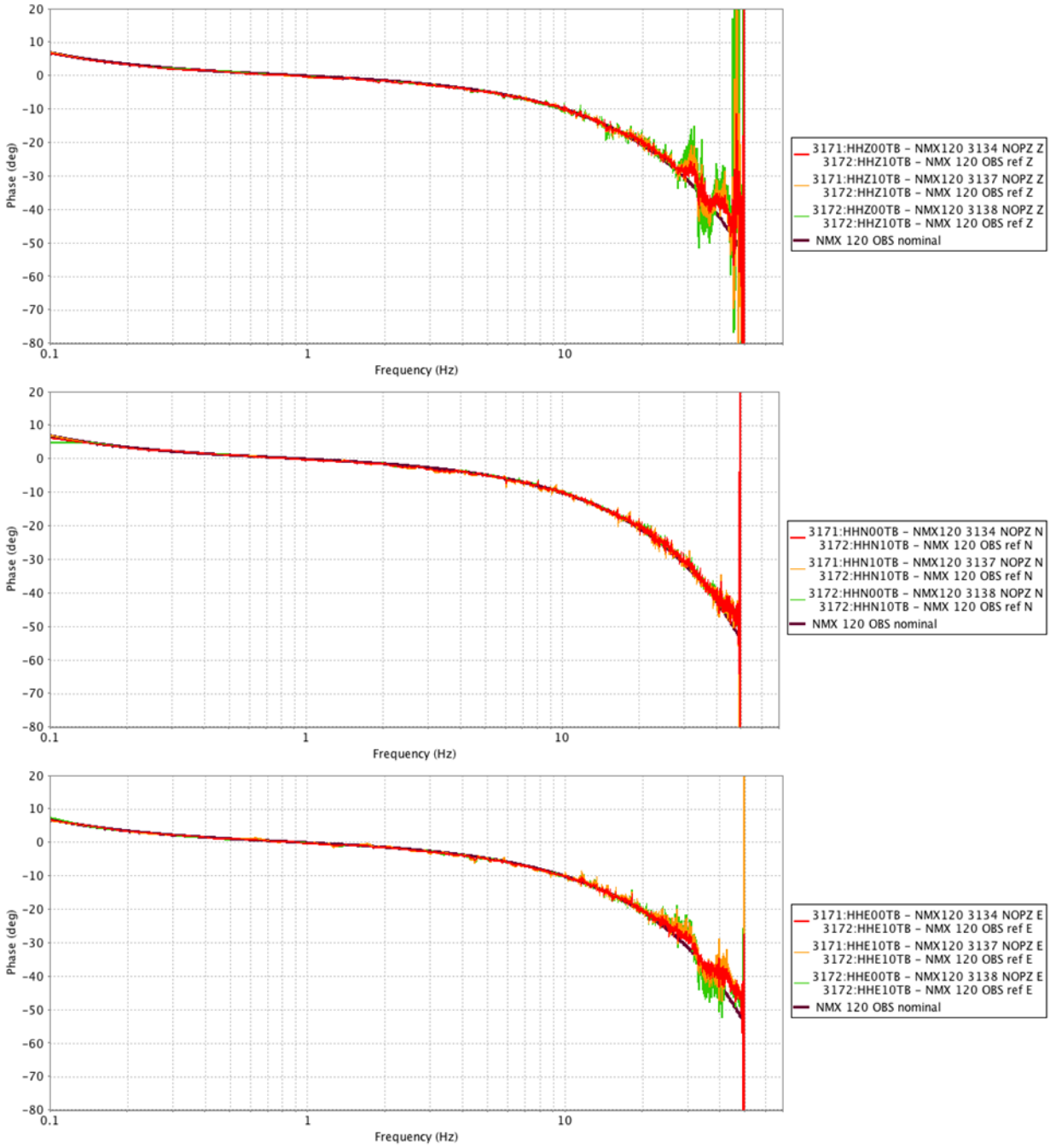

Figure 31 Broadband sensor phase response comparisons, local earthquake source, between the reference sensor and sensors under test: Vertical (top), North (middle) and East (bottom).

Across components and sensors, phases are within the 5° maximum of the nominal phase response, as specified in Table 1 SHDAS Seismometer Requirements, over the frequency band with highest coherence 0.2 Hz to 25 Hz. The north components in particular are within the specification for phase up to frequencies approaching the Nyquist. The phase deviations on the Vertical and East components occur over frequency ranges (in the 25 Hz to 50 Hz) over which the respective components exhibit reduced coherence, however this is also the range over which coherence decreases.

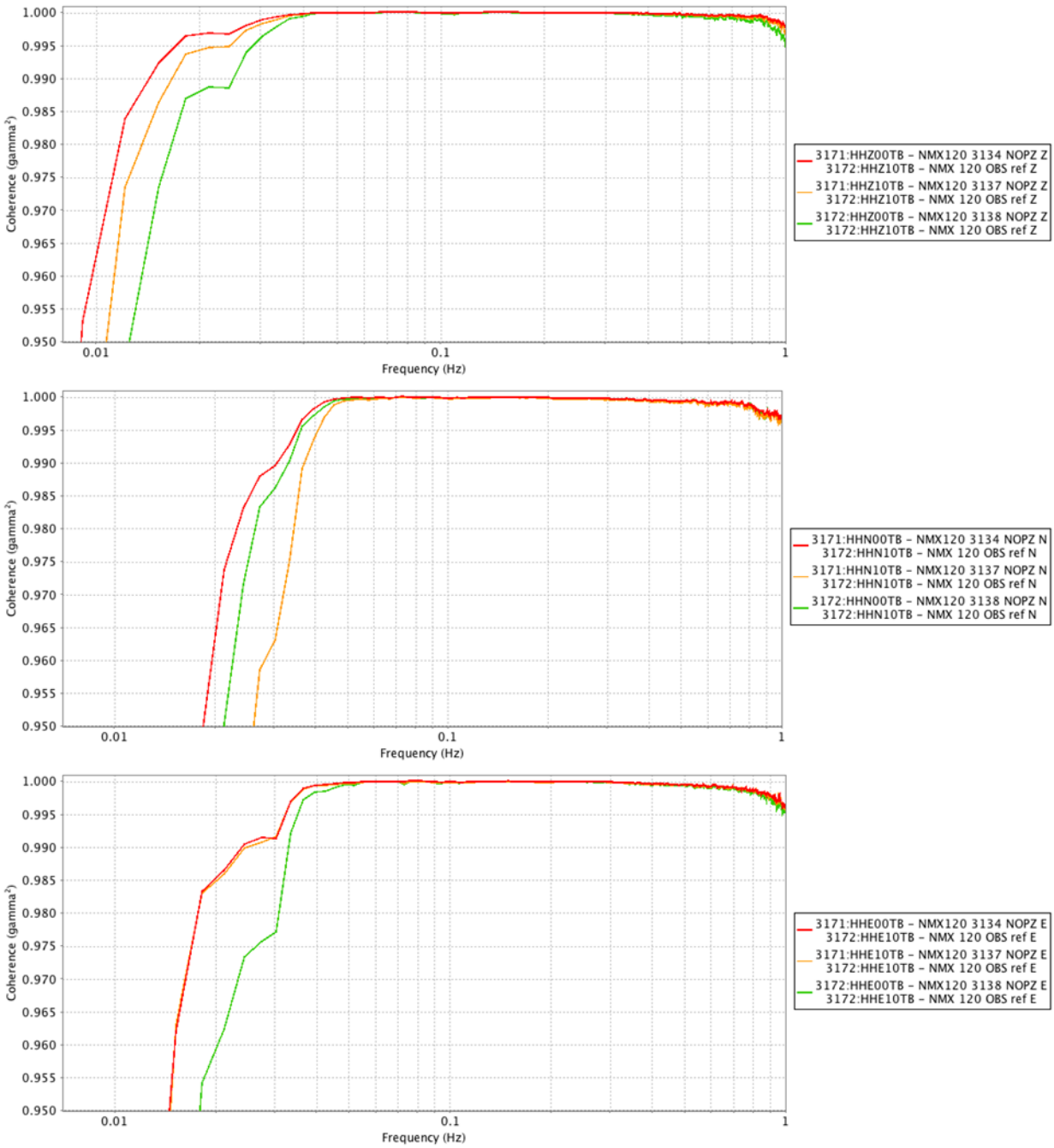

Figure 32 Coherence between the broadband reference sensor and sensors under test, tele-seismic source: Vertical (top), North (middle) and East (bottom).

Coherence between the reference sensor and sensors under test is excellent (at least 0.995 gamma^2) on the horizontal components to as low as 0.03 Hz to 0.04 Hz and even over a broader range, to frequencies as low as 0.02 Hz 0.03 Hz, for the vertical components and is sufficient between the sensors under test and the reference sensor to be able to comment on the relative magnitude and phase response over these frequency ranges.

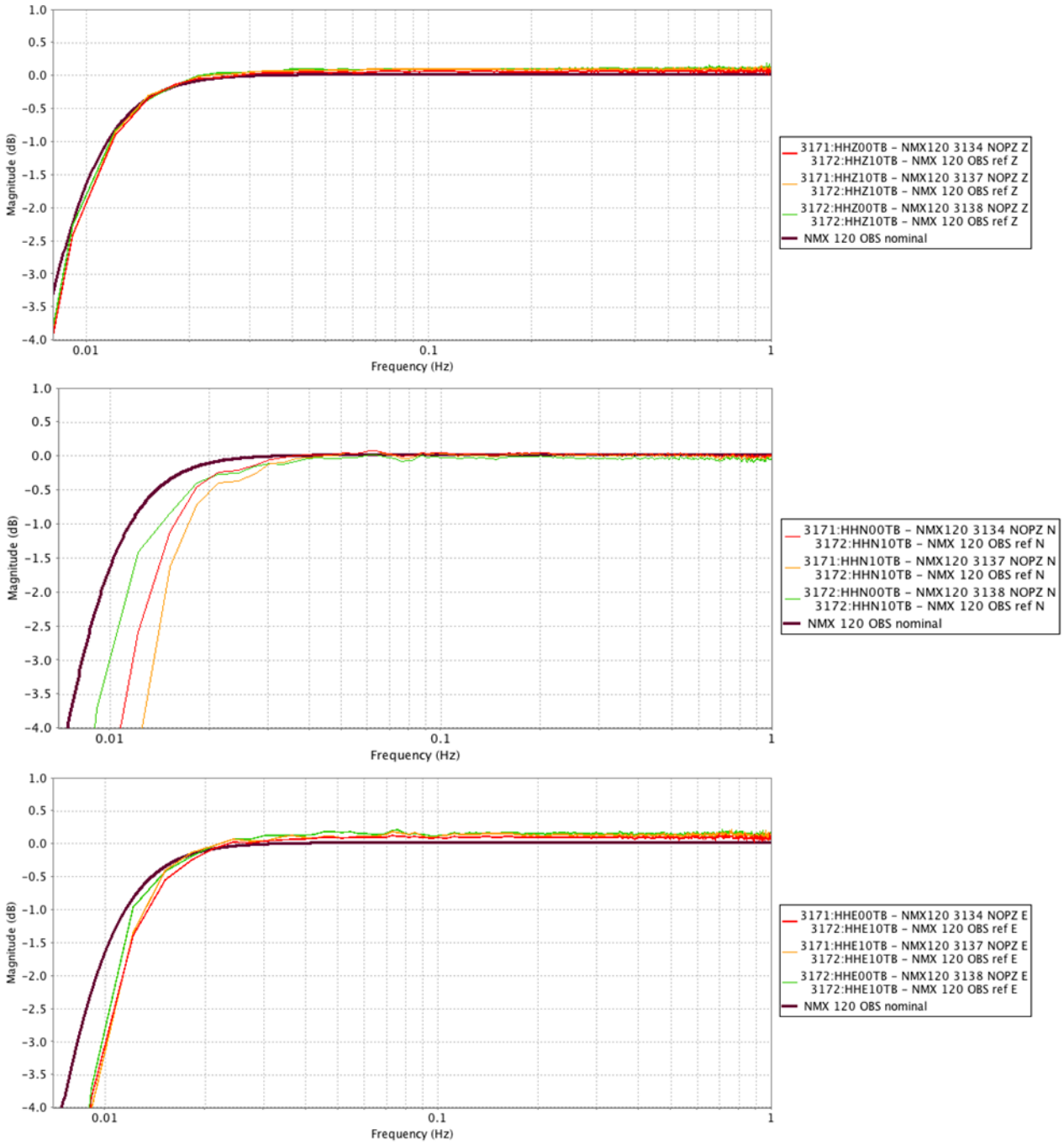

Figure 33 Broadband sensor magnitude response comparisons, tele-seismic source, between the reference sensor and sensors under test: Vertical (top), North (middle) and East (bottom).

Relative magnitudes of the vertical components are in good agreement with the nominal response of the sensor, from 0.01 Hz through 1 Hz, however the horizontal components both exhibit a higher frequency roll-off than the nominal response (the north more so than the east components). Recall though the coherence of the horizontal components drops off at a higher frequency than the vertical. The east components, perhaps sensor 3138 more than the others, exceed the desired criterion of 0.1 dB deviation in magnitude, similar to results at higher frequencies found with the analysis of a local earthquake.

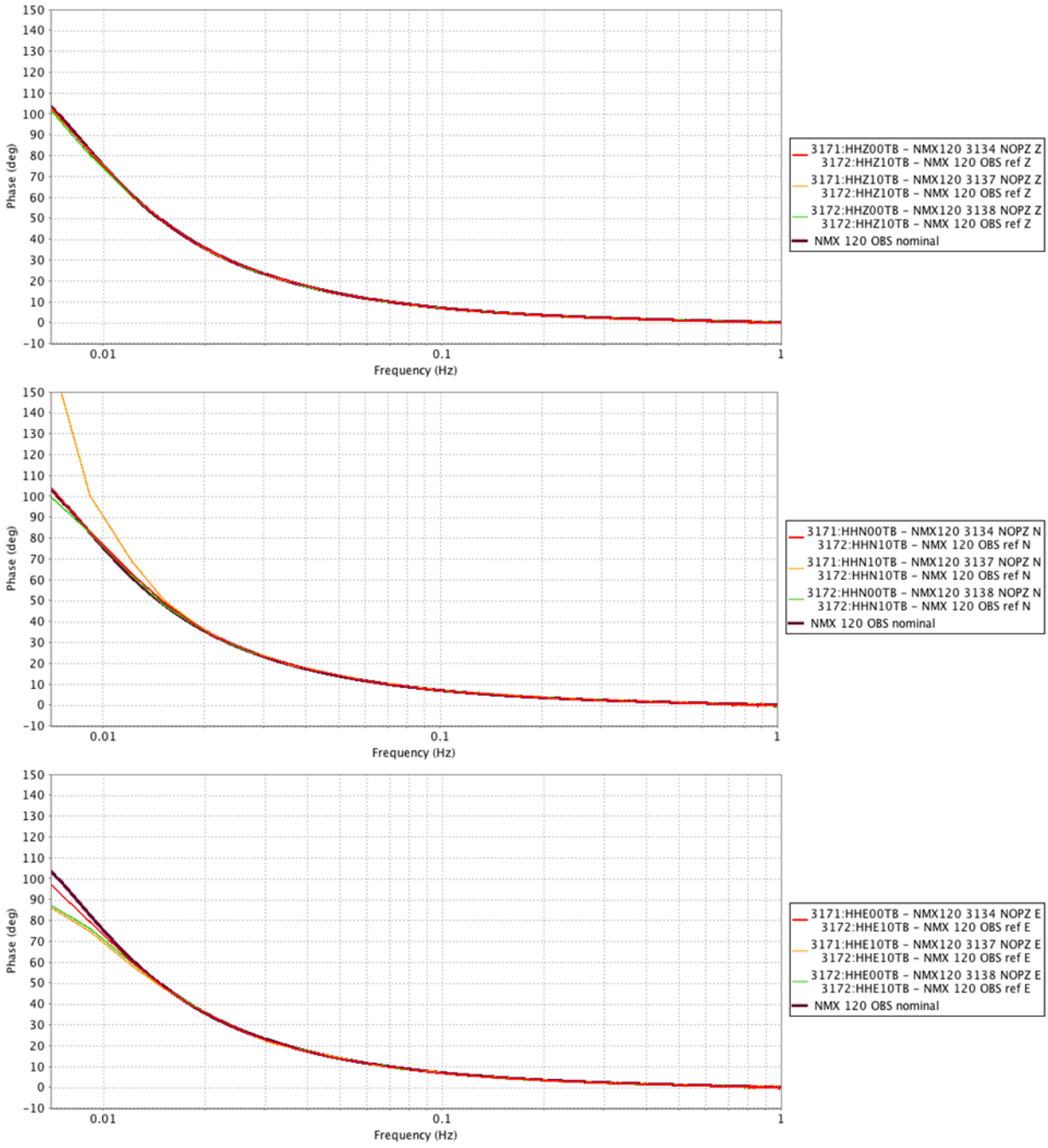

Figure 34 Broadband phase response comparisons, tele-seismic source, between the reference sensor and sensors under test: Vertical (top), North (middle) and East (bottom).

The relative phase response of all components are in good agreement with the nominal response of the sensor, in the frequency bands over which there is coherence; e.g. the deviations in phase of the horizontal components below 0.02 Hz should be viewed with caution.

3.1.3.3 Nanometrics OBS 3130, 3132 and 3139

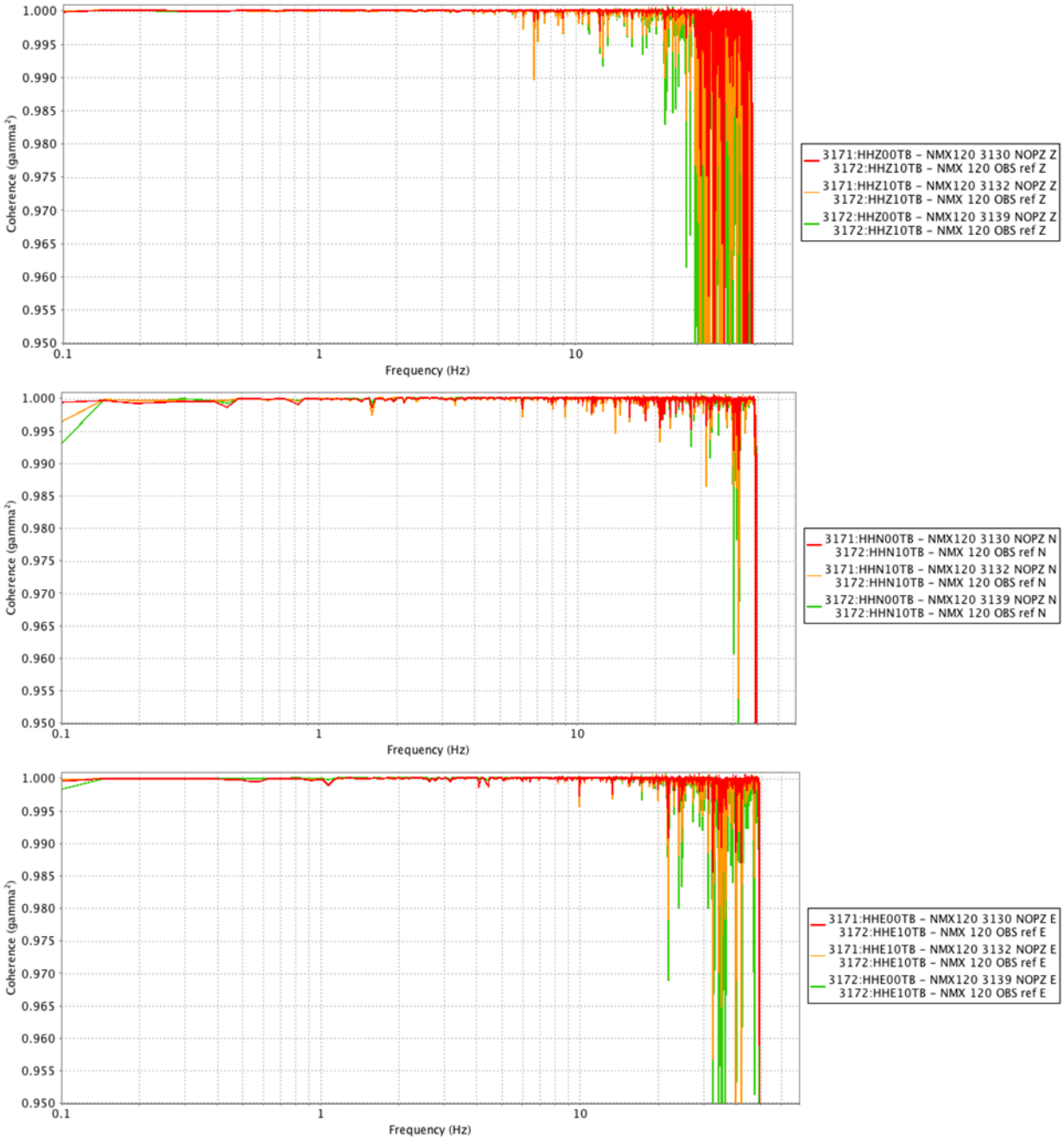

Figure 35 Coherence between the broadband reference sensor and sensors, local earthquake source, under test with a local earthquake source: Vertical (top), North (middle) and East (bottom).

Coherence between the reference sensor and sensors under test is excellent (at least 0.995 gamma^2) between 0.1 Hz and 30 Hz on all components (even higher frequencies on the north components – 40 Hz). Generally, sensor 3130 has best coherence at the highest frequencies, in particular on the horizontal components. Coherence levels are sufficient between the sensors under test and the reference sensor to be able to comment on the relative magnitude and phase response over these frequency ranges.

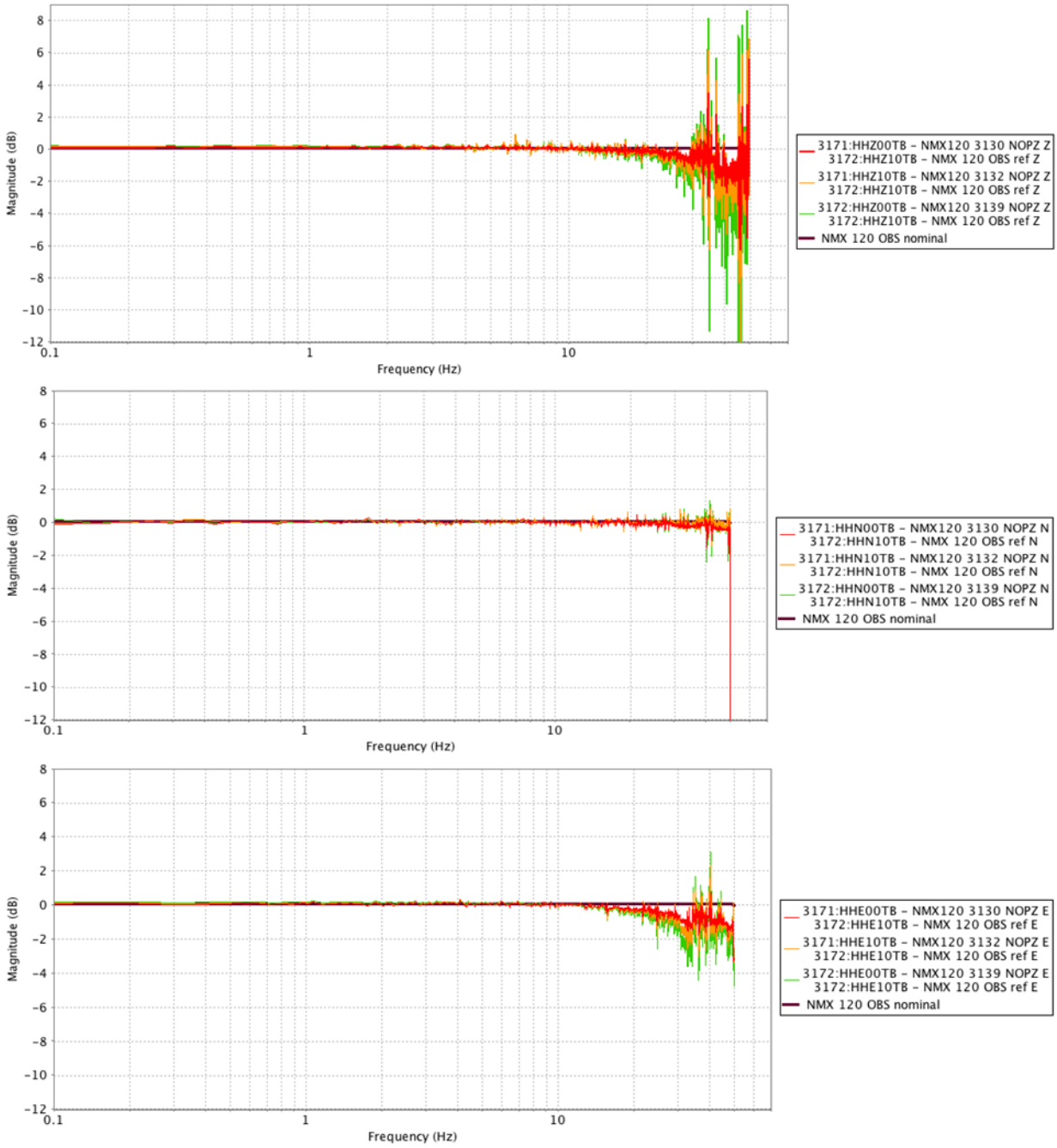

Figure 36 Broadband sensor magnitude response comparisons, local earthquake source, between the reference sensor and sensors under test: Vertical (top), North (middle) and East (bottom).

Relative magnitudes of the vertical components are relatively flat over the widest frequency, 0.1 Hz to 10 Hz; the largest divergence in magnitude response also corresponds to the frequencies with lower coherence. The vertical and east components of sensors 3139 have consistent deviations from the ideal response over a wide frequency band; its vertical and east components are at or near 0.1 dB above or 0.1 to 0.2 dB above, respectively.

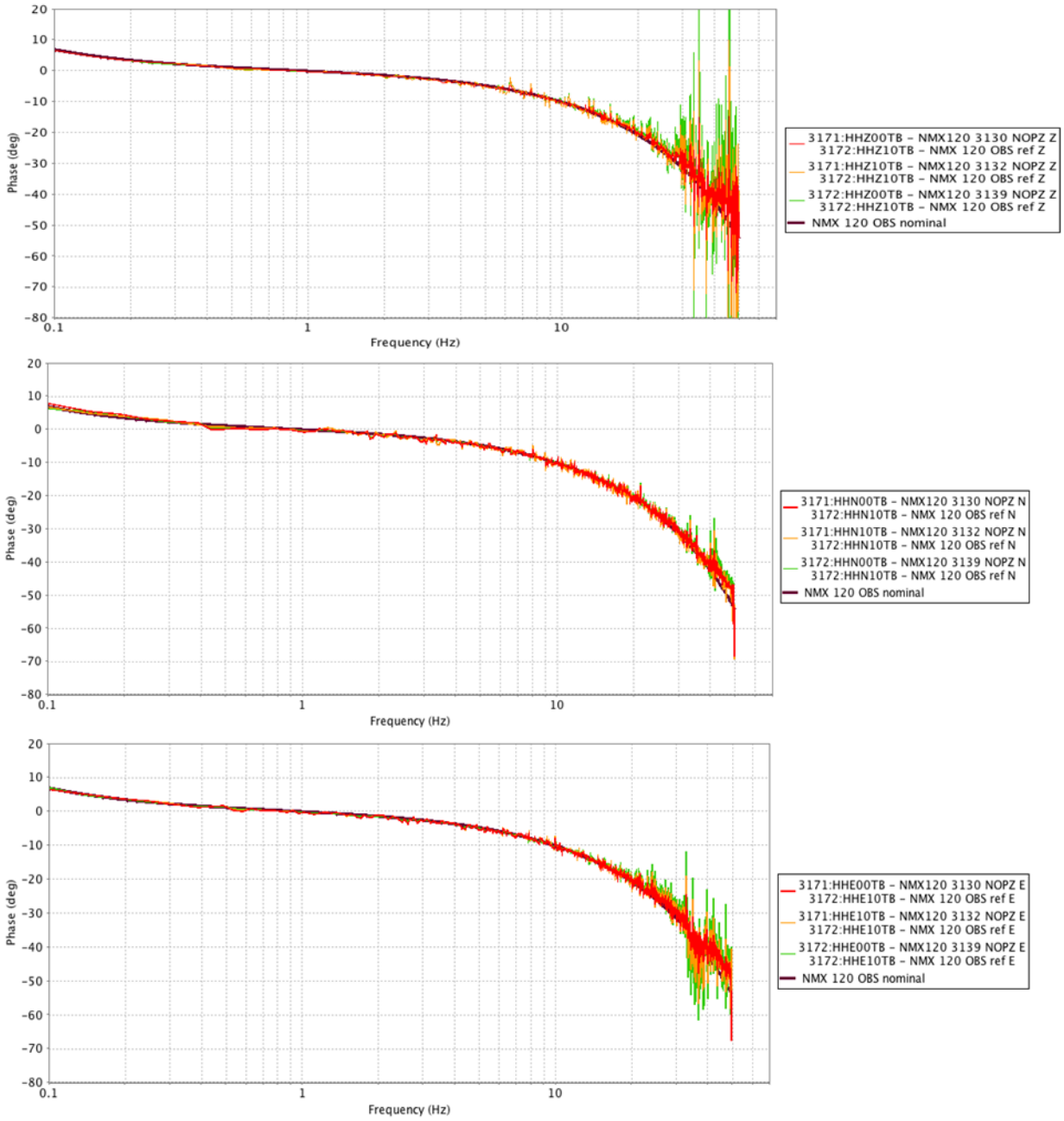

Figure 37 Broadband sensor phase response comparisons, local earthquake source, between the reference sensor and sensors under test: Vertical (top), North (middle) and East (bottom).

Across components and sensor phases are within the 5° maximum of the nominal phase response, as specified in Table 1 SHDAS Seismometer Requirements, over the frequency band with highest coherence.

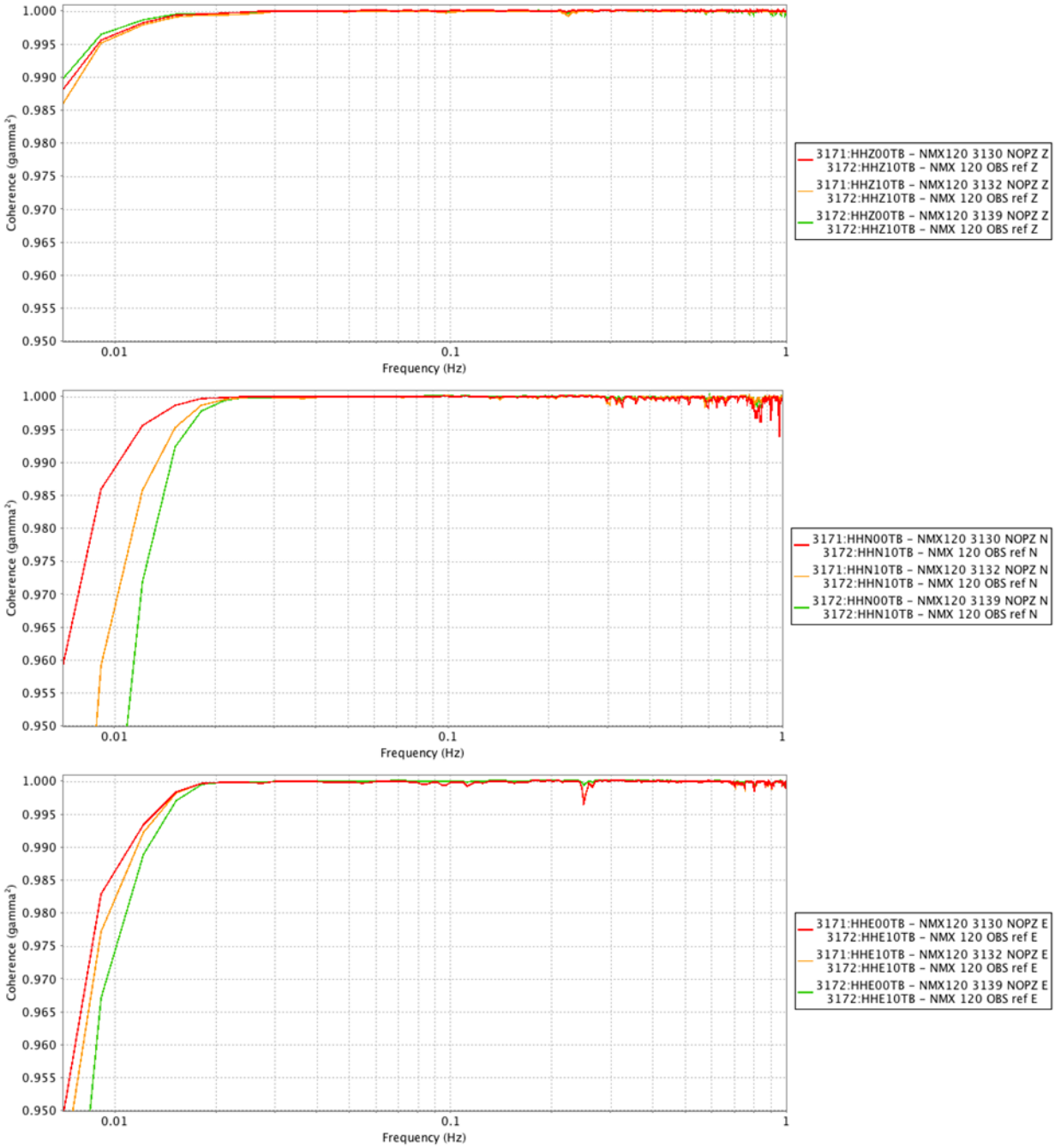

Figure 38 Coherence between the broadband reference sensor and sensors under test, tele-seismic source: Vertical (top), North (middle) and East (bottom).

Coherence between the reference sensor and sensors under test is excellent (at least 0.995 gamma^2) on the vertical to below 0.01 Hz; horizontal components to as low as 0.012 Hz to 0.018 Hz on the North to 0.015 Hz on the East, and is sufficient between the sensors under test and the reference sensor to be able to comment on the relative magnitude and phase response to frequencies as low as mentioned here.

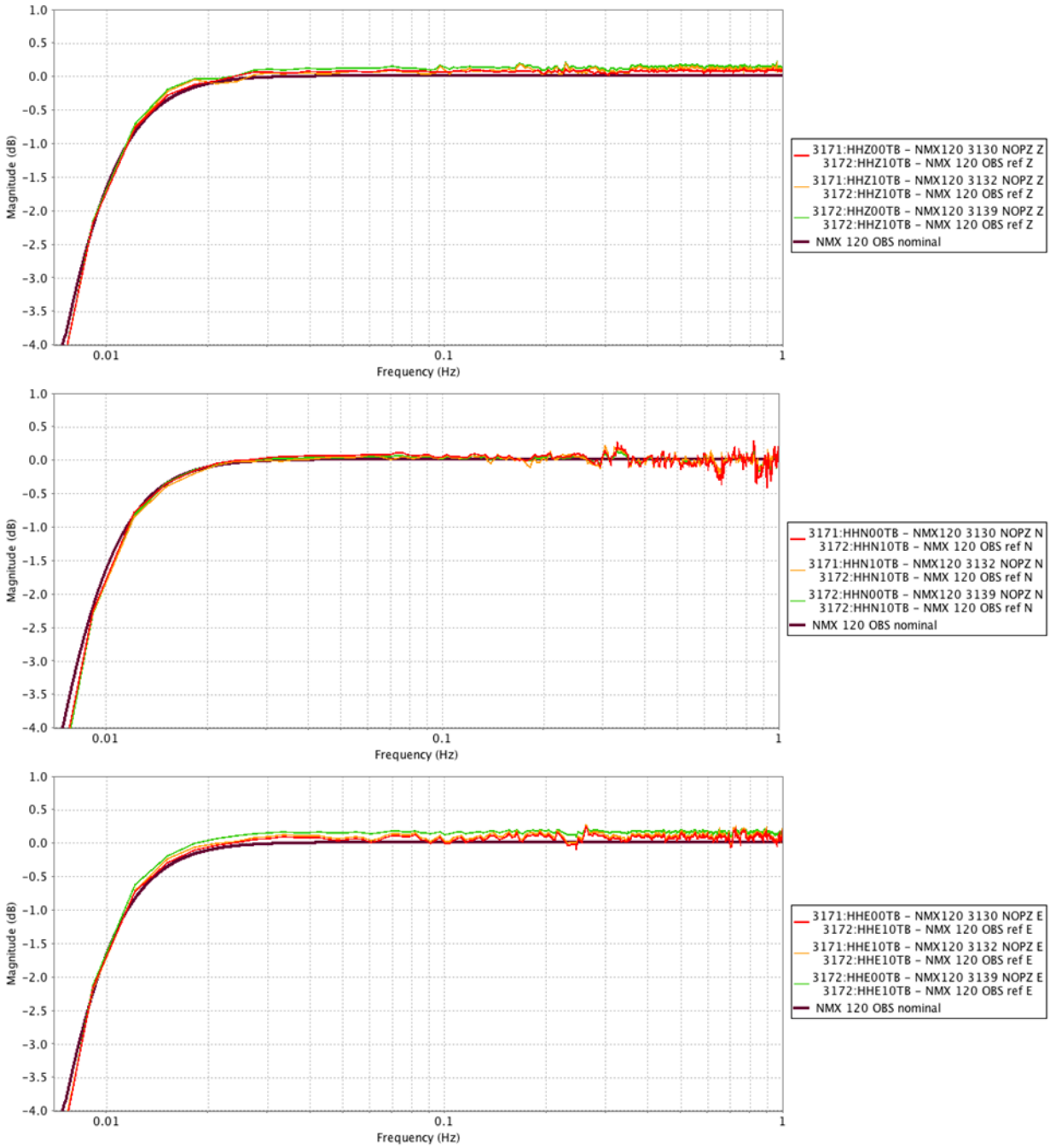

Figure 39 Broadband sensor magnitude response comparisons, tele-seismic source, between the reference sensor and sensors under test: Vertical (top), North (middle) and East (bottom).

Similar to the relative magnitudes values found at higher frequencies, from a local earthquake source, vertical and east components of all three sensors show the largest deviations (=> 0.1 dB) from an ideal response, in particular the east component of sensor 3139. There is good agreement at the lowest frequencies of the vertical and north components and east components of 3130 and 3132, despite their respective coherence levels dropping off.

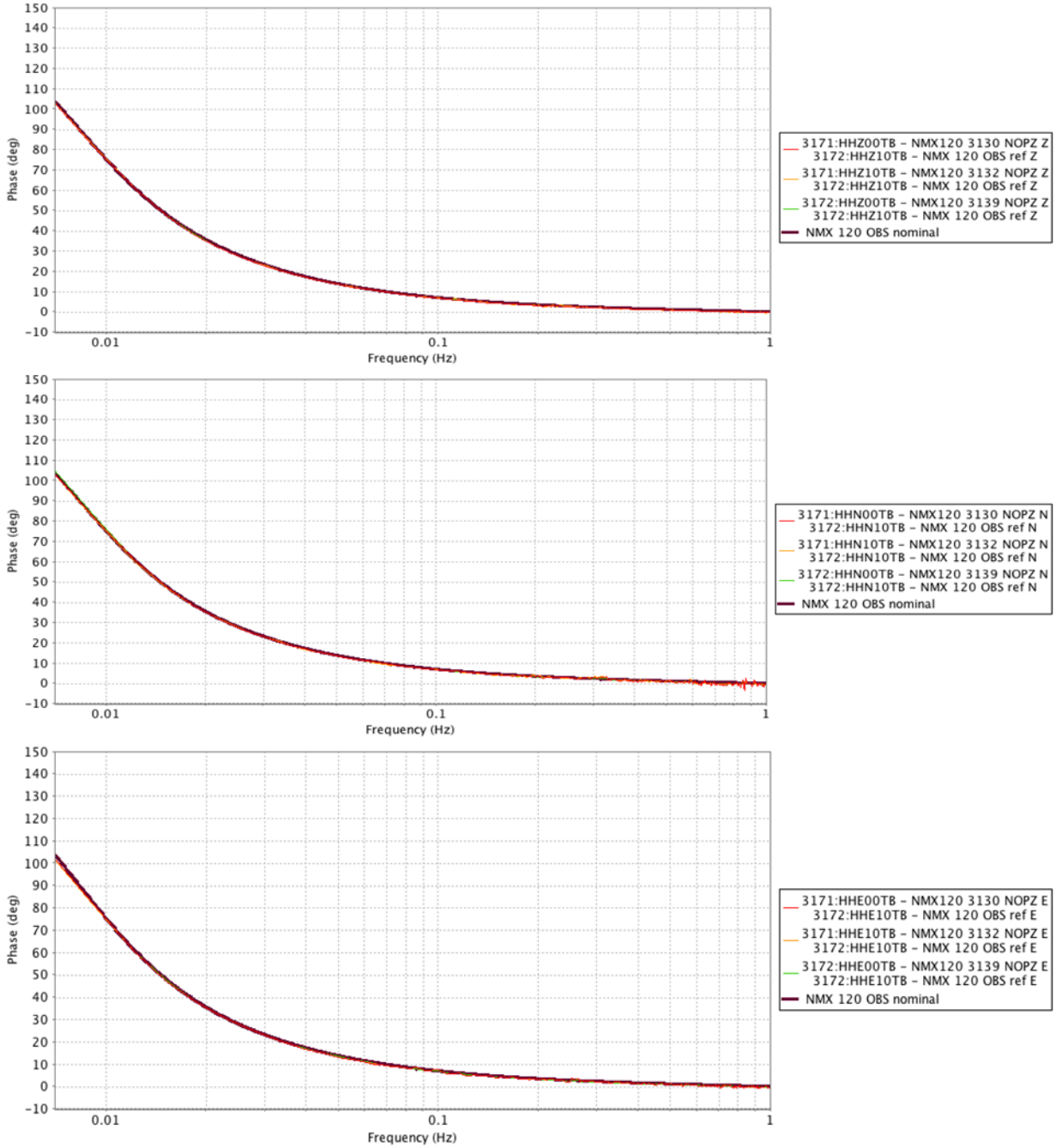

Figure 40 Broadband phase response comparisons, tele-seismic source, between the reference sensor and sensors under test: Vertical (top), North (middle) and East (bottom).

The relative phase response of all components is in good agreement with the nominal response of the sensor over the frequencies plotted.

3.1.3.4 Nanometrics OBS 3129, 3136 and 3142

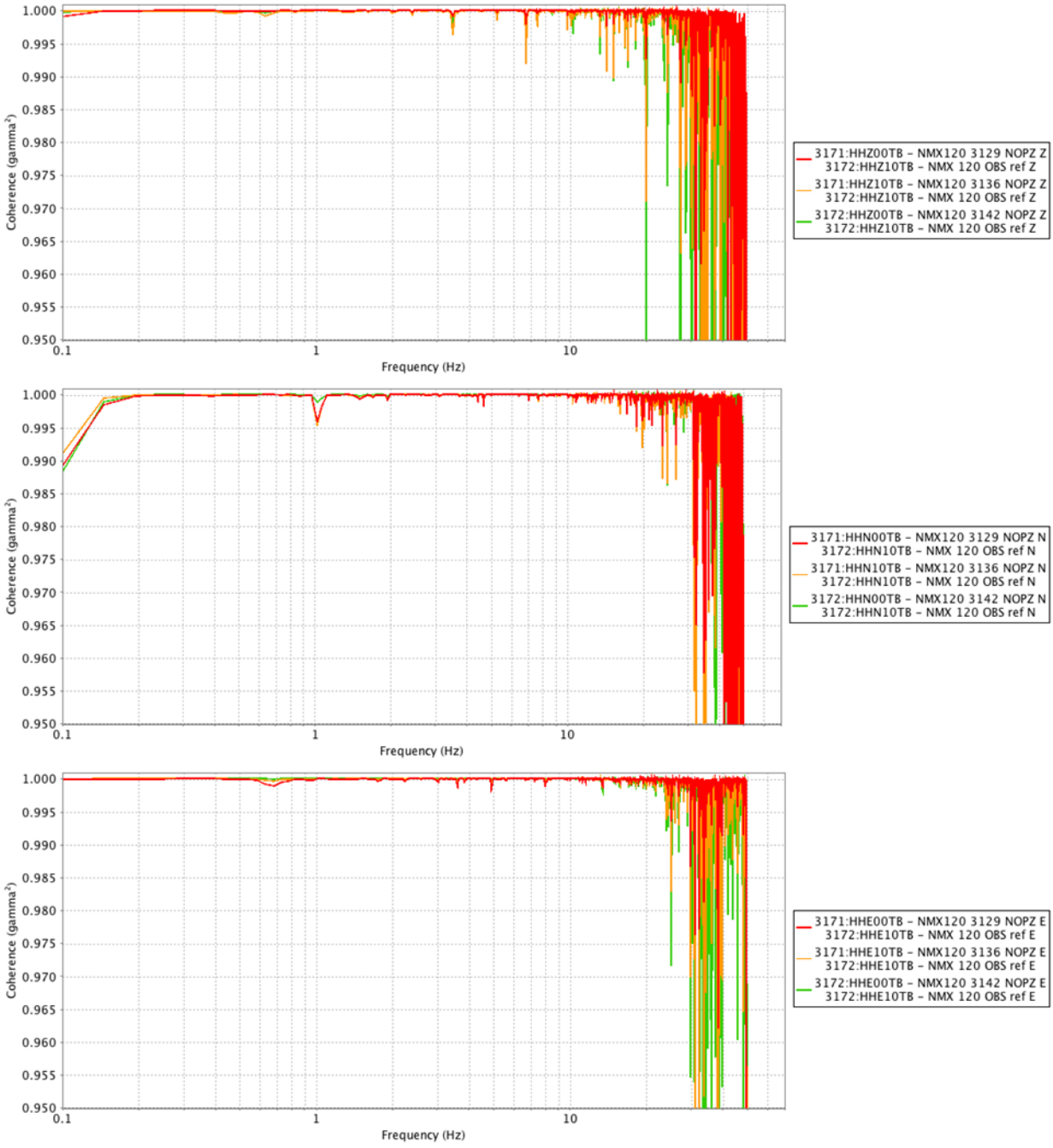

Figure 41 Coherence between the broadband reference sensor and sensors under test, local earthquake source: Vertical (top), North (middle) and East (bottom).

Coherence between the reference sensor and sensors under test is excellent between 0.1 Hz and 28 Hz to 29 Hz on the vertical and east components, with coherence levels highest on sensor 3129. North component coherence is excellent just above 0.1 Hz through 31 Hz at which point the north component of 3129 has a larger drop in coherence than its counterparts. Coherence levels are sufficient between the sensors under test and the reference sensor to be able to comment on the relative magnitude and phase response over these frequency ranges.

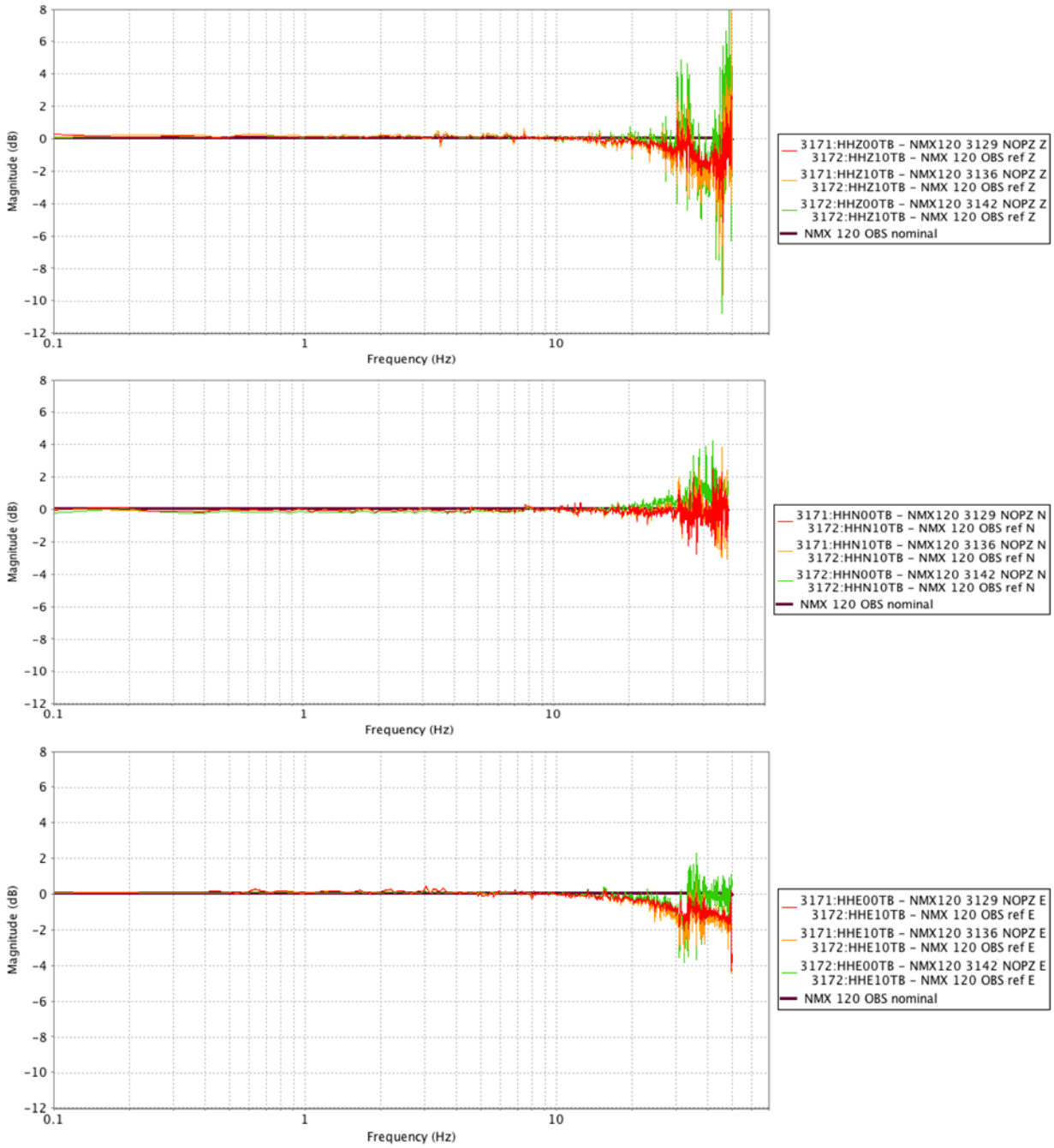

Figure 42 Broadband sensor magnitude response comparisons, local earthquake source, between the reference sensor and sensors under test: Vertical (top), North (middle) and East (bottom).

Relative magnitudes of the vertical components exceed the ideal response by at least 0.1 dB over a broad frequency range; essentially 0.1 Hz to 10 Hz. The north and east components of 3129 and 3136 exhibit some variability in magnitude over the frequency band where each exhibit high coherence; the north component of sensor 3142 is consistently at least 0.1 dB below the ideal. The east components of sensors 3129 and 3136 exhibit some variability and, in general, both exceed the 0.1 dB threshold over much of their frequency range.

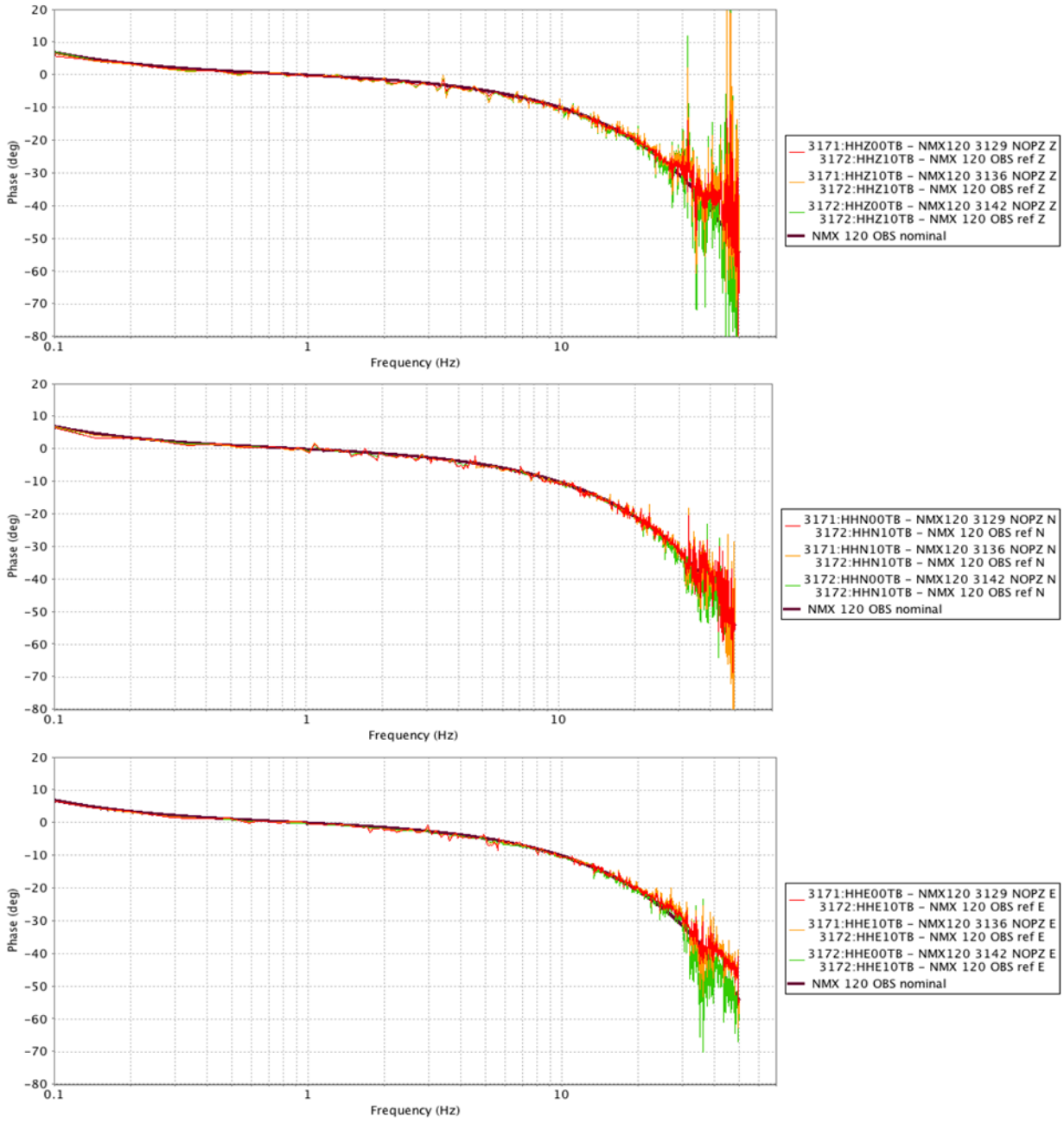

Figure 43 Broadband sensor phase response comparisons, local earthquake source, between the reference sensor and sensors under test: Vertical (top), North (middle) and East (bottom).

The relative phase response of all components are in good agreement with the nominal response of the sensor in the frequency bands over which there is coherence; e.g. the deviations in phase at frequencies above approximately 30 Hz should be treated as suspect.

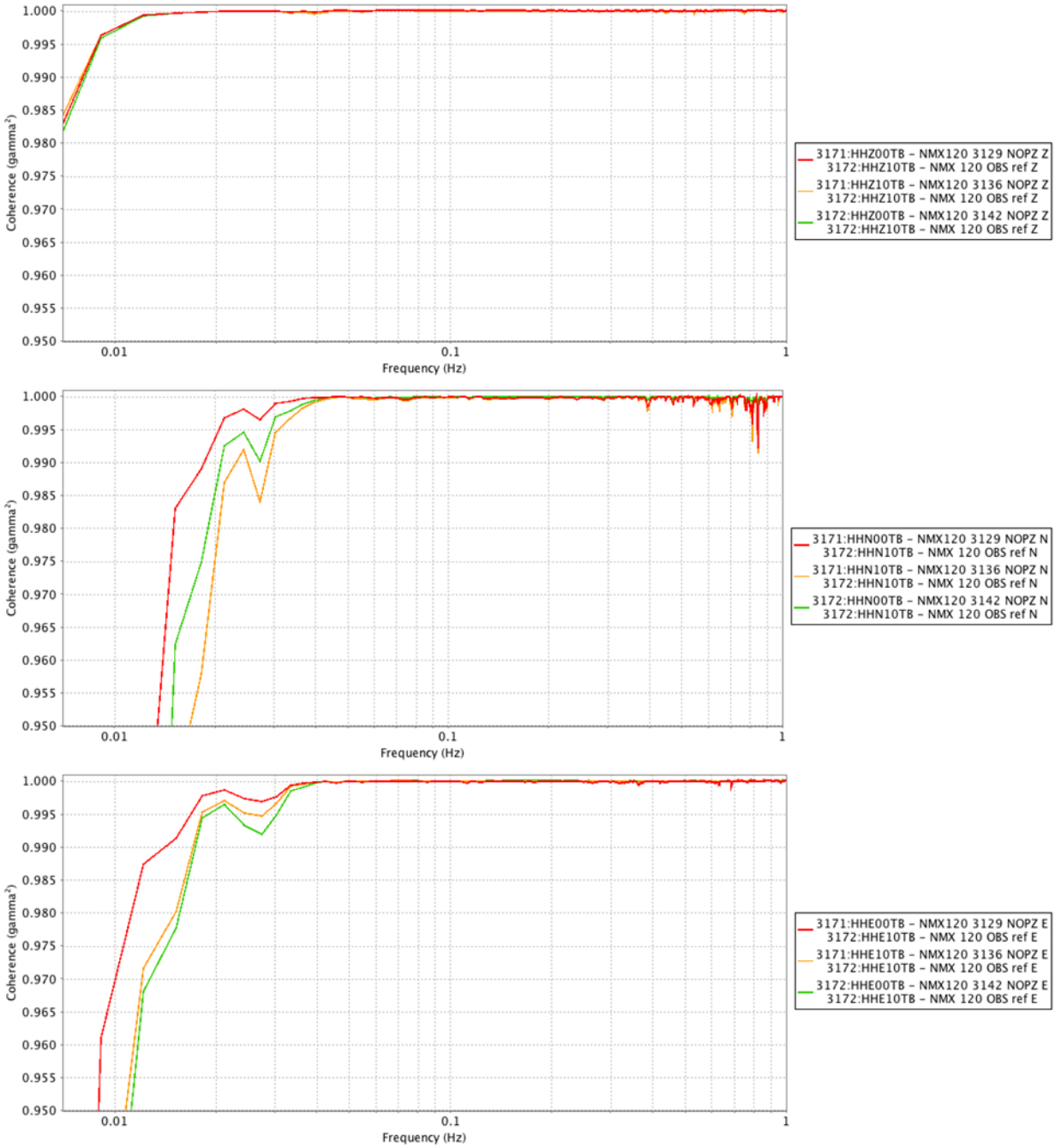

Figure 44 Coherence between the broadband reference sensor and sensors under test, tele-seismic source: Vertical (top), North (middle) and East (bottom).

Coherence between the reference sensor and sensors under test is excellent (at least 0.995 gamma^2) on all components: the verticals consistently to below 0.01 Hz, the horizontals to as low as 0.02 Hz to 0.03 Hz; sensor 3129's coherence extending slightly lower in frequency than its counterparts. Coherence is sufficient between the sensors under test and the reference sensor to be able to comment on the relative magnitude and phase response over these frequency ranges.

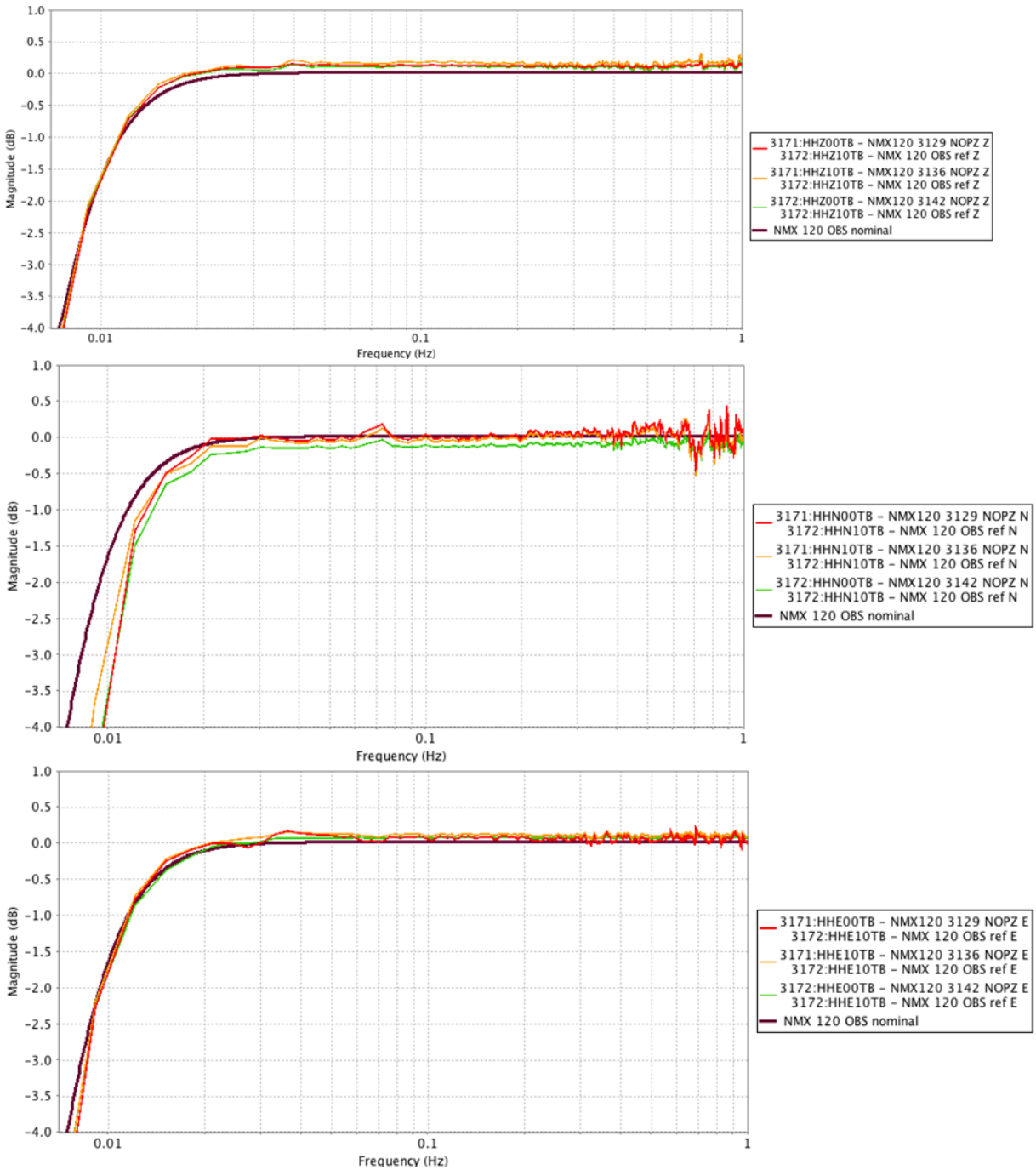

Figure 45 Broadband sensor magnitude response comparisons, tele-seismic source, between the reference sensor and sensors under test: Vertical (top), North (middle) and East (bottom).

Relative magnitudes of vertical components are in general agreement with the nominal response of the sensor; however the vertical components exceed the 0.1 dB criterion, except perhaps sensor 3142 between 0.2 Hz and 0.6 Hz. The north component exceeds the 0.1 dB criterion below 0.2 Hz; sensors 3129 and 3136 below approximately 0.02 Hz. Recall the coherence of the north components drops off between 0.02 and 0.03 Hz, therefore the higher roll-off shown should be treated as suspect. Of the east components, sensor 3136 exceeds the 0.1 dB criterion below 0.3 Hz; sensor 3129 between 0.3 and 0.5 Hz.

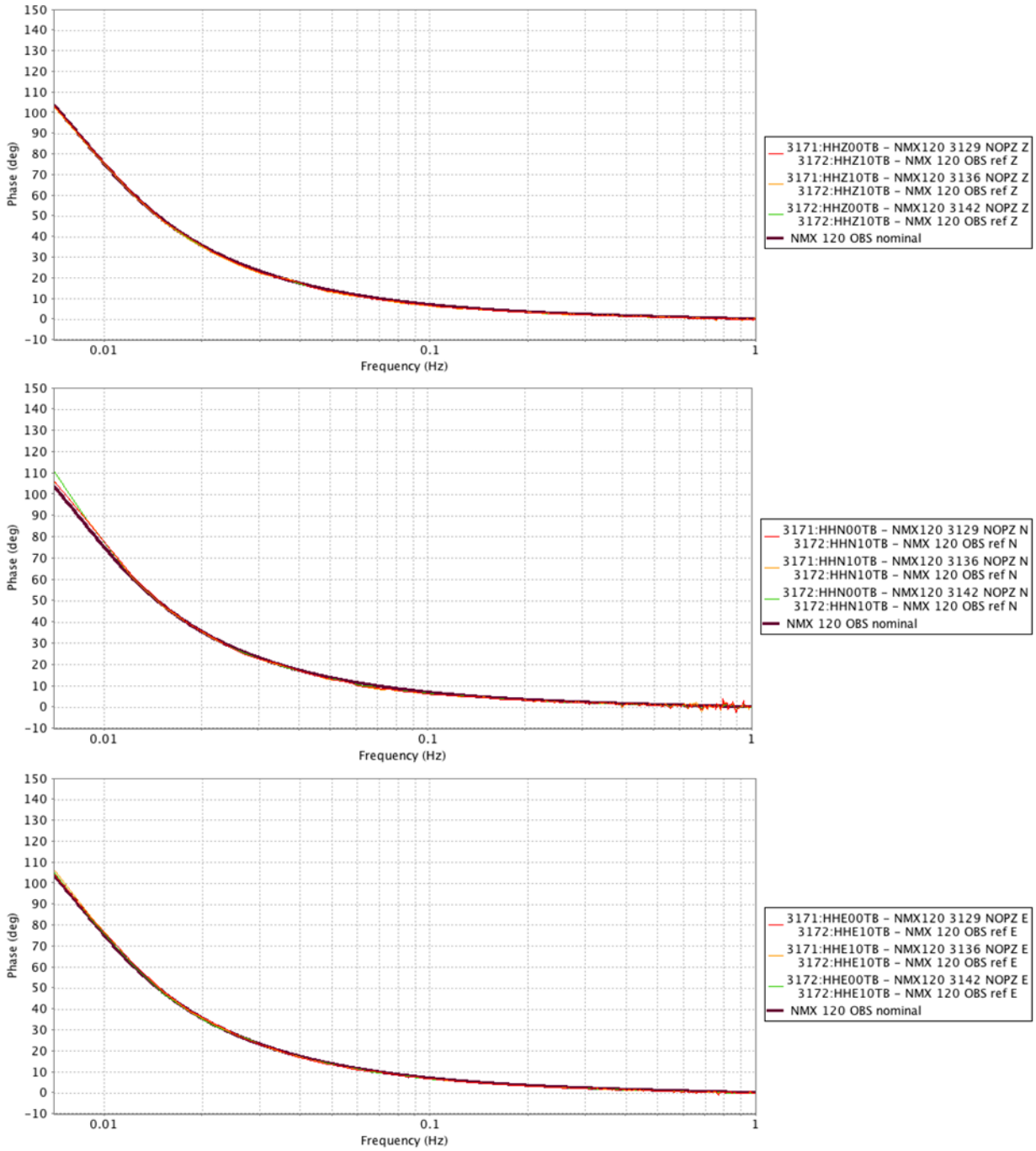

Figure 46 Broadband phase response comparisons, tele-seismic source, between the reference sensor and sensors under test: Vertical (top), North (middle) and East (bottom).

The relative phase response of all components is in good agreement with the nominal response of the sensor over the frequencies of interest.

3.1.3.5 Nanometrics OBS 3127, 3133 and 3135

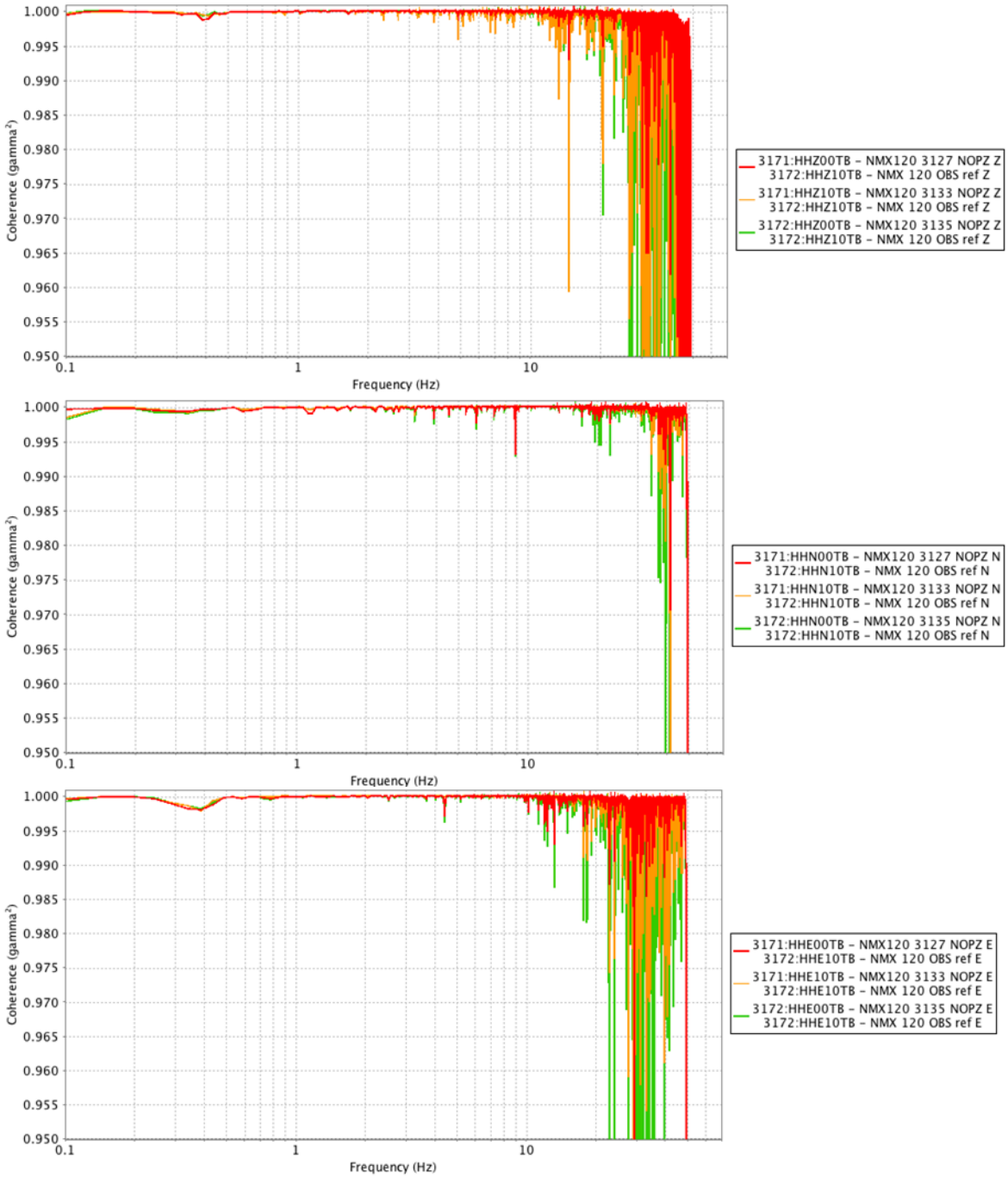

Figure 47 Coherence between the broadband reference sensor and sensors under test, local earthquake source: Vertical (top), North (middle) and East (bottom).

Coherence between the reference sensor and sensors under test is excellent (at least 0.995 gamma^2) between 0.1 Hz and 25 Hz, 37 Hz and 27 Hz for the vertical, north and east components respectively. Sensor 3127 consistently has the widest band of coherence, regardless of component. Coherence levels are sufficient between the sensors under test and the reference

sensor to be able to comment on the relative magnitude and phase response over this frequency range.

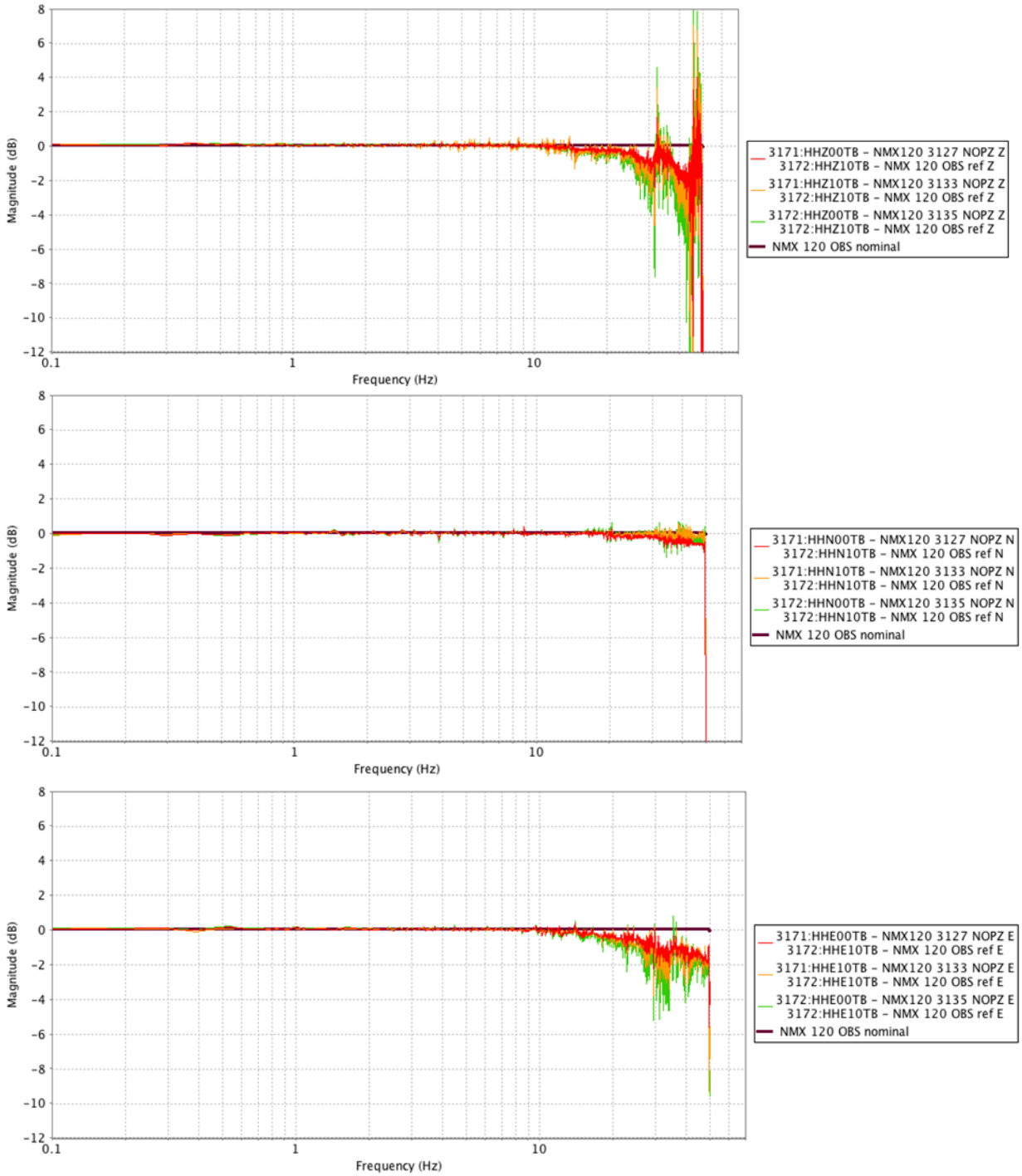

Figure 48 Broadband sensor magnitude response comparisons, local earthquake source, between the reference sensor and sensors under test: Vertical (top), North (middle) and East (bottom).

Relative magnitudes of the vertical components are relatively flat over the widest frequency, 0.1 Hz to 10 Hz, however each sensor exceeds the 0.1 dB criterion: all above approximately 10 Hz; at lower frequencies: 3127 between 0.3 Hz and 0.4 Hz, 3133 between 0.4 Hz and 1 Hz and 3135 below 0.9 Hz. The east components begin a roll-off above 10 Hz; however coherence is reduced at these high frequencies, requiring caution of the significance of the roll-off.

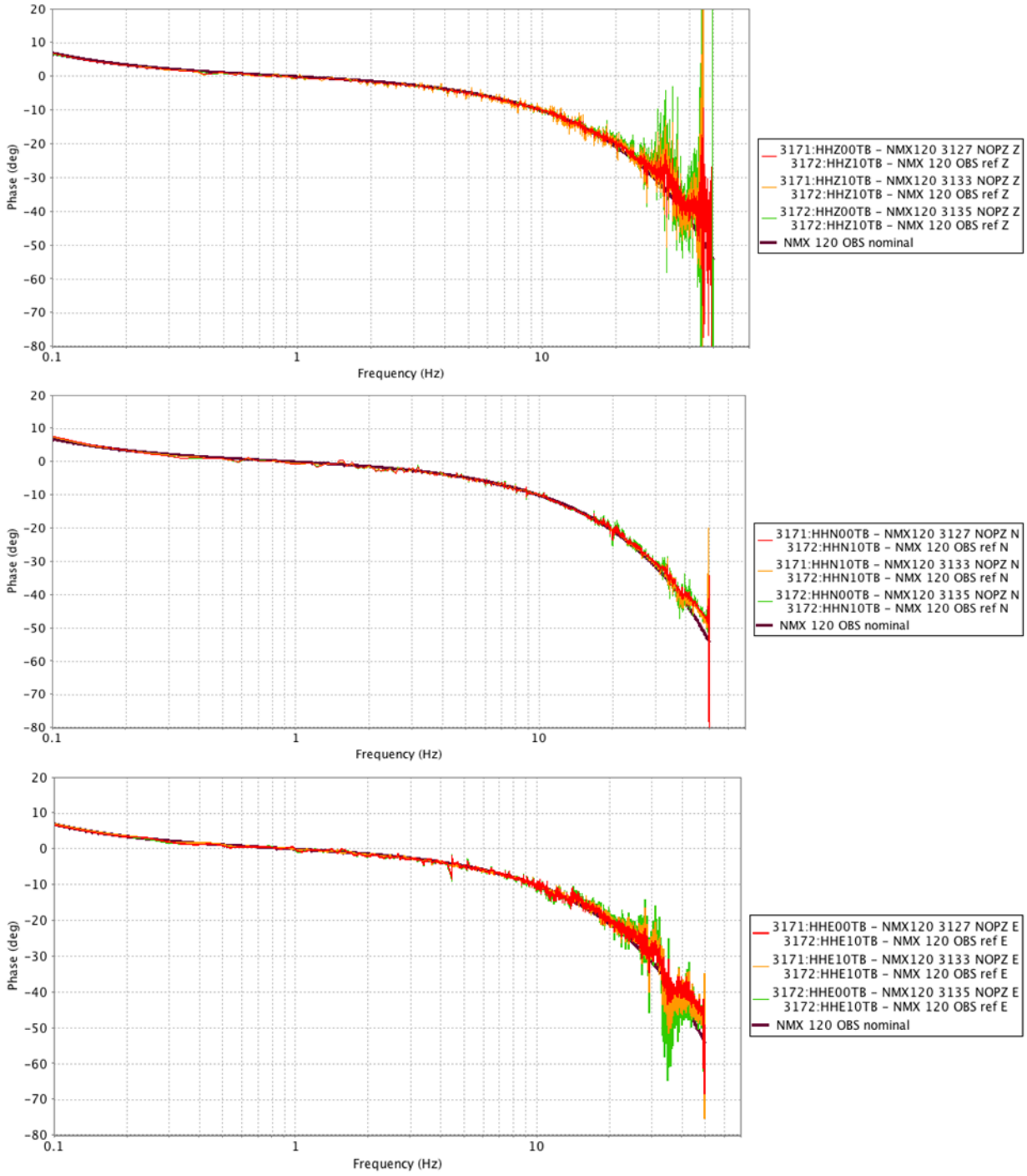

Figure 49 Broadband sensor phase response comparisons, local earthquake source, between the reference sensor and sensors under test: Vertical (top), North (middle) and East (bottom).

Across components and sensors phases are in good agreement with the nominal phase response. Any outliers in phase occur at frequencies with relatively low coherence levels.

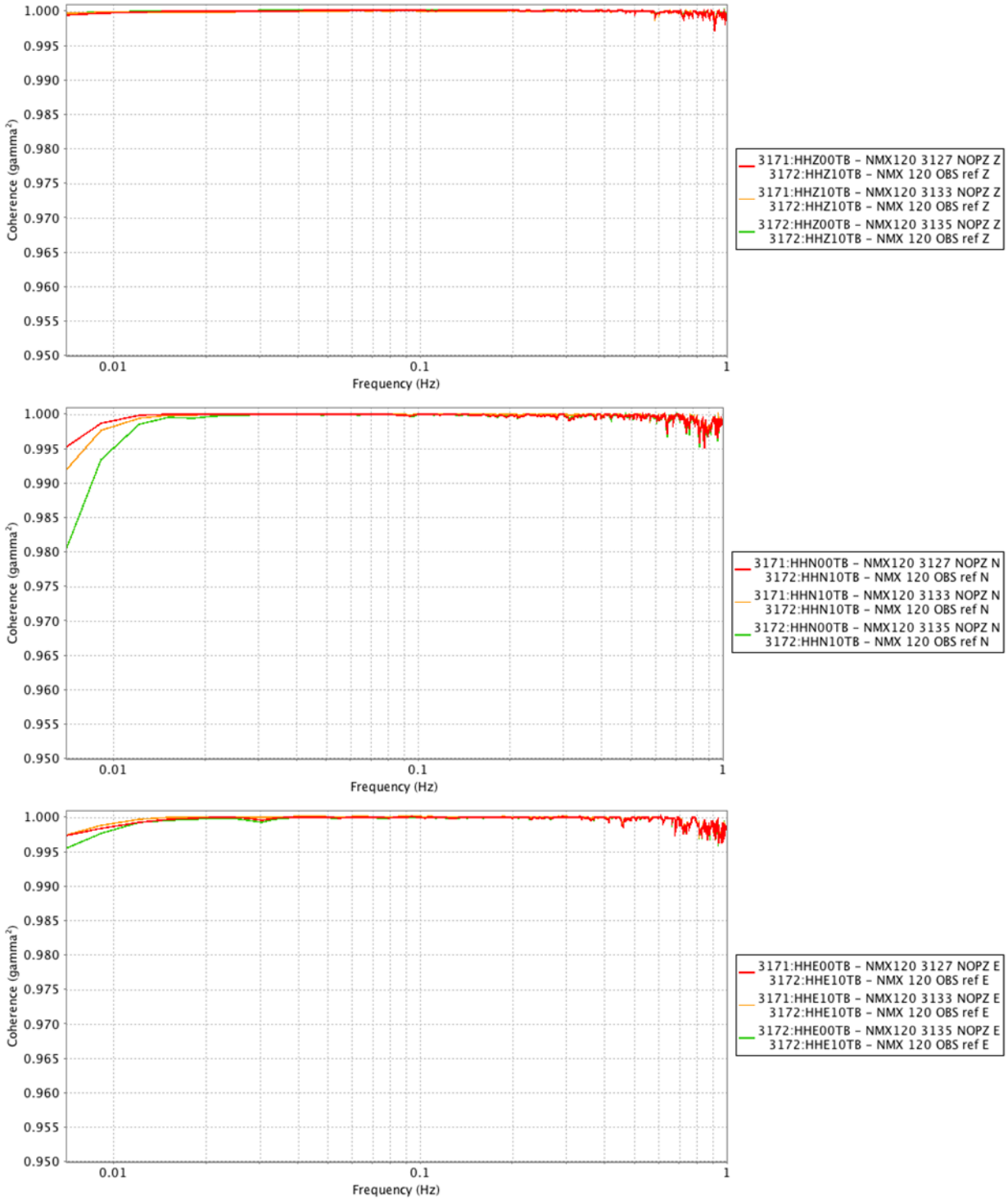

Figure 50 Coherence between the broadband reference sensor and sensors under test, tele-seismic source: Vertical (top), North (middle) and East (bottom).

Coherence between the reference sensor and sensors under test is excellent (at least 0.995 gamma^2) across all sensors, from 0.01 Hz through 1 Hz and provides one with high confidence in the subsequent magnitude and phase response calculations.

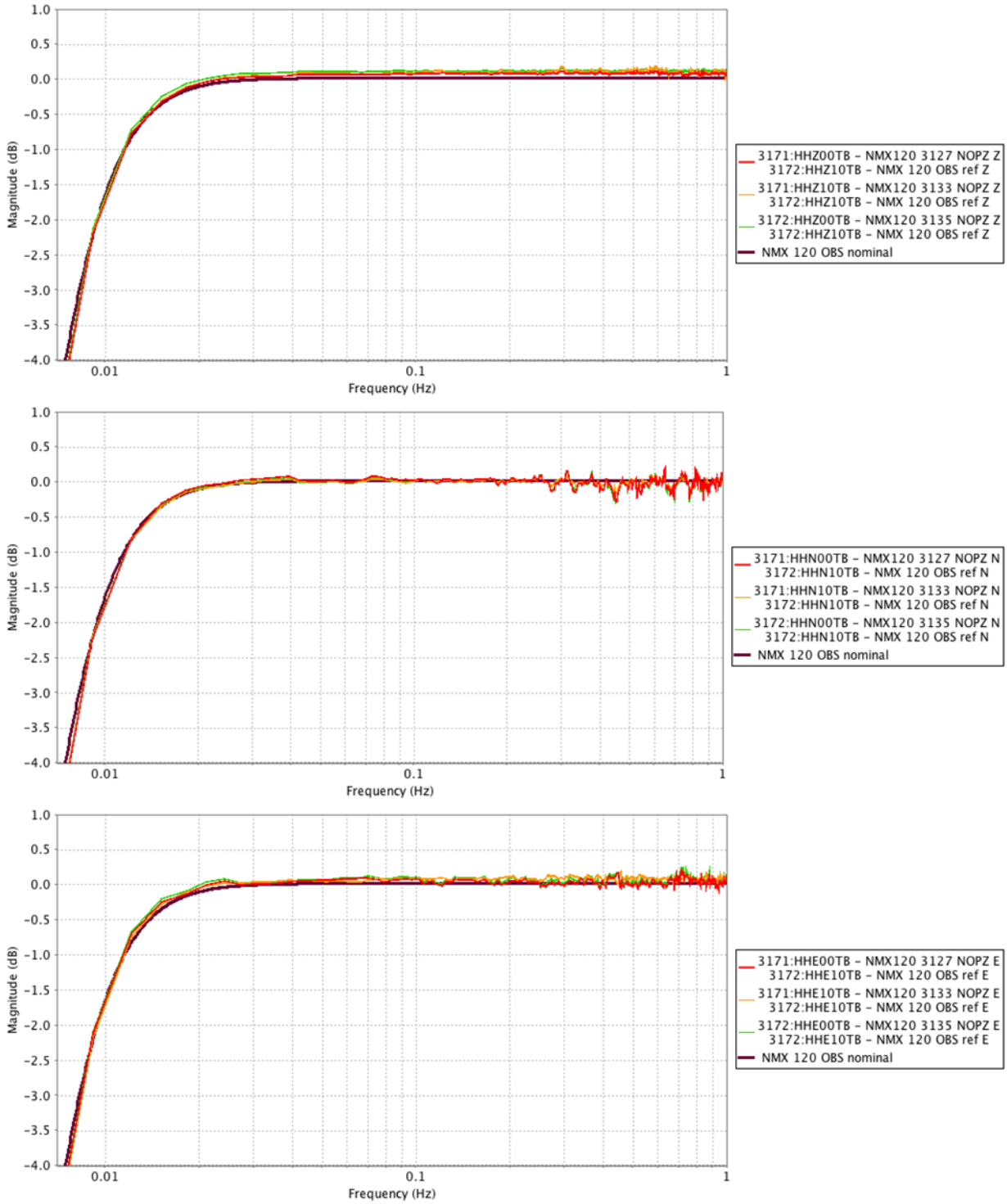

Figure 51 Broadband sensor magnitude response comparisons, tele-seismic source, between the reference sensor and sensors under test: Vertical (top), North (middle) and East (bottom).

Relative magnitudes of vertical components are very flat, though sensor 3135 just exceeds the 0.1 dB criterion from 0.04 Hz to 1 Hz. The north components show slight variability, perhaps exceeding the 0.1 dB criterion between 0.4 Hz and 0.5 Hz; the east, also exhibits slight variability, exceeding the 0.1 dB criterion from 0.7 Hz to 0.8 Hz.

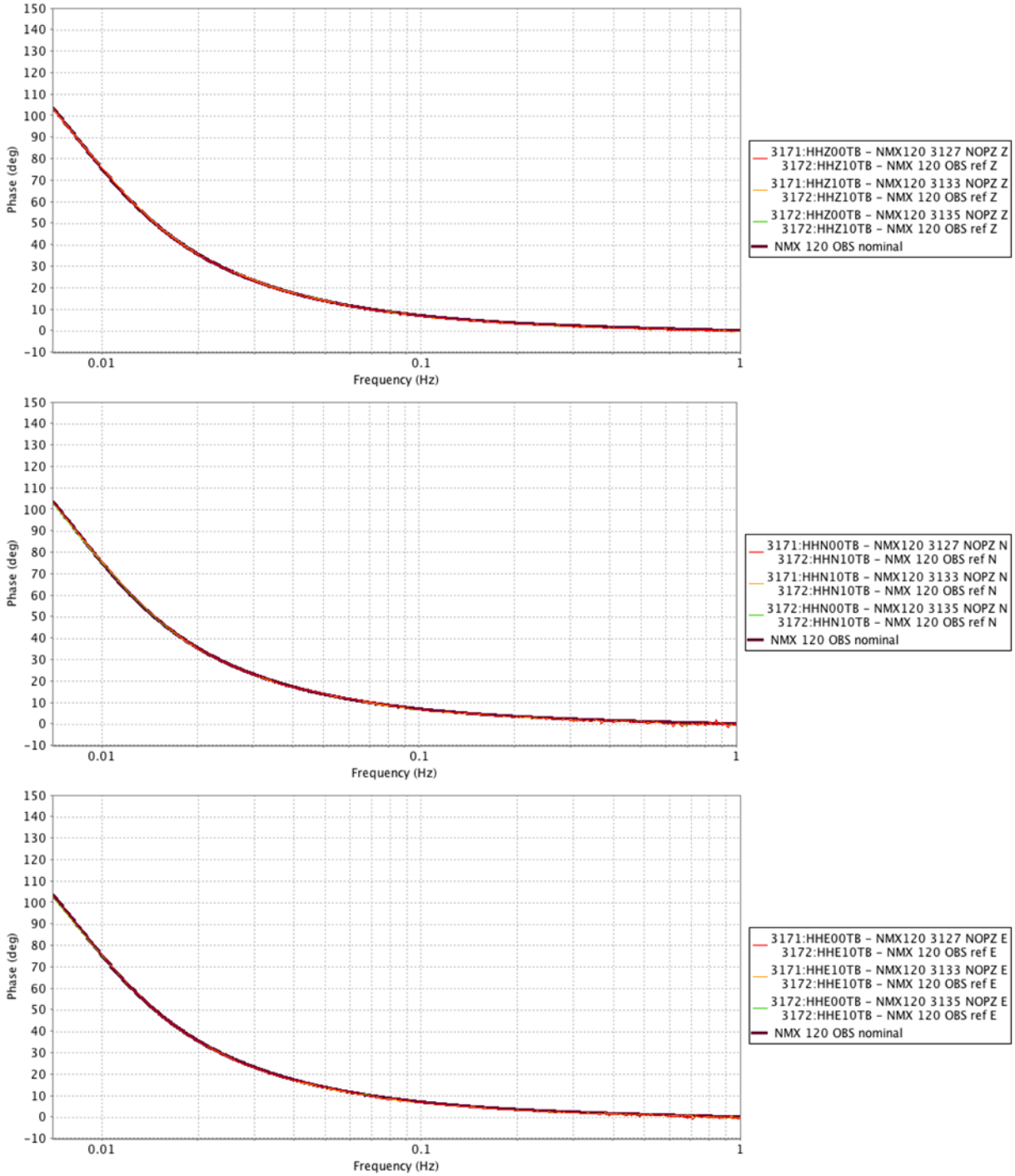

Figure 52 Broadband phase response comparisons, tele-seismic source, between the reference sensor and sensors under test: Vertical (top), North (middle) and East (bottom).

The relative phase response of all components is in good agreement with the nominal response of the sensor over the frequencies plotted.

3.1.3.6 Nanometrics OBS 3128, 3140 and 3141

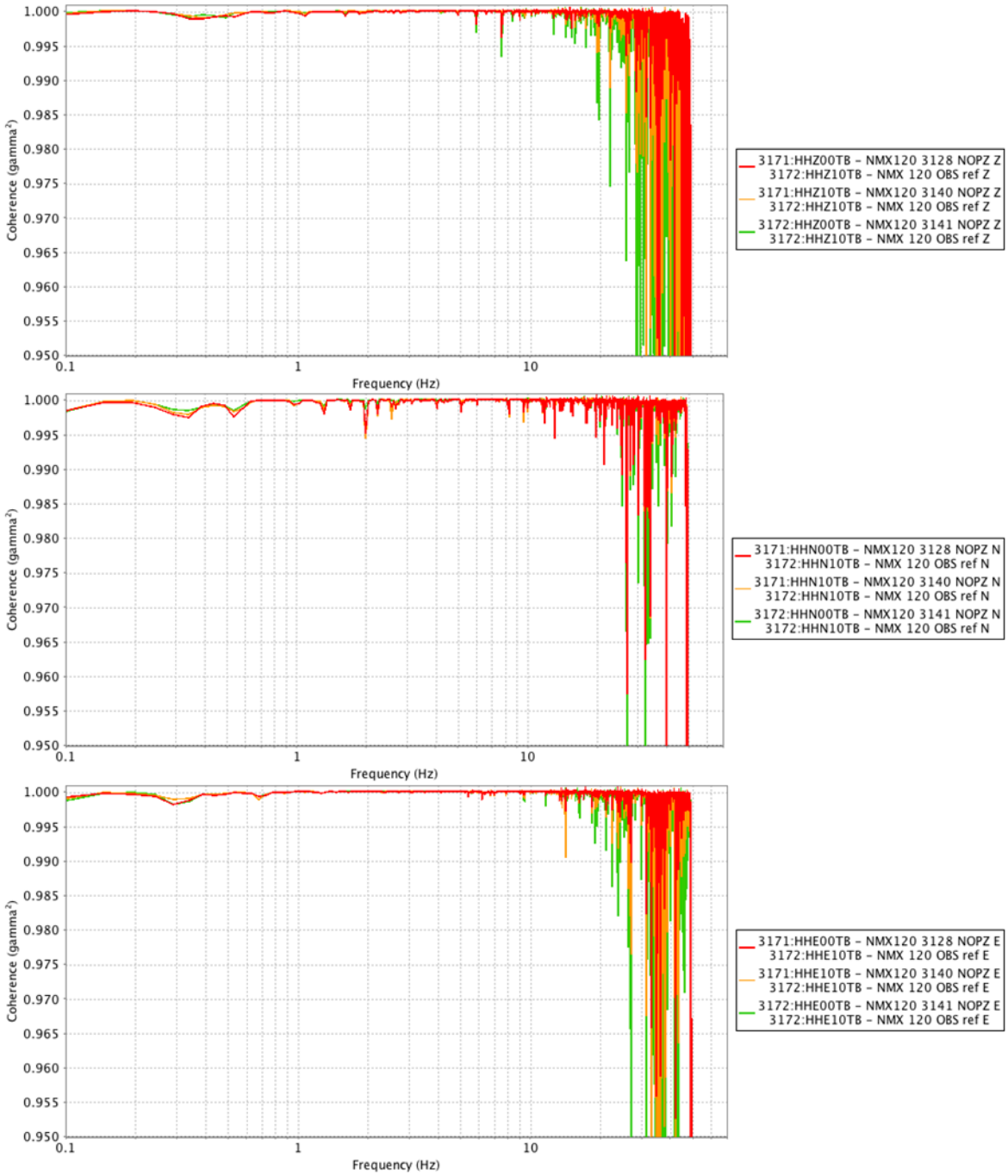

Figure 53 Coherence between the broadband reference sensor and sensors under test, local earthquake source: Vertical (top), North (middle) and East (bottom).

Coherence between the reference sensor and sensors under test is excellent (at least 0.995 gamma^2) between 0.1 Hz and 29 Hz, 25 Hz and 23 Hz for the Vertical, North and East components respectively. Generally, sensor 3128 has the highest level of coherence, where coherence drops. Coherence levels are sufficient between the sensors under test and the reference sensor to be able to comment on the relative magnitude and phase response over these frequency ranges.

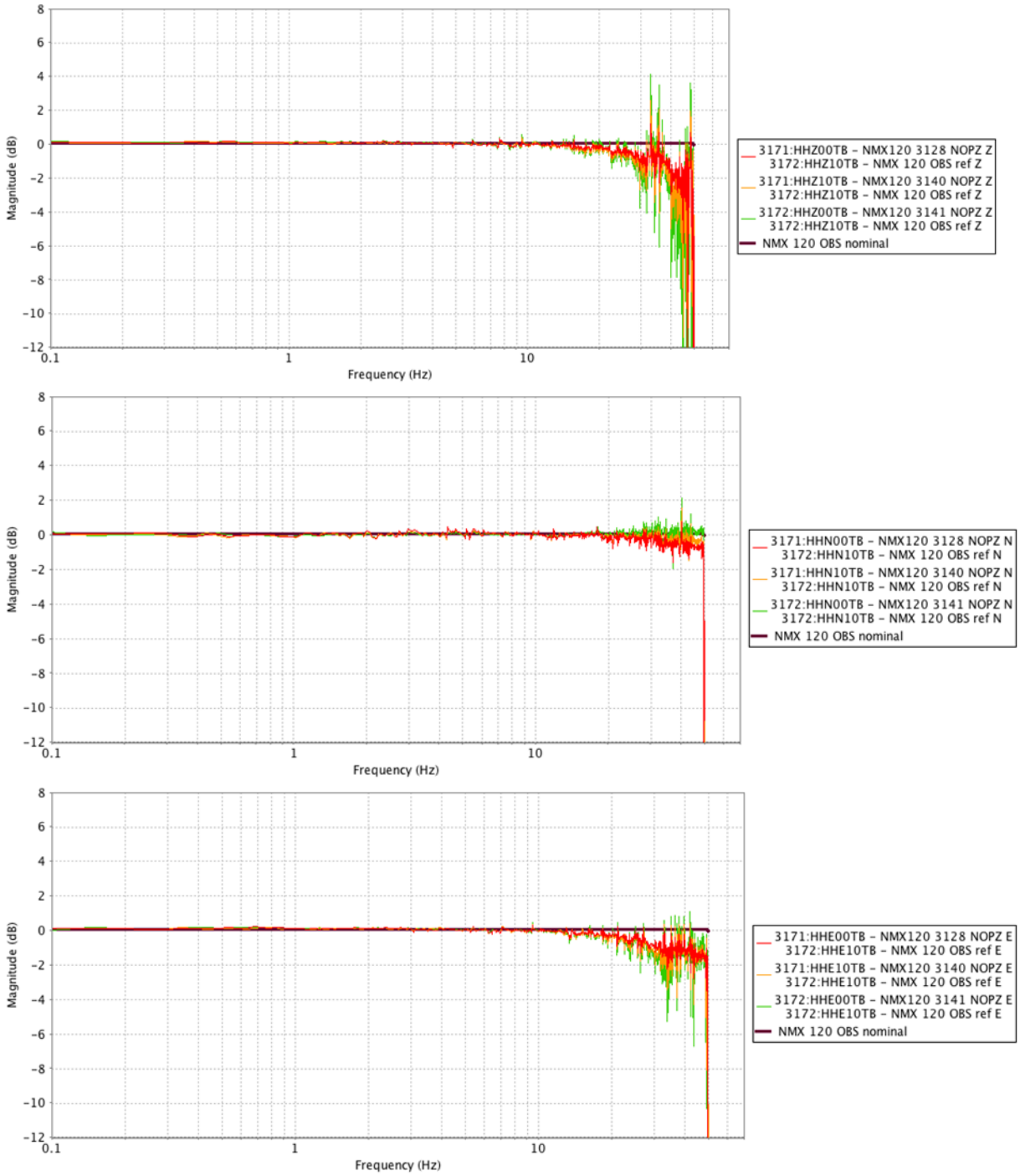

Figure 54 Broadband sensor magnitude response comparisons, local earthquake source, between the reference sensor and sensors under test: Vertical (top), North (middle) and East (bottom).

Relative magnitudes of the vertical components are relatively flat over the widest frequency range, 0.1 Hz to 10 Hz, however each sensor exceeds the 0.1 dB criterion: all above approximately 10 Hz; at lower frequencies: 3128 below 0.6 Hz, 3140 between 0.3 Hz and 6 Hz and 3141 below 2 Hz.

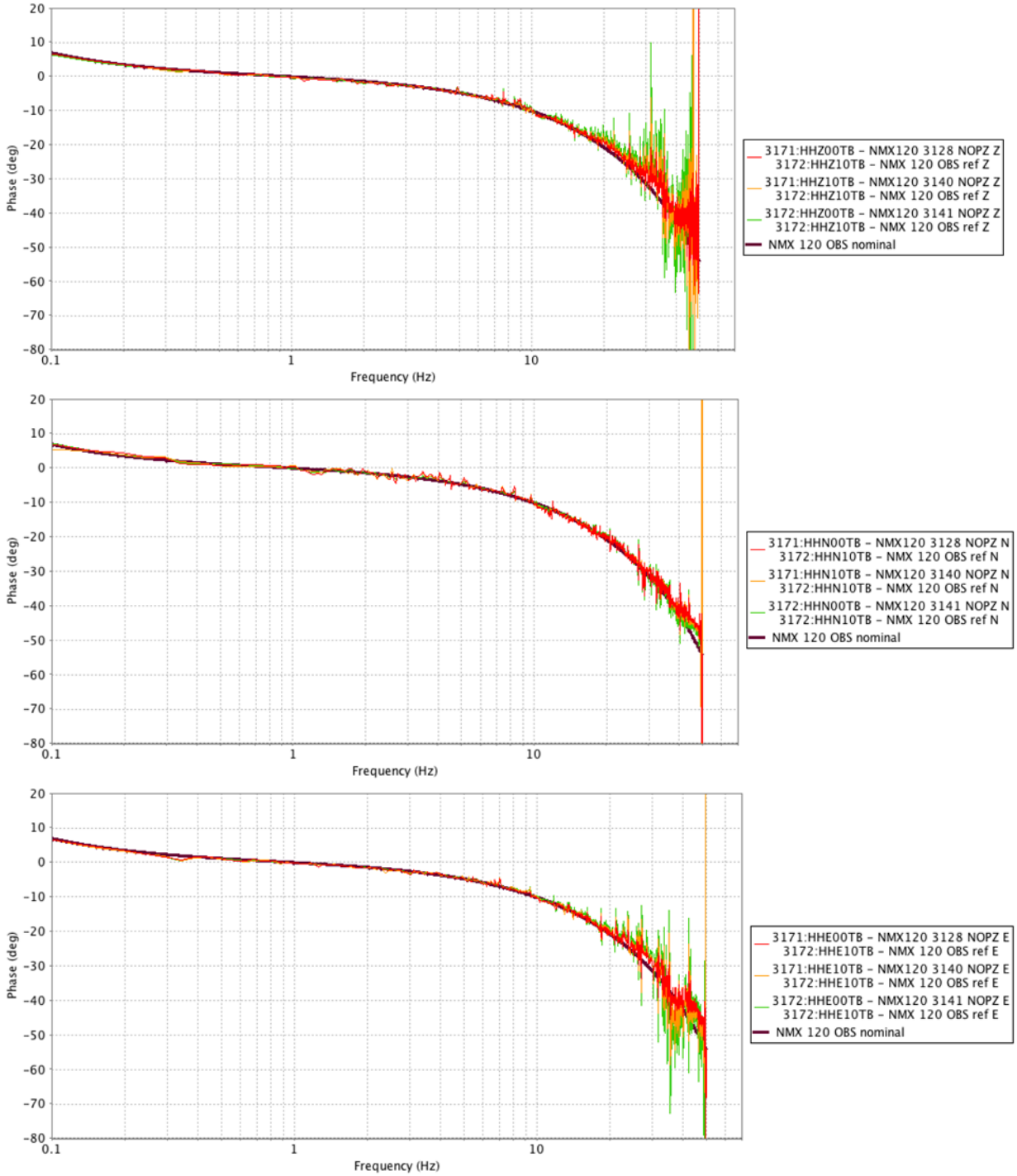

Figure 55 Broadband sensor phase response comparisons, local earthquake source, between the reference sensor and sensors under test: Vertical (top), North (middle) and East (bottom).

Across components and sensors phases are in good agreement with the nominal phase response. Any outliers in phase occur at frequencies with relatively low coherence levels, at higher frequencies.

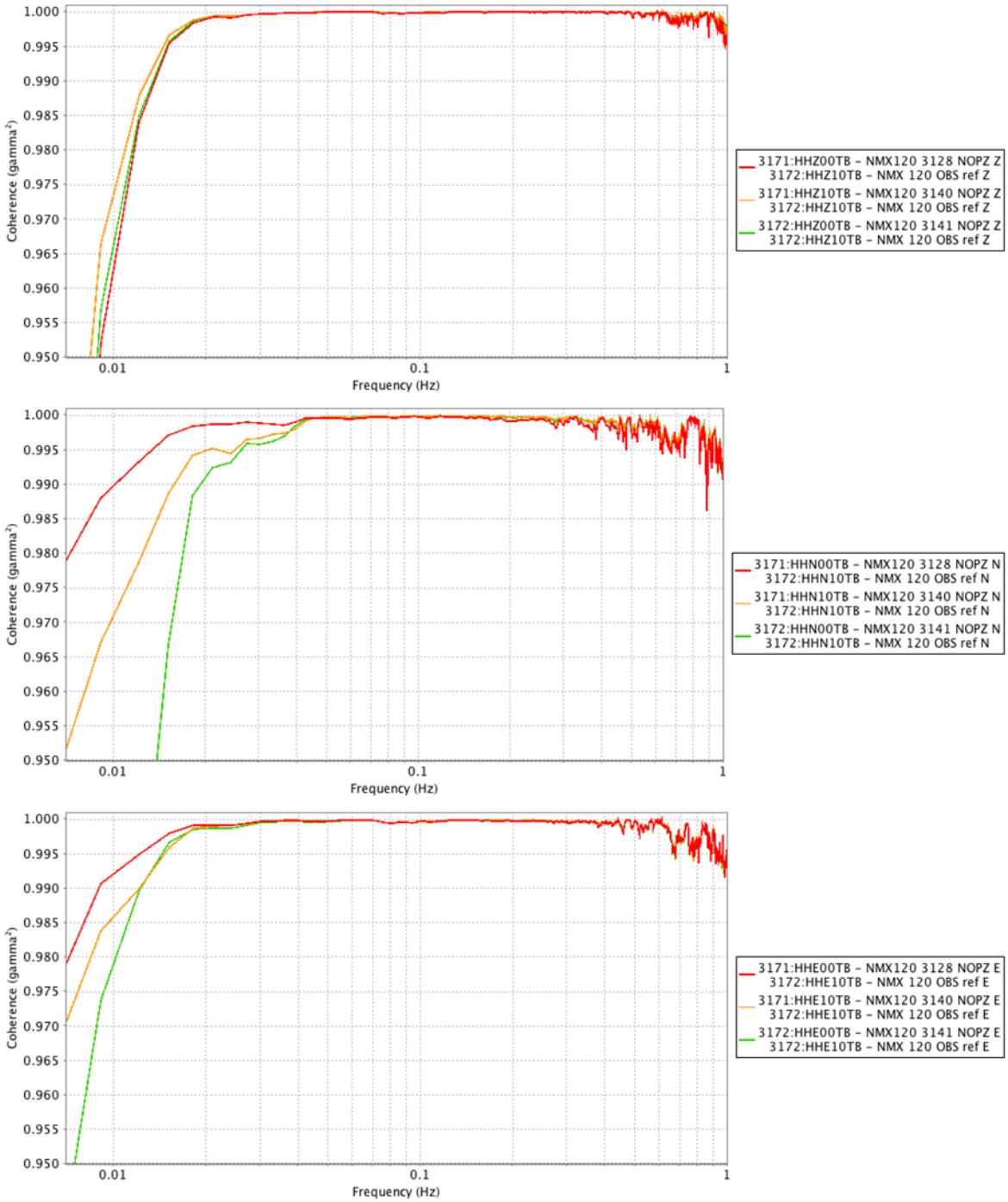

Figure 56 Coherence between the broadband reference sensor and sensors under test, tele-seismic source: Vertical (top), North (middle) and East (bottom).

Coherence between the reference sensor and sensors under test is excellent (at least 0.995 gamma^2) on all components: the verticals above 0.015 Hz, north components to as low as 0.024 Hz (sensor 3141) and 0.016 Hz (sensor 3128) and the east components above 0.012 Hz for sensor 3128 and 0.015 Hz for sensors 3140 and 3141. Coherence is sufficient between the sensors under test and the reference sensor to be able to comment on the relative magnitude and phase response over these frequency ranges.

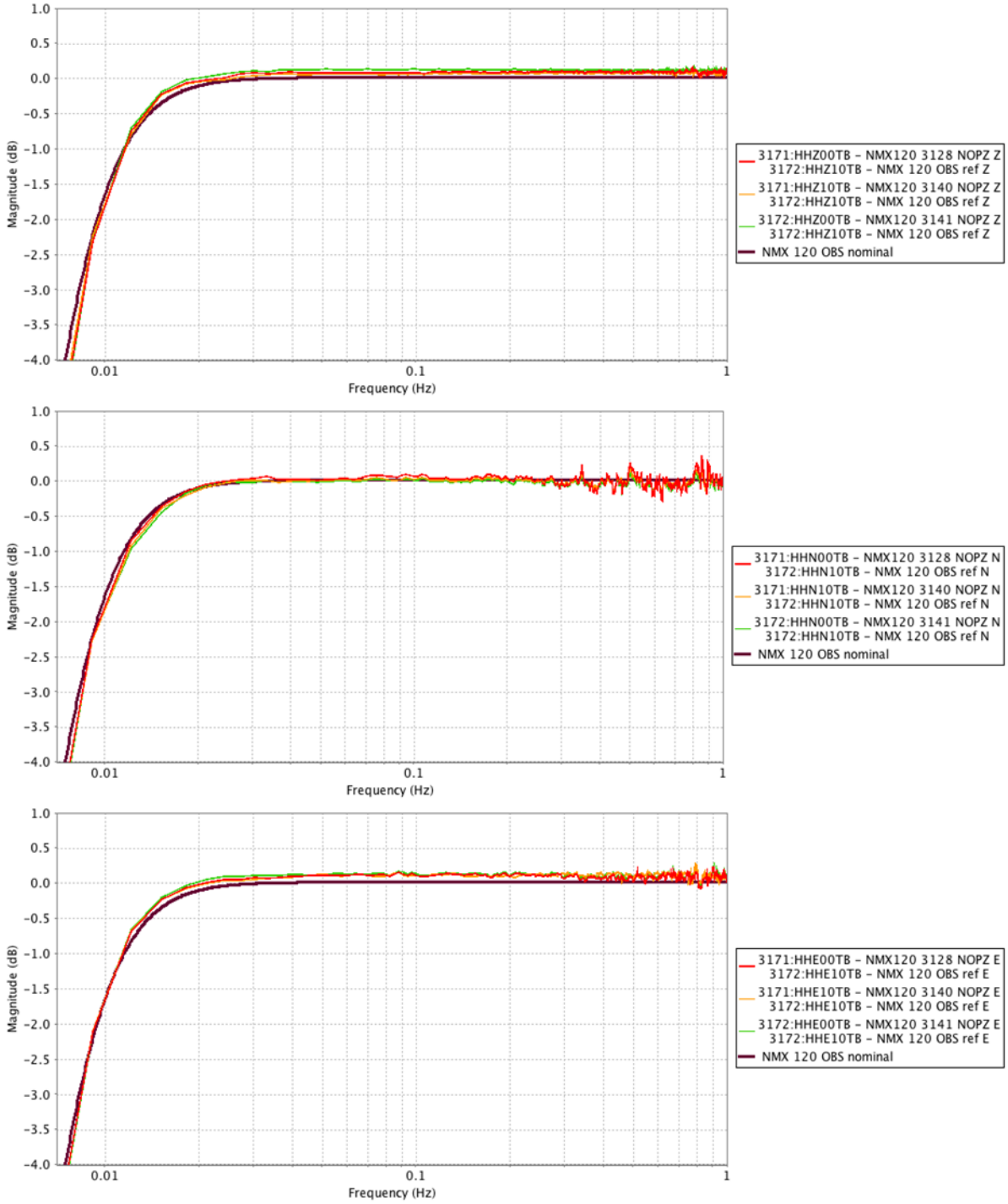

Figure 57 Broadband sensor magnitude response comparisons, tele-seismic source, between the reference sensor and sensors under test: Vertical (top), North (middle) and East (bottom).

Relative magnitudes of vertical components are very flat, though sensor 3141 exceeds the 0.1 dB criterion from approximately 0.01 to 1 Hz. The north components show slight variability, perhaps 3128 and 3140 exceeding the 0.1 dB criterion at approximately 0.5 Hz and between 0.8 and 0.9 Hz. The east, also exhibits slight variability, exceeding the 0.1 dB criterion below 0.3 Hz for 3128 and 3141 and 0.5 Hz for sensor 3140.

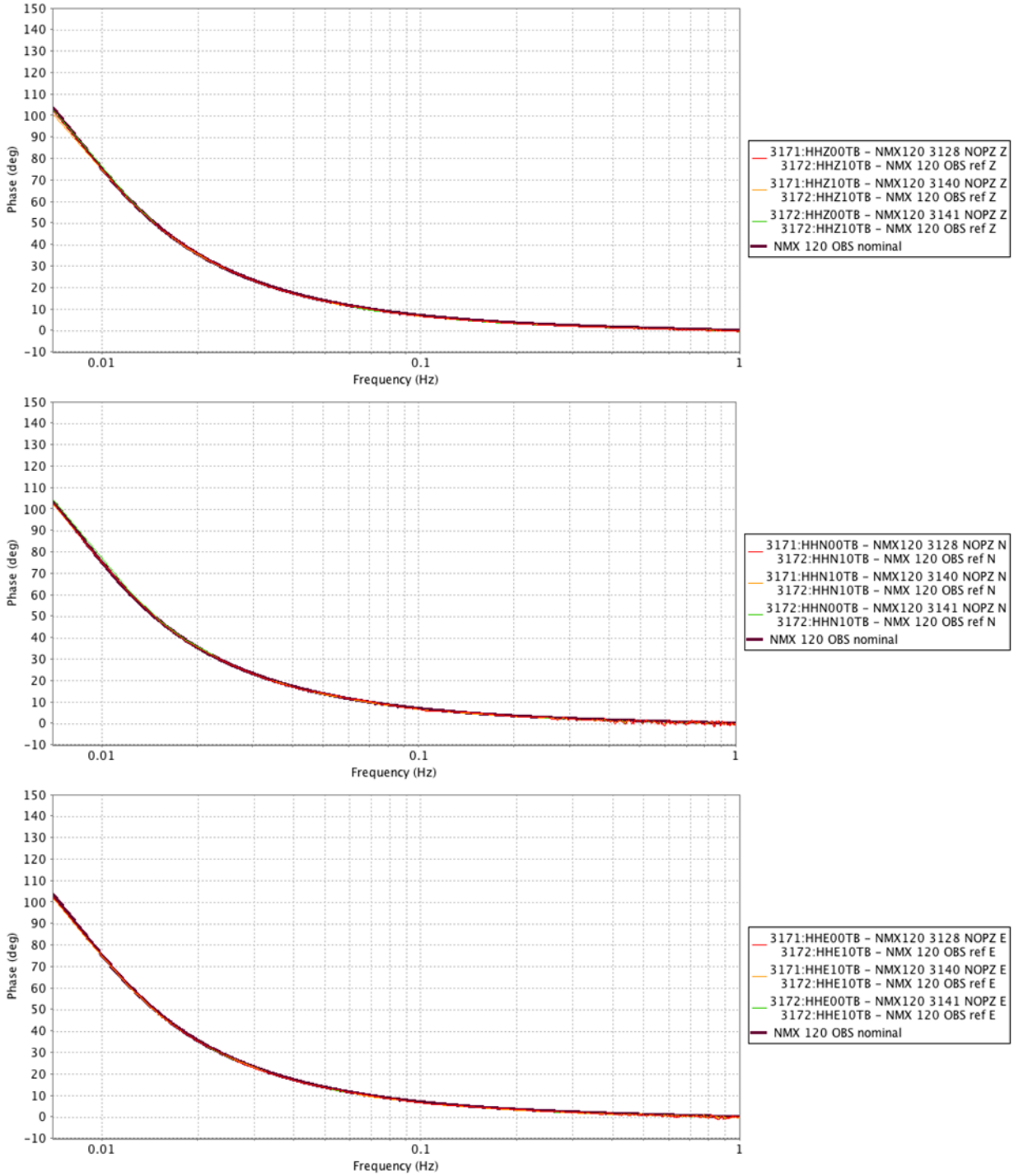

Figure 58 Broadband phase response comparisons, tele-seismic source, between the reference sensor and sensors under test: Vertical (top), North (middle) and East (bottom).

The relative phase response of all components is in good agreement with the nominal response of the sensor over the frequencies plotted.

3.1.3.7 Navy OBS 82, 88 and 89

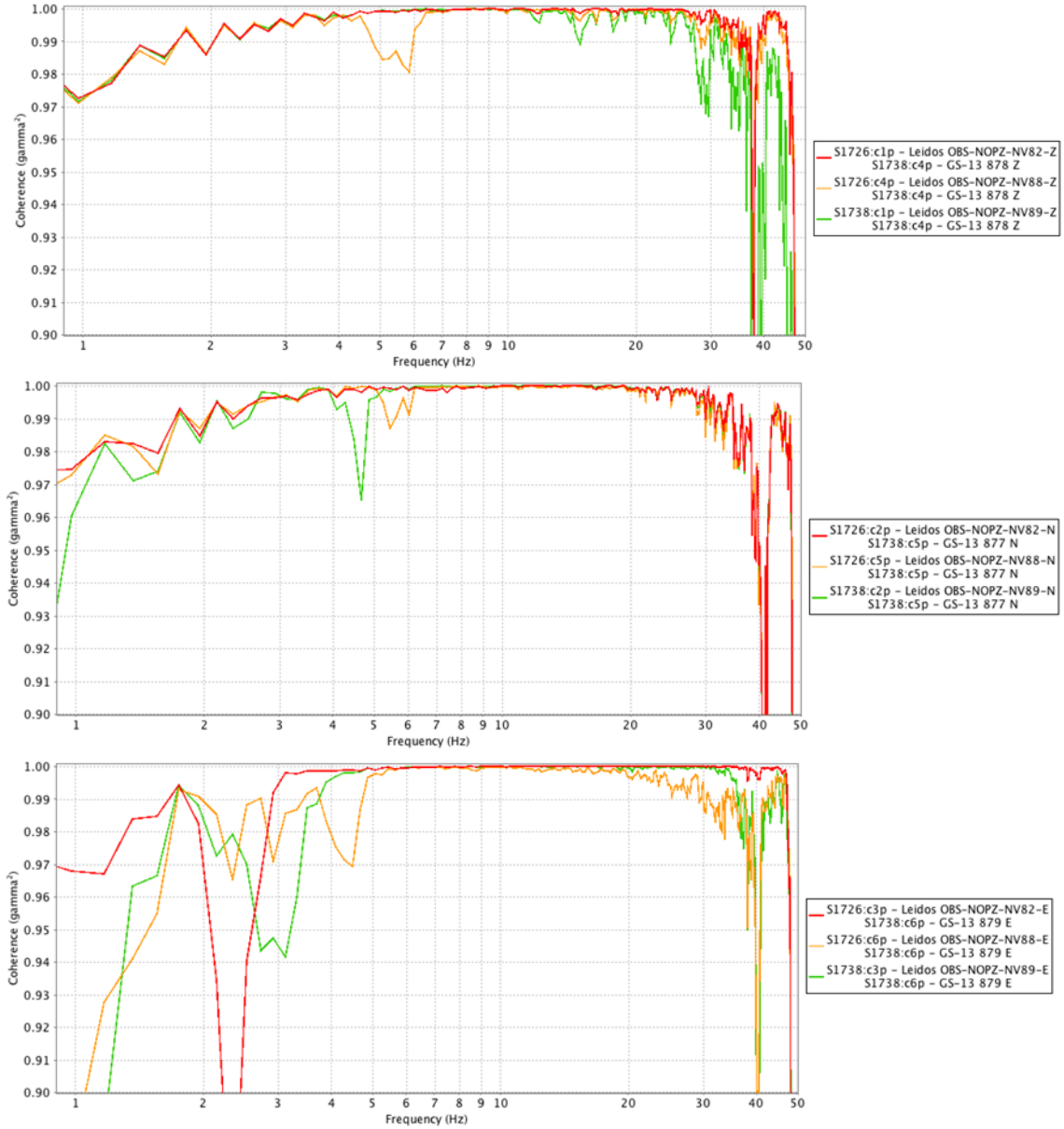

Figure 59 Coherence between short-period reference sensor and sensors under test: Vertical (top), North (middle) and East (bottom).

Coherence between the reference sensor and sensors under test is excellent (at least 0.995 gamma^2) on all components over varying ranges: the verticals consistently from as low as approximately 4.5 Hz for sensors 82 and 89 and 6 Hz for sensor 88, to as high as 26 Hz and 34 Hz, for 89 and 82, respectively; the north component from as low as 3.3 Hz to 6.1 Hz, for sensors 82 and 88 respectively, up to 30 Hz across all sensors; and the east as low as 3 Hz to 4.8 Hz, sensors 82 and 88, respectively, to as high as 25 to 47 Hz, sensors 88 and 82. Coherence is sufficient between the sensors under test and the reference sensor to be able to comment on the relative magnitude and phase response over these frequency ranges.

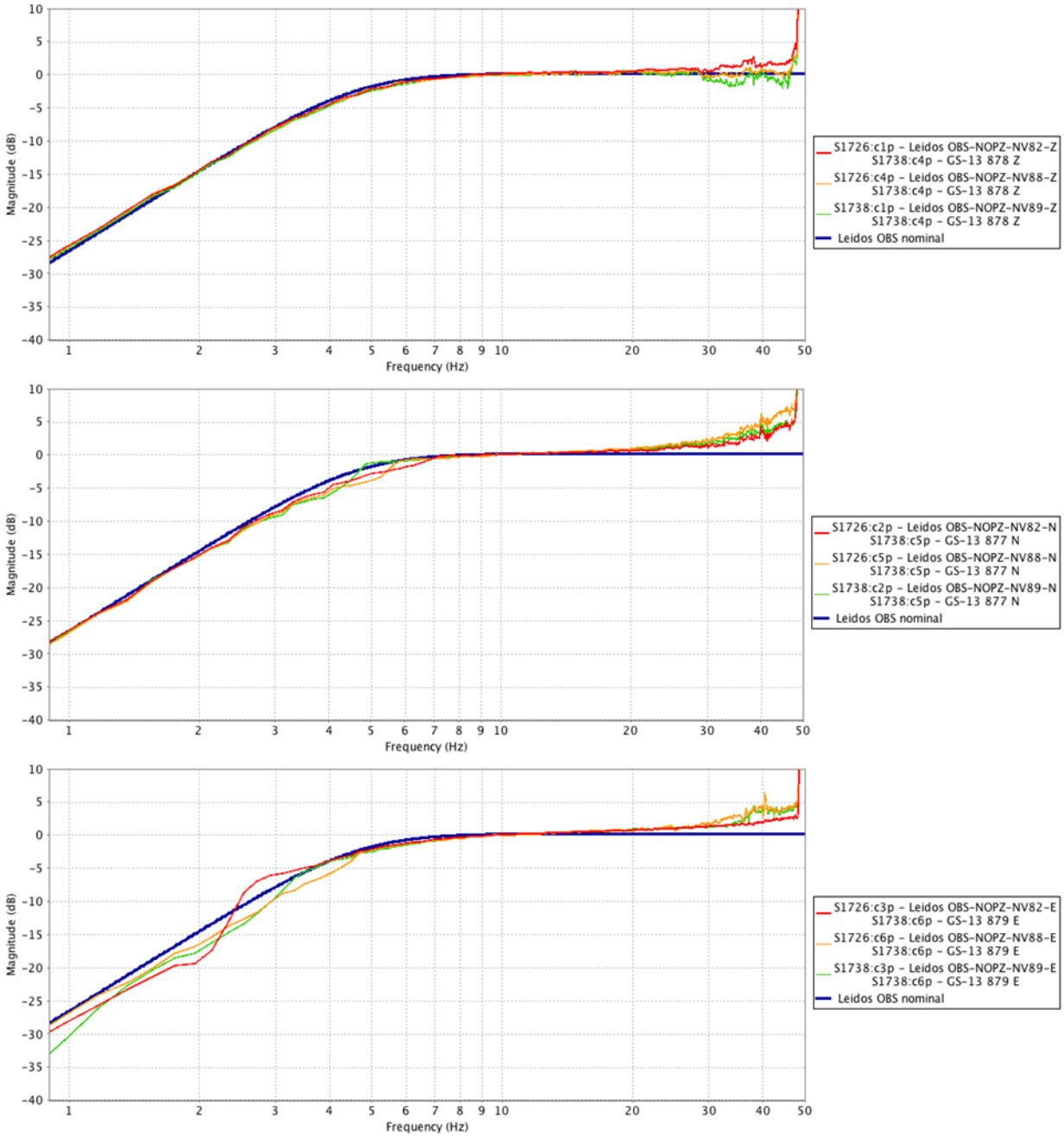

Figure 60 Short-period sensor magnitude response comparisons between the reference sensor and sensors under test: Vertical (top), North (middle) and East (bottom).

While the relative magnitudes generally follow the nominal response model at mid to low frequencies (excluding the east component of sensor 82, though recall its coherence is very low at the point at which the large magnitude deviation occurs), the magnitudes only remain within 0.1 dB generally over a 1 Hz to 20 Hz range approximately centered at 10 Hz, the frequency at which sensitivities are calculated. Notice the horizontal components, to varying degrees, have upward sloping responses from approximately 10 Hz and up. As with the broadband sensor plots large deviations in response are usually accompanied by lower coherence.

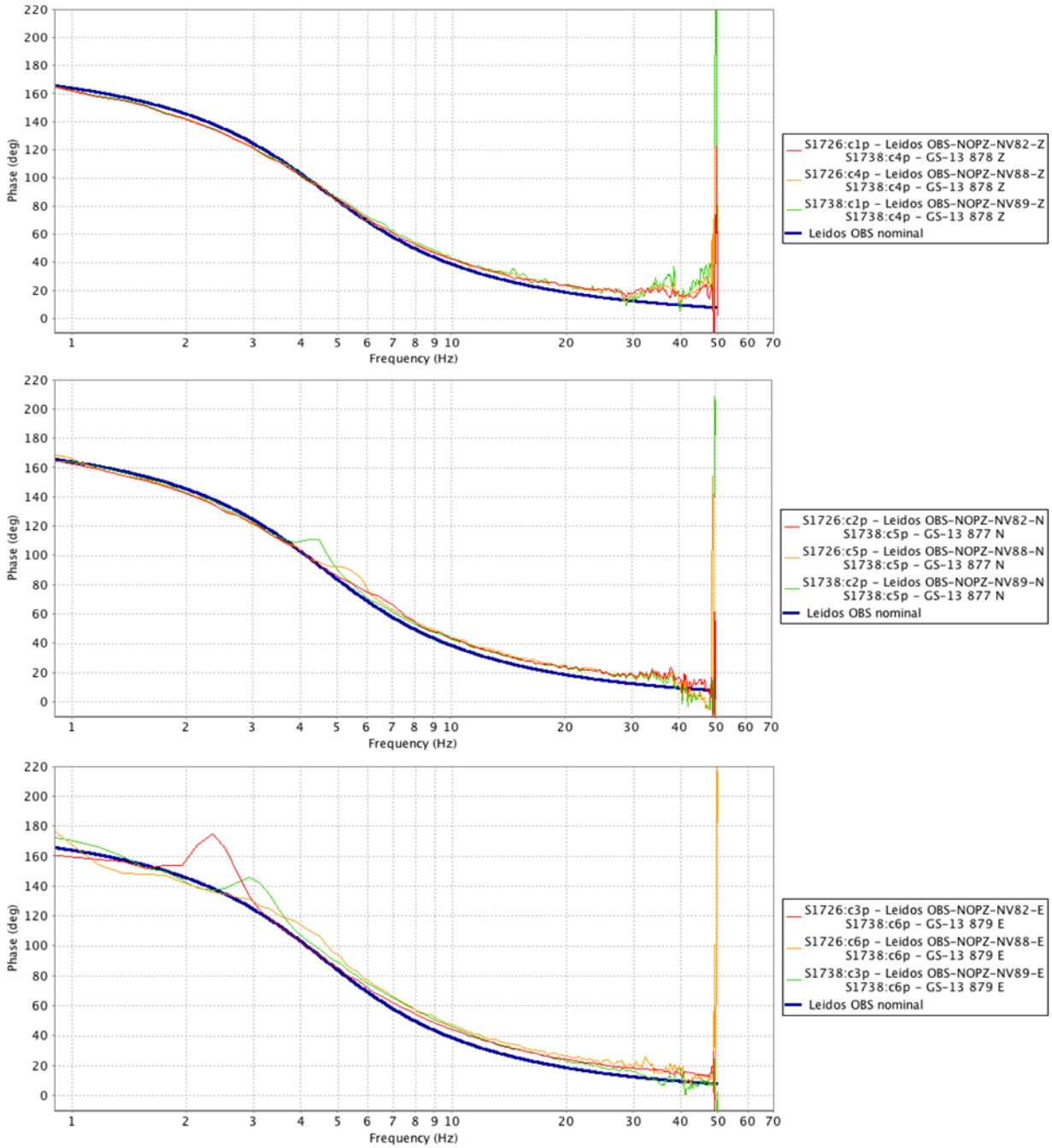

Figure 61 Short-period sensor phase response comparisons between the reference sensor and sensors under test: Vertical (top), North (middle) and East (bottom).

The relative phase response of the vertical components is in good agreement with the nominal response of the sensor up to approximately 12 Hz across sensors. The horizontal components did not fare as well; the north components exceed the 5° deviation criterion beginning approximately at 6 Hz (ignoring the lower frequencies deviations near 4 and 5 Hz of sensors 89 and 88, respectively, as at these frequencies coherence is down slightly). The east components deviated significantly, only remaining within the 5° criterion (with high coherence) between 3.2 Hz and 5 Hz for sensor 82.

3.1.3.8 Navy OBS 86, 92 and 93

Figure 62 Coherence between short-period reference sensor and sensors under test: Vertical (top), North (middle) and East (bottom).

Coherence between the reference sensor and sensors under test is excellent (at least 0.995 gamma^2) on all components over varying ranges: the verticals as low as 2.7 Hz across all sensors to high frequency limits of 25 Hz, sensor 93, and to 29 Hz, sensors 86 and 92; the north to as low as 3.8 Hz to 5.3 Hz, sensors 92 and 93, respectively, up to 27 Hz across all sensors; and the east as low as 2.5 Hz to 4.5 Hz, sensors 93 and 86, respectively to as high as 35 to 39 Hz, sensors 93 and 86, respectively. Coherence is sufficient between the sensors under test and the reference sensor to be able to comment on the relative magnitude and phase response over these frequency ranges.

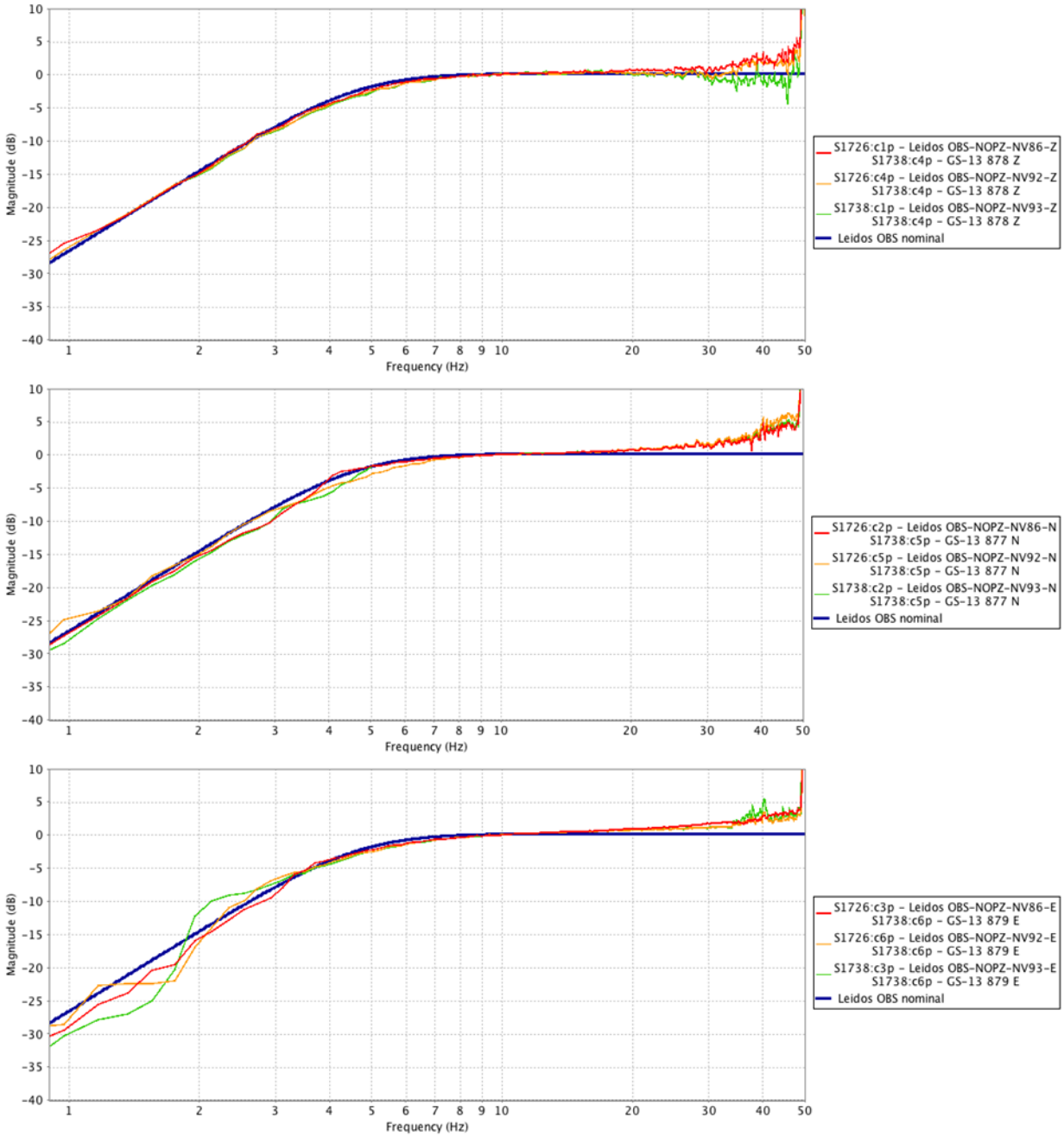

Figure 63 Short-period sensor magnitude response comparisons between the reference sensor and sensors under test: Vertical (top), North (middle) and East (bottom).

While the relative magnitudes generally follow the nominal response model at mid to low frequencies (excluding the East component of sensor 93, though recall its coherence is very low in the low frequency range over which the large magnitude deviation occurs). The relative magnitude of the vertical components of sensors 92 and 93 remain very close, if not often below the 0.1dB criterion between approximately 10 and 25 Hz. The horizontal components exhibit only a narrow range of frequency, centered on 10 Hz, over which deviations are within 0.1 dB. The horizontal components, to varying degrees, have upward sloping responses from approximately 10 Hz and up.

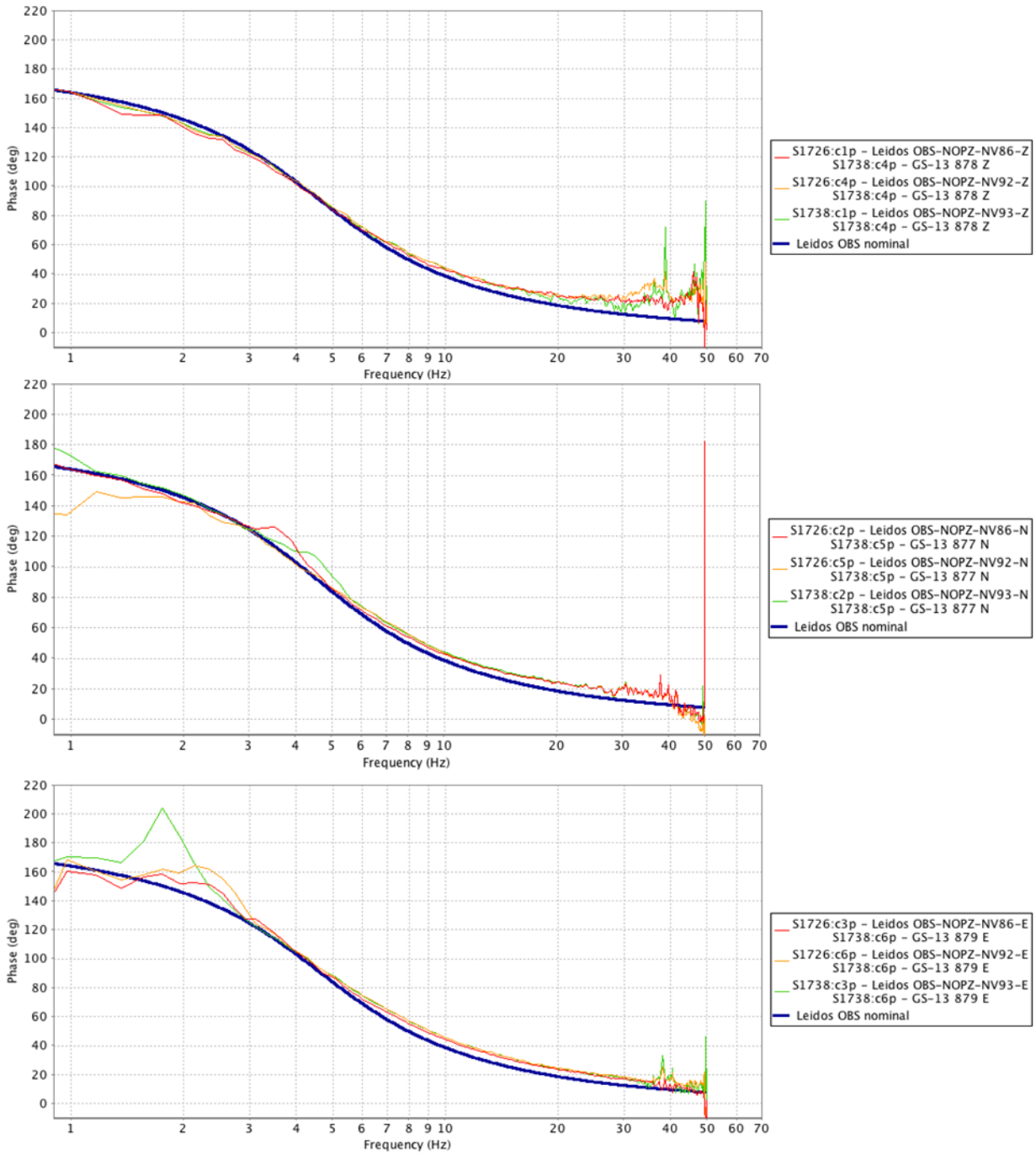

Figure 64 Short-period sensor phase response comparisons between the reference sensor and sensors under test: Vertical (top), North (middle) and East (bottom).

The relative phase response of the vertical components is in good agreement with the nominal response of the sensor up to approximately 12 Hz across sensors. The horizontal components did not fare as well; the north components exceed the 5° deviation criterion beginning approximately at 6 Hz (ignoring the lower frequencies deviations near 4 and 5 Hz of sensors 86 and 93, respectively, as at these frequencies coherence is down slightly). The east components deviated

significantly, only staying within the 5° criterion (with high coherence) between 3.2 Hz and 5 Hz for sensor 93.

3.1.3.9 Navy OBS 84, 91 and 94

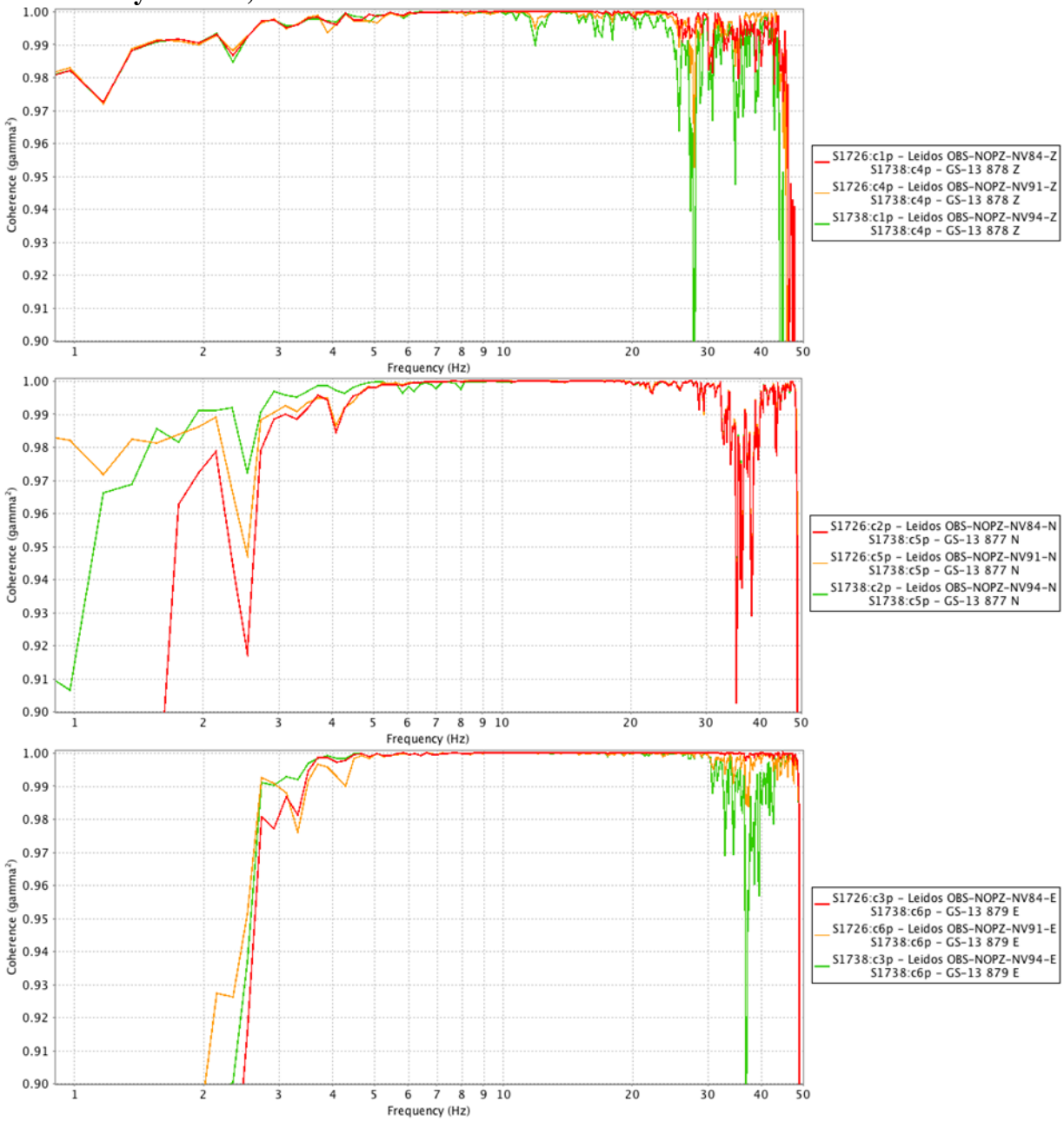

Figure 65 Coherence between short-period reference sensor and sensors under test: Vertical (top), North (middle) and East (bottom).

Coherence between the reference sensor and sensors under test is excellent (at least 0.995 gamma^2) on all components over varying ranges (in particular the East component of sensor 84): the verticals to as low as 2.7 Hz across all sensors to high frequency limits of 24 Hz, sensor 94, and 26 Hz, sensors 84 and 91; the North to as low as 2.7 Hz to 4.5 Hz, sensors 94 and sensors 84 and 91, respectively, up to 32 Hz across all sensors; and the east to as low as 3.4 Hz to 3.6 Hz, sensors 94 and 91, respectively, to as high as 31 to 48 Hz, sensors 94 and 84, respectively! Coherence is sufficient between the sensors under test and the reference sensor to be able to comment on the relative magnitude and phase response over these frequency ranges.

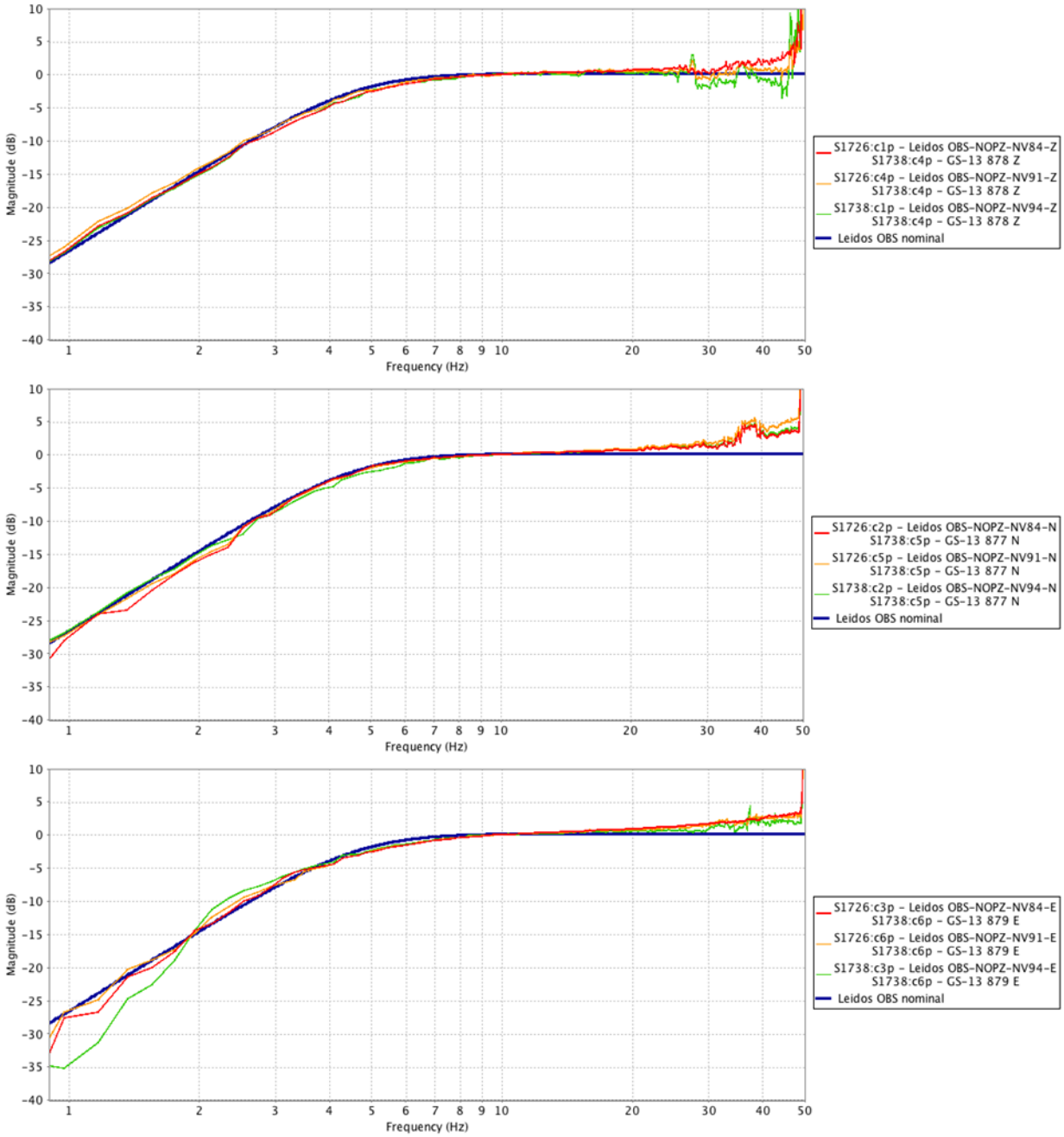

Figure 66 Short-period sensor magnitude response comparisons between the reference sensor and sensors under test: Vertical (top), North (middle) and East (bottom).

While the relative magnitudes generally follow the nominal response model from low to high frequencies; deviations at both the lower and higher frequencies are accompanied by lower coherence and should be treated as suspect. Across components sensors 84 and 91 only remain within 0.1 dB over a narrow band centered at 10 Hz. While sensor 94 exceeds 0.1 dB at higher frequencies, it arguably has a flatter slope at higher frequencies than the other sensors.

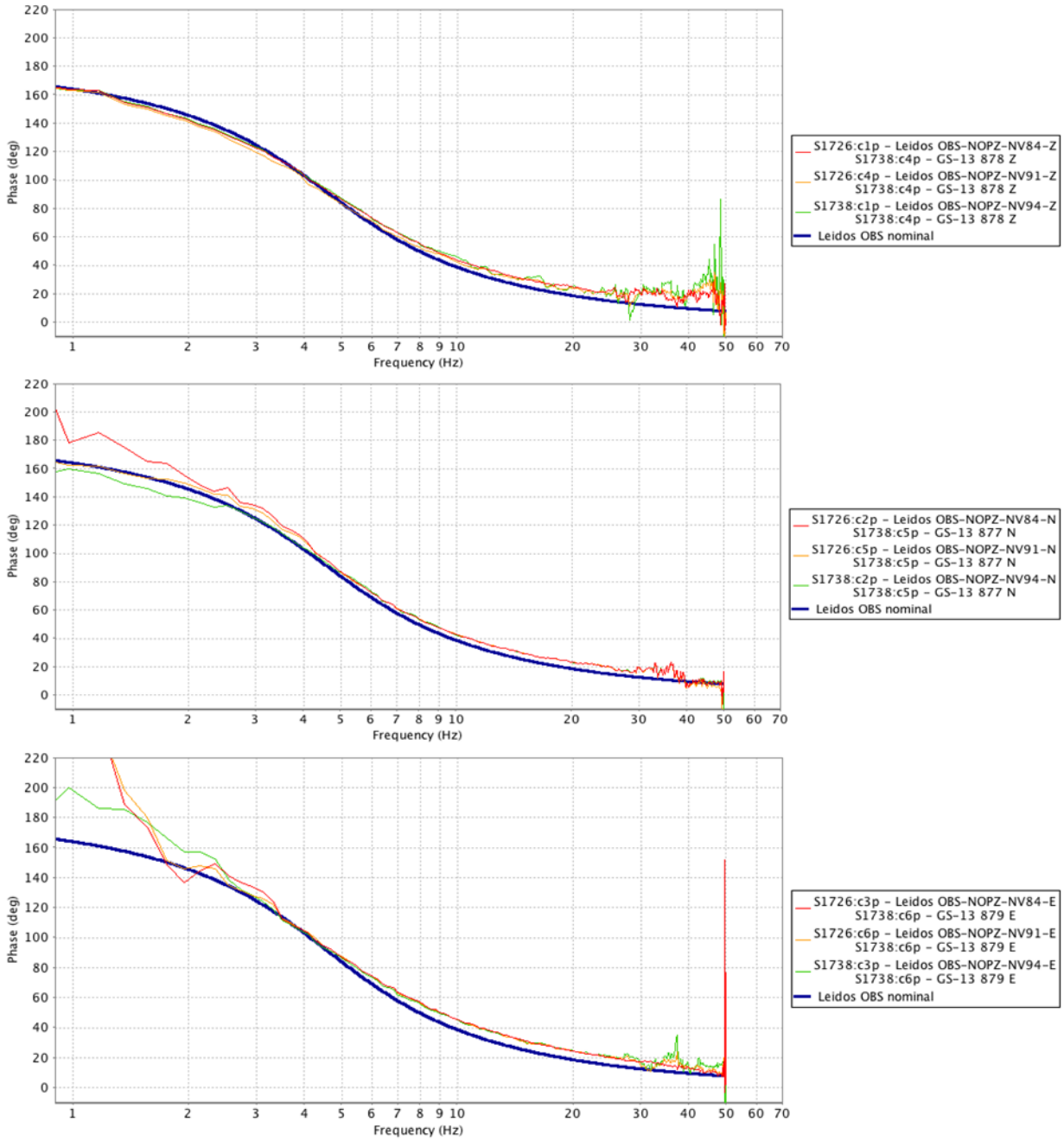

Figure 67 Short-period sensor phase response comparisons between the reference sensor and sensors under test: Vertical (top), North (middle) and East (bottom).

Over frequencies where coherence is good, the relative phase response of the vertical components are in good agreement with the nominal response of the sensor up to 6 Hz for sensors 84 and 94 and up to 15 Hz for sensor 91 (though near 4 Hz the deviation exceeds 5°). The north components fall within the 5° deviation criterion from as low as 2 Hz, sensor 94, to frequencies approaching 20 Hz. The east components deviated significantly, only staying within the 5° criterion (with high coherence) between 2.5 Hz and 3.1 Hz, for sensors 91 and 94 and sensor 84, respectively. Note, the east components of sensors 84 and 91 rise above scale: at 1.17 Hz, 247.7 dB and 244 dB, at 0.98 Hz 280.2 dB and 272.6 Hz, respectively.

3.1.3.10 Navy OBS 87, 90 and 81

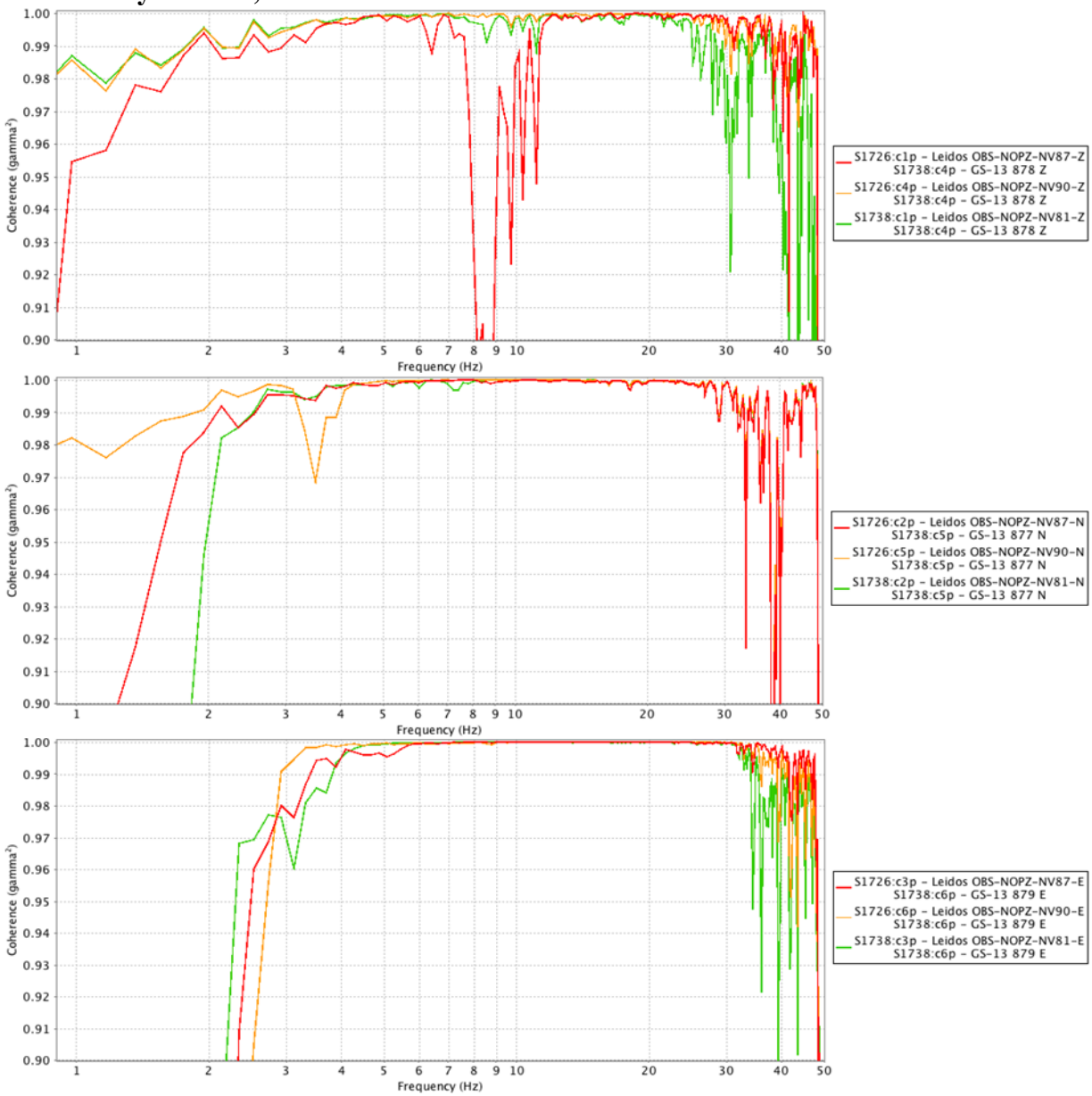

Figure 68 Coherence between short-period reference sensor and sensors under test: Vertical (top), North (middle) and East (bottom).

Coherence between the reference sensor and sensors under test is excellent (at least 0.995 gamma^2) on all components over varying ranges, though the vertical of sensor 87 has a sharp drop in coherence between 7.6 Hz and 11.3 Hz. Sensor 81 coherence begins to wane above 25 Hz and the others follow by approximately 30 Hz. Coherence of the north component of sensor 90 drops between 3.1 and 4.1 Hz, but otherwise the north component high coherence ranges from as low as 2.7 Hz to as high as 29.5 Hz across all sensors. The east components' coherence remains high between 3.1 Hz (sensor 90) to 4.0 Hz (sensors 81 and 87) through 33 Hz (sensor 81) to 35 Hz (sensor 90). Coherence is sufficient between the sensors under test and the reference sensor to be able to comment on the relative magnitude and phase response over these frequency ranges.

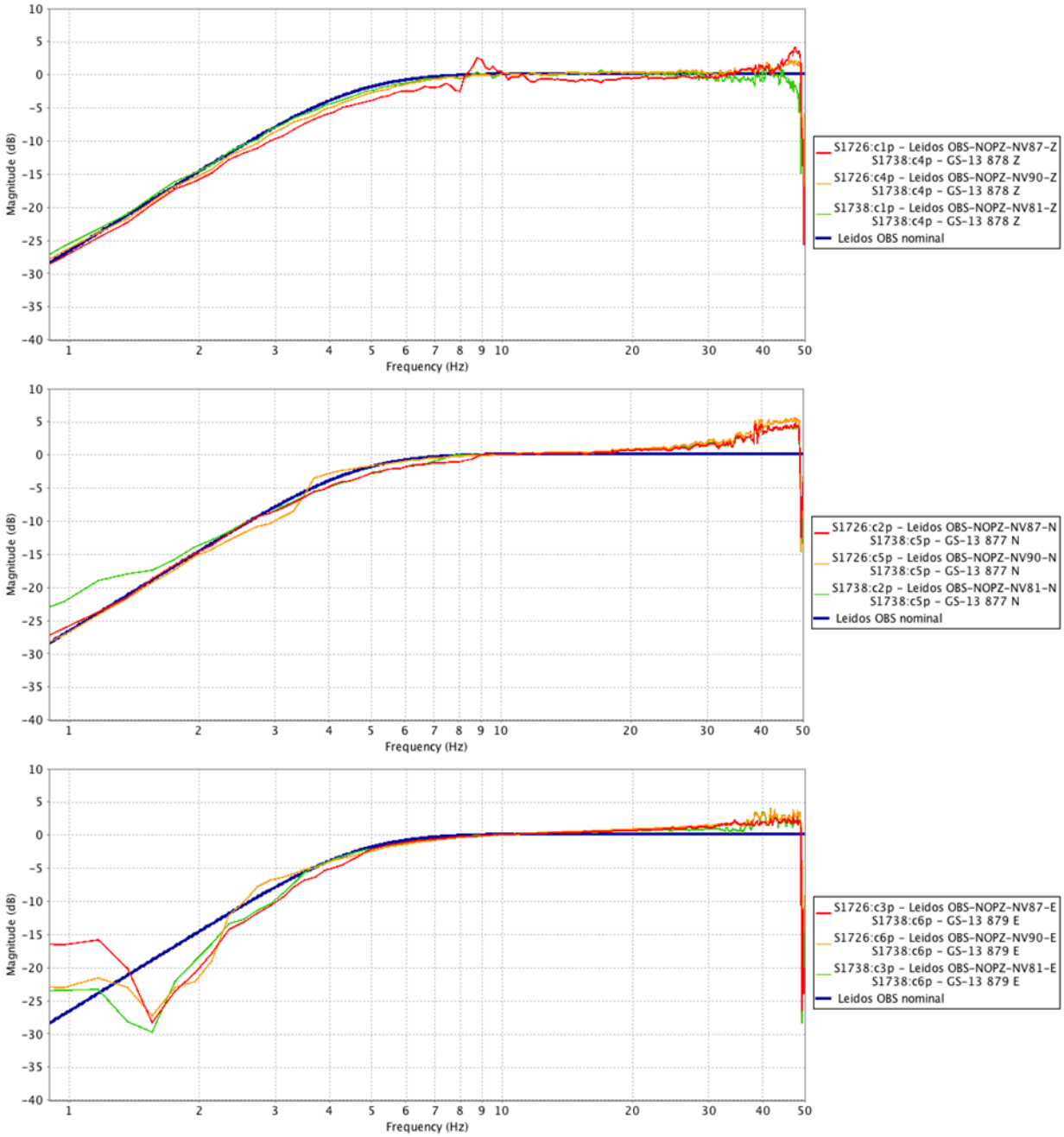

Figure 69 Short-period sensor magnitude response comparisons between the reference sensor and sensors under test: Vertical (top), North (middle) and East (bottom).

Relative magnitudes of the vertical components generally follow the nominal response, excluding the aforementioned range of low coherence between 7 and 11 Hz. There is less of a trend of increase magnitude with frequency on the vertical components. The decreases in magnitude of the north and east components below the expected response (between 4 Hz and 10Hz) are associated with high coherency. In all cases there are only relatively narrow bands of frequency at which magnitude deviations are within 0.1 dB.

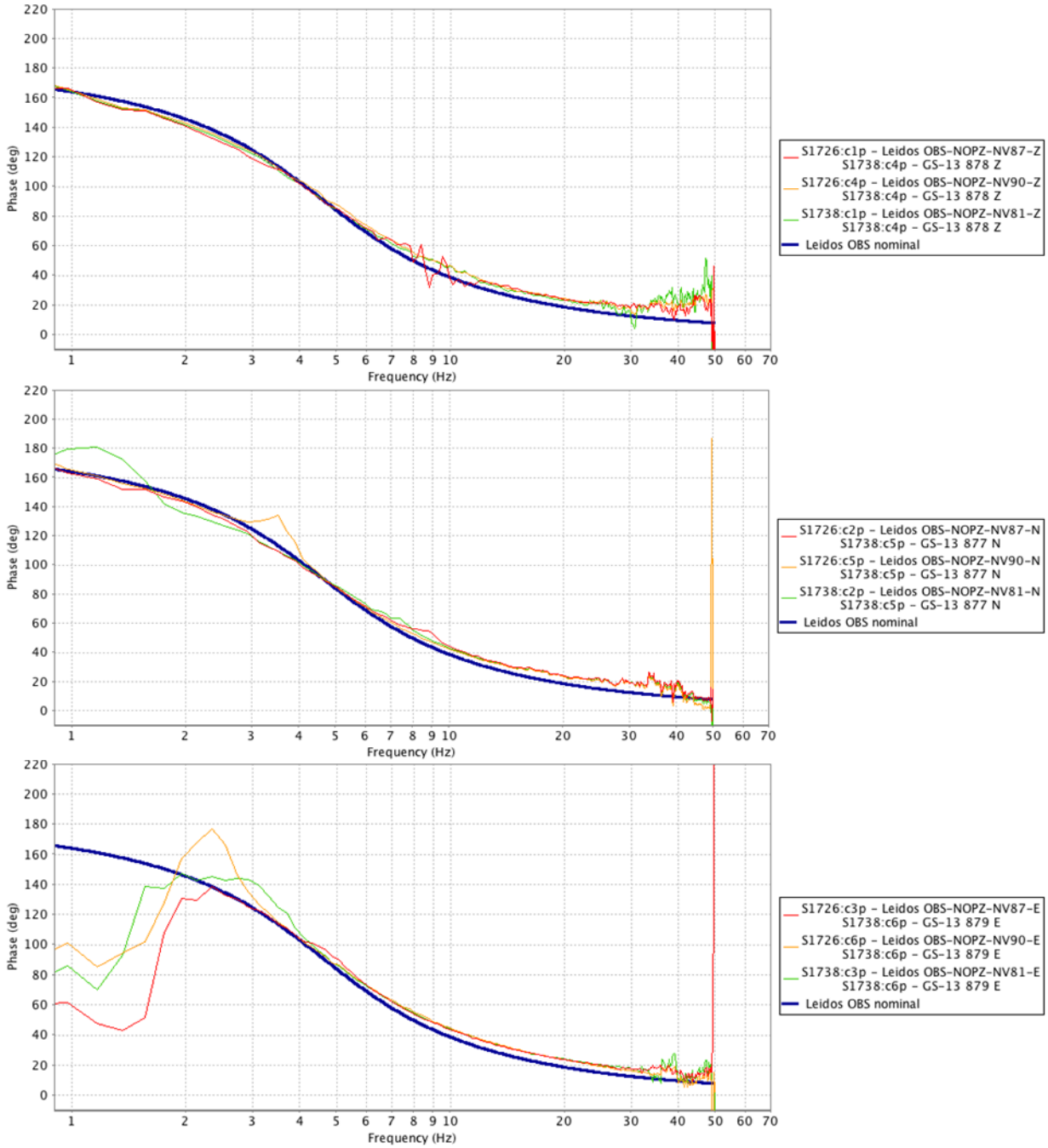

Figure 70 Short-period sensor phase response comparisons between the reference sensor and sensors under test: Vertical (top), North (middle) and East (bottom).

Where coherence is high, the relative phase response of the vertical components are in good agreement with the nominal response at lower frequencies (disregarding the anomalies of sensor 87 between 7 and 11 Hz, a region with lower coherence) through 9 Hz, though sensor 81's coherence improves slightly into higher frequencies. The north components of the sensors fall within the 5° deviation criterion up to approximately 16 Hz, disregarding anomaly between 3 and 4 Hz on sensor 90, where there is lower coherence. The east components show good agreement

from the lowest frequencies of high coherence to 7 Hz (sensor 90) to approximately 10 Hz for sensors 81 and 87.

3.1.3.11 Navy OBS 85, 95 and 96

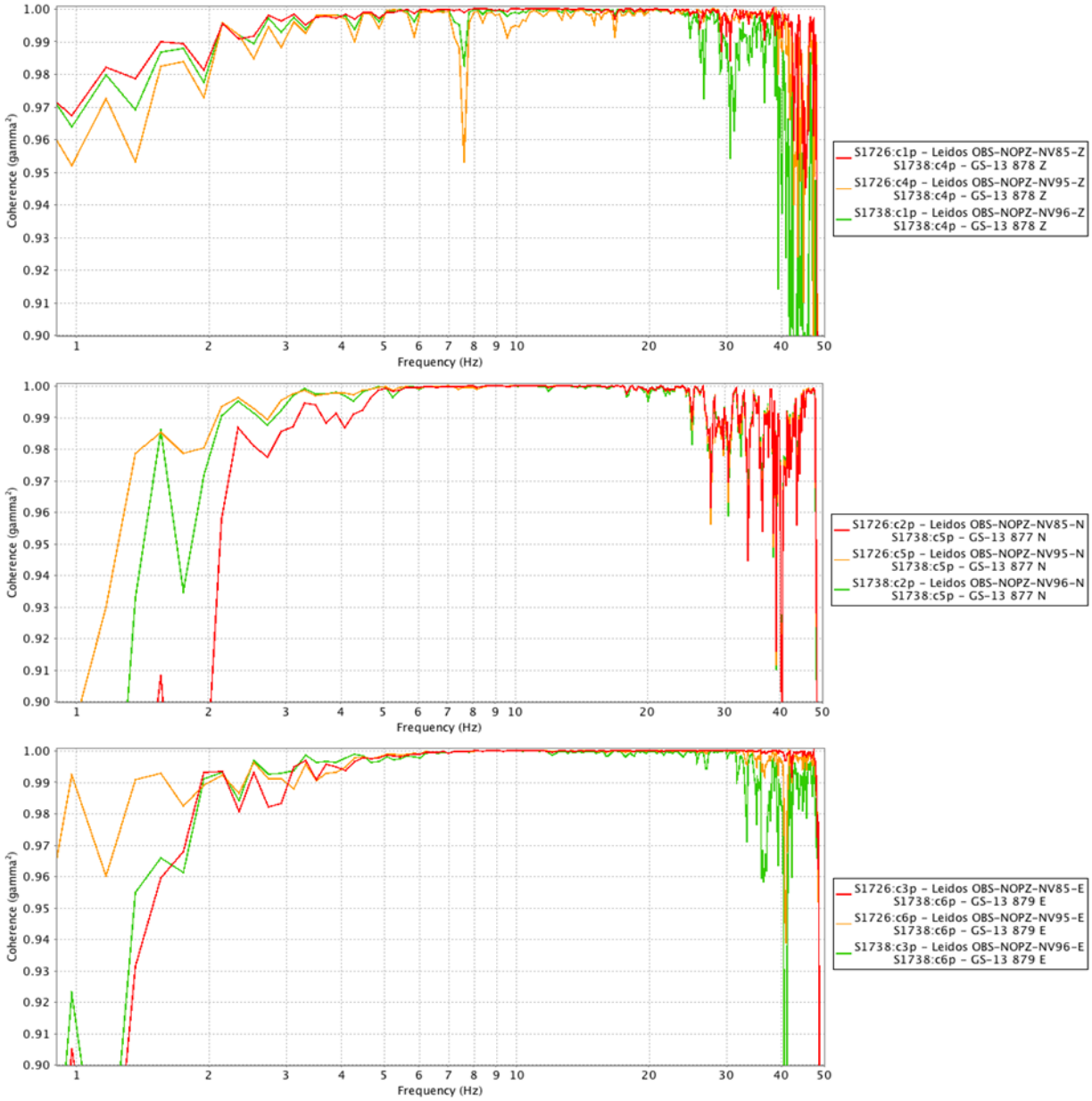

Figure 71 Coherence between short-period reference sensor and sensors under test: Vertical (top), North (middle) and East (bottom).

Coherence between the reference sensor and sensors under test is excellent (at least 0.995 gamma^2) on all components over varying ranges (in particular the east component of sensor 85). Coherence is highest on the vertical components over the widest range for sensor 85, while there is a sharp drop in coherence on both sensors 95 and 96 centered on 7.6 Hz. The north components of sensors 95 and 96 prove to have widest range of high coherence, from 3 Hz to 25 Hz and of the east components sensor 85 exhibits the widest band of high coherence, from nearly 4 Hz to 42 Hz.

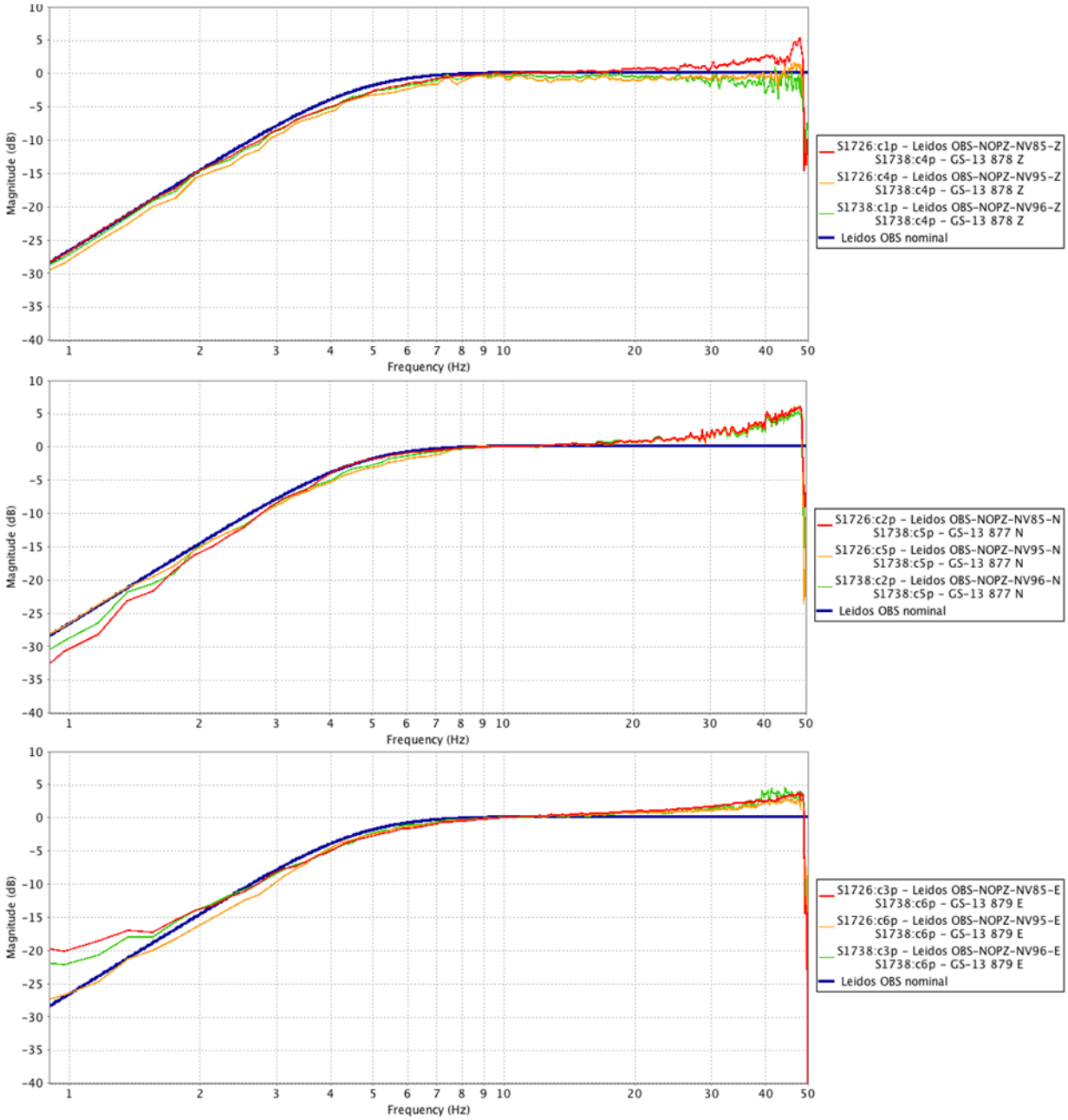

Figure 72 Short-period sensor magnitude response comparisons between the reference sensor and sensors under test: Vertical (top), North (middle) and East (bottom).

Relative magnitudes of the vertical components generally follow the nominal response, over the frequencies of interest. There is less of a trend of an increase magnitude with frequency on the vertical components than that found on the horizontal components. It should be noted the calculation of the sensitivity of the vertical component was done with a large FFT window, allowing finer scale, which led to increased variability in amplitude near 10 Hz. When calculating the relative magnitudes, the short FFT window tends to smooth the variability and, with the sensitivity applied that was calculated with the large FFT window, the relative magnitude curves are shifted lower, 0.5 dB or less. With this caveat, as with other relative magnitude comparisons, only over a narrow band do the magnitudes remain within 0.1 dB.

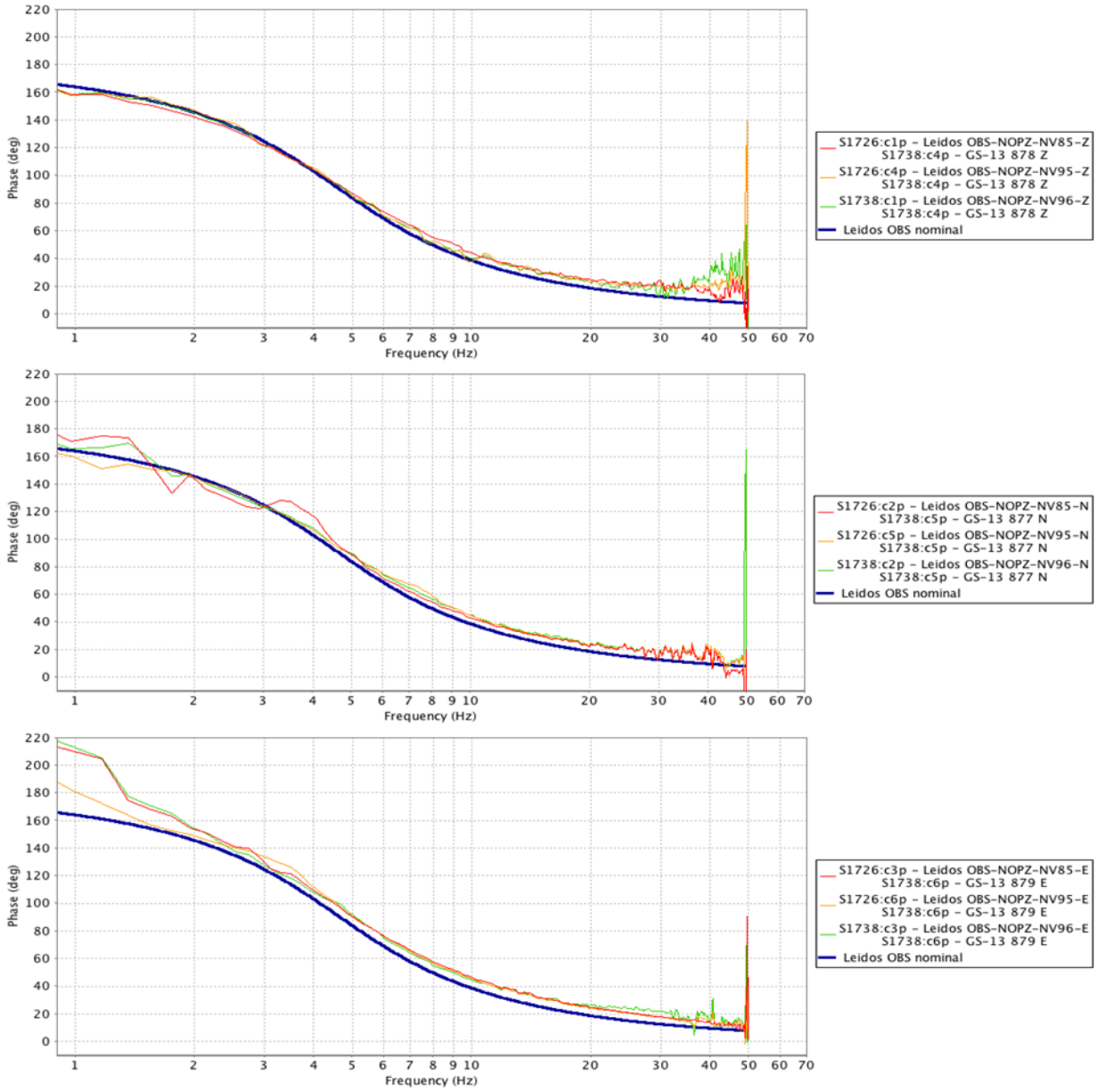

Figure 73 Short-period sensor phase response comparisons between the reference sensor and sensors under test: Vertical (top), North (middle) and East (bottom).

Over frequencies where coherence is good, the relative phase response of the vertical components is in good agreement with the nominal response of the sensor up to 6 Hz for sensor 85; sensors 95 and 96 begin to exceed the 5° criterion beyond 10.5 Hz. The north components fall within the 5° deviation criterion over a relatively narrow band from approximately 2 to 5 Hz, disregarding the anomaly in sensor 85, as it has lower coherence in this range. Similarly, the east components are within 5° of the nominal phase response over a narrow range centered on 2 Hz to 3 Hz, however coherence drops in this region so the phase should be treated as suspect.

3.1.3.12 Navy OBS 83, 97 and 98

Figure 74 Coherence between short-period reference sensor and sensors under test: Vertical (top), North (middle) and East (bottom).

Coherence between the reference sensor and sensors under test is excellent (at least 0.995 gamma^2) on all components over varying ranges. The verticals have high coherence uniformly to as low as 2.3 Hz. Sensor 97's coherence remains high through 43 Hz, whereas sensors 83 and 98 coherence levels generally degrade between 24 Hz to 26 Hz. The North coherence levels are high from as low as 2.7 Hz (sensors 97 and 98) to 4.0 Hz (sensor 83; each north component coherence remains high up to 27 Hz. All east components see a coherency drop off below 3 Hz to 4 Hz and as well as above 34 Hz (sensors 83 and 98) and over 48 Hz for sensor 97. Coherence is

sufficient between the sensors under test and the reference sensor to be able to comment on the relative magnitude and phase response over these frequency ranges.

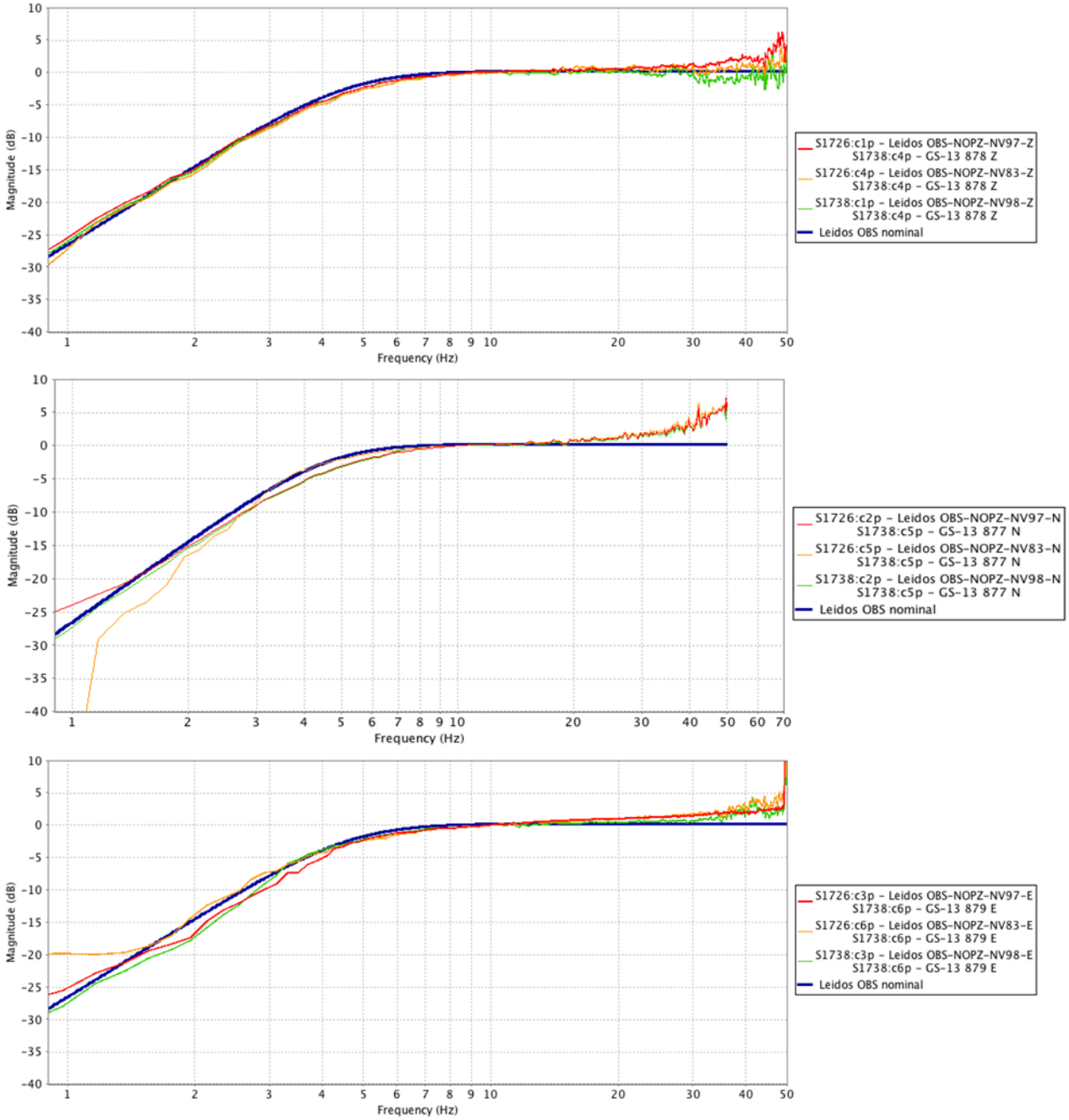

Figure 75 Short-period sensor magnitude response comparisons between the reference sensor and sensors under test: Vertical (top), North (middle) and East (bottom). Sensor 83's north component falls off scale to -55.9 dB at 0.98 Hz.

Relative magnitudes of the vertical components generally follow the nominal response over ranges of high coherence. Interestingly the vertical component of sensors 83 and 98 do not exhibit the typical increase in magnitude with frequency as observed with other sensors. Still, there exists only a tight band over which the 0.1 dB deviation criterion is met, on any sensor.

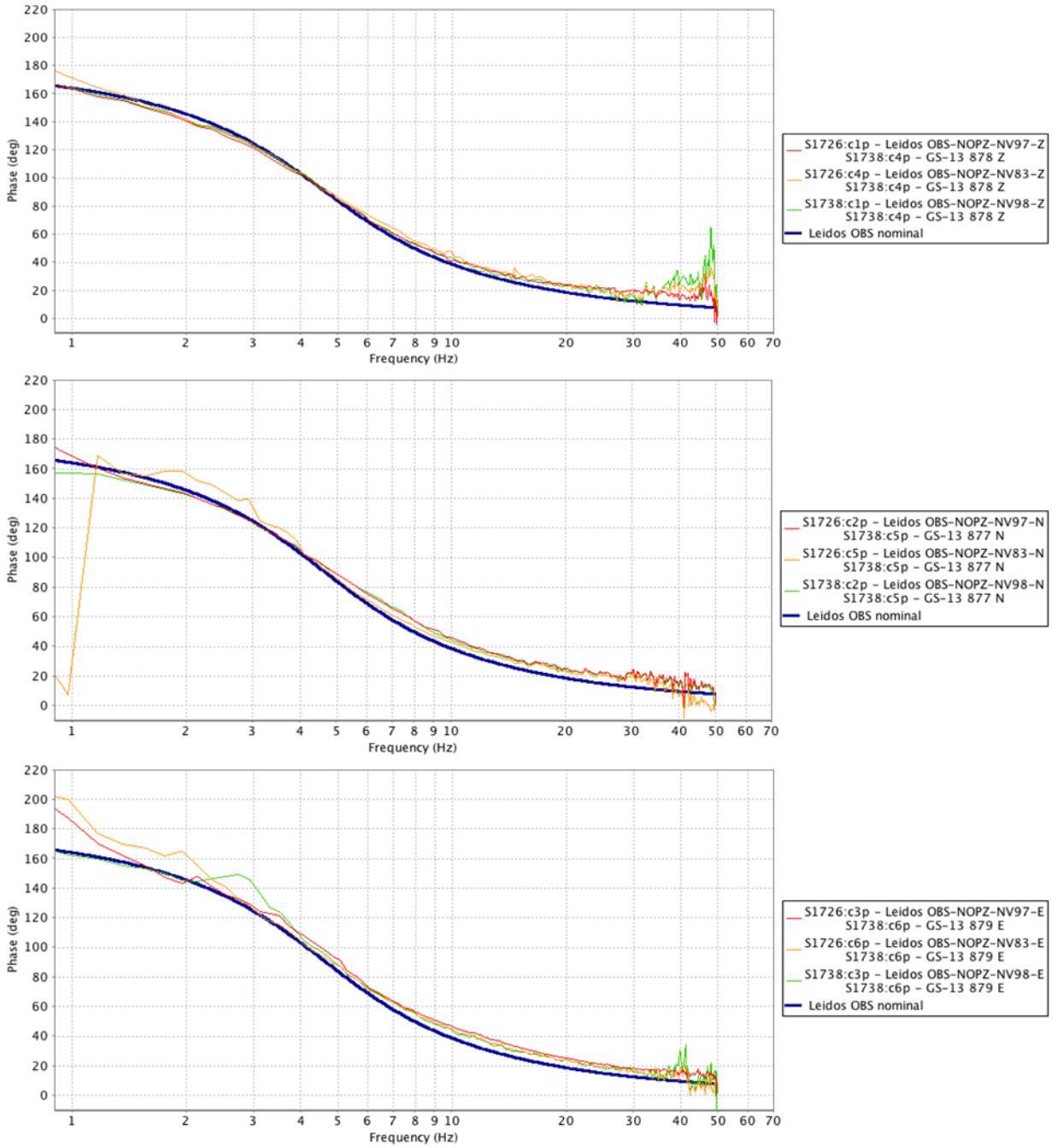

Figure 76 Short-period sensor phase response comparisons between the reference sensor and sensors under test: Vertical (top), North (middle) and East (bottom).

Over frequencies where coherence is high, the relative phase response of all components is in good agreement with the nominal response (within 5°) at lower frequencies, as seen with previous tests. Sensor 97 has the broadest range of agreement of the vertical components, sensor 83 of the north components and sensor 98 of the east components.

3.1.4 Passband Determination

Test description: Similar to the Seismic Sensitivity and Response Verification test, data are collected from a local earthquake and a teleseism from the co-located reference sensor and sensors under test. Their data are quantitatively compared in the frequency domain, removing the instrument response from the reference sensor and applying the calculated sensitivities of the sensors-under-test. The extents to which the relative magnitude and phase are zero represent how close the sensors are to a flat response in magnitude and phase and serves to validate the pass band of the sensor.

3.1.4.1 Broadband Results

The Trillium OBS sensors are expected to have a passband from approximately 120 seconds to 100 Hz, broader than the passband requirements of Table 1 SHDAS Seismometer Requirements, 0.02 Hz to 40 Hz. The ability to comment on seismometer passband may be limited at times by degradation in coherence between the sensor under test and the reference sensor. To robustly sample the low frequency range of interest we focus our analysis on teleseisms as these have relatively strong amplitudes in the low to mid frequency ranges. Similarly, at the high frequency range of interest, we focus our analysis on select local earthquakes due to the strong mid to high frequency content in their waveforms. However, there still exists instances in which there is not sufficient coherent energy (or coherent output from the sensors) to allow comments at the lowest and/or highest frequencies of interest. Therefore, we limit our comments regarding the passband to a range with lower and upper frequency bounds imposed by any degradation in coherence ($gamma^2 < 0.995$). The following table provides the low frequency corner (-3 dB point) and high frequency limit in the analysis due to low coherence. Instances in which the calculated low frequency corner is accompanied by low coherence are noted.

Table 8. Nanometrics OBS Passband (-3 dB points) and Passband Determination

Sensor	Vertical		North		East	
	Low Freq Corner (Hz)	High Freq. Limit (Hz)	Low Freq Corner (Hz)	High Freq. Limit (Hz)	Low Freq Corner (Hz)	High Freq. Limit (Hz)
3125	0.0063*	28.6	0.0064	49.1	0.0068	49.2
3126	0.0063*	28.6	0.0063	40.4	0.0067	42.7
3127	0.0064*	30.1	0.0064	41.5	0.0063	29.1
3128	0.0066	29.1	0.0065	27.0	0.0063	31.7
3129	0.0064	30.1	0.0087	31.7	0.0069	30.0
3130	0.0063	30.9	0.0065	47.1	0.0065	32.0
3131	0.0063*	25.8	0.0063	40.4	0.0068	30.9
3132	0.0062	24.7	0.0065	32.0	0.0064	32.6
3133	0.0064*	20.7	0.0064	38.8	0.0064	22.9
3134	0.0076	33.1	0.0091	38.9	0.0082	37.8
3135	0.0063*	22.5	0.0064	37.2	0.0063	17.8
3136	0.0063	27.1	0.0078	31.7	0.0067	25.3
3137	0.0077	29.8	0.011	33.7	0.0083	25.6
3138	0.0074	27.8	0.0088	33.7	0.0082	26.2
3139	0.0062	22.4	0.0066	31.6	0.0065	33.1
3140	0.0065	25.2	0.0064	27.0	0.0064	27.4
3141	0.0066	26.0	0.0065	27.0	0.0064	27.4
3142	0.0063	27.1	0.0085	32.4	0.0066	25.3

***high coherence exists at the calculated low frequency corner for these components.**

Note that the earlier plots of amplitude response have units of dB relative to signal power $(V/m/s)^2$, and not amplitude, V/m/s. Therefore, the -3 dB point in amplitude corresponds to -6 dB on the power response curve presented in the previous section.

In most cases a degradation in coherence in both the teleseismic and local earthquake analysis occurs at the frequencies calculated at the low corner frequency and at the higher frequencies approaching the Nyquist frequency (50 Hz) for the sample rate; the notable exceptions, in which there is high coherence at the calculated lower corner frequencies are the vertical components of sensors 3125, 3126 and 3131, which recorded a M=7.5 earthquake located in Afghanistan, and the vertical and east components of sensors 3127, 3133 and 3135, which recorded a M=7.8 earthquake which occurred in Ecuador. (Please refer to APPENDICES
Appendix A: , for further details regarding the events utilized in this analysis).

The local earthquake data analysis has shown there are also limits in the coherence between the sensors under test and the reference sensor. Unlike coherence behavior at low frequencies, where coherence generally dropped off and remained low as frequency decrease, coherence at high frequencies dropped below and rose above the threshold of $gamma^2 = 0.995$ a number of times in a given plot. This behavior is evident in the plots of relative magnitude in the previous section. As suggested previously comment regarding the high frequency corner frequency is limited by the frequency at which high frequency coherence drops below the threshold of 0.995 $gamma^2$.

3.1.4.2 Short-period Results

With the short-period sensors, the coherence between the reference sensor and the sensor under test limits, in some cases, comments regarding the passband low and high frequency bounds. A coherence (gamma^2) of 0.995 was used to define a limiting frequency allowing for comment on the passband corners. The earthquakes had sufficient size and duration to provide energy at sufficiently low frequency to allow for the opportunity to define the low frequency corner. Coherence, if not the Nyquist frequency, is the determining factor at the high frequencies. A note is made when coherence between the sensor under test and the reference sensor is limiting the determination of the low corner frequency.

Note, the Navy OBS are comprised of several geophones (GS-11D model) strung together to increase the gain and reduce instrument noise, over that of a single geophone. It is suspected that this assembly of exploration-focused geophones results in a relatively large variation in the sensitivity of the sensors and the observed roll-off of the sensors' response below the low frequency corner.

Table 9. Navy OBS Passband (-3 dB points) and Passband Determination

Sensor	Vertical		North		East	
	Low Freq. Corner (Hz)	High Freq. Limit (Hz)	Low Freq. Corner (Hz)	High Freq. Limit (Hz)	Low Freq. Corner (Hz)	High Freq. Limit (Hz)
81	3.5	25.0	3.6	31.2	3.0	34.2
82	3.6	34.8	3.9*	30.0	4.0*	47.1
83	3.6	26.8	4.0*	27.0	3.4*	34.2
84	3.4	26.6	3.6*	32.6	3.3*	48.4
85	3.6	42.0	3.7	25.4	3.2*	42.3
86	3.6	28.4	4.0*	31.0	3.3*	38.7
87	3.6	38.3	3.4*	31.2	3.2*	40.6
88	3.5	29.9	3.5*	30.0	3.4*	25.0
89	3.6	26.8	3.6	30.0	3.2*	35.8
90	3.9*	29.7	3.6	31.2	3.8*	35.7
91	3.7	25.5	3.5*	32.6	3.2	34.4
92	3.5	28.4	3.6	31.0	3.5*	37.7
93	3.7	24.6	3.6*	31.0	3.7	34.2
94	3.9*	24.8	3.8	32.6	3.7	31.1
95	3.7*	38.6	3.7	25.4	3.7	36.3
96	3.5	29.1	3.8	25.4	3.7	33.0
97	3.6	42.8	3.4*	27.0	3.3*	48.4
98	3.6	23.8	3.9	27.0	3.3*	33.4

***Low coherence exists at the calculated low frequency corner**

Note that the earlier plots of amplitude response have units of dB relative to signal power $(V/m/s)^2$, and not amplitude, V/m/s. Therefore, the -3 dB point in amplitude corresponds to -6 dB on the power response curve. The low corner frequency, defining the lower end of the passband, ranges from 3.0 to 4.0 Hz. In all cases the passband for the short-period sensors fall short of the desired lower frequency band of 1 Hz. The aforementioned lower coherence, widely varying across sensors and components, limits comment regarding the upper limit of the passband, on some components, to frequencies as low as 23.8 Hz (Sensor 98, vertical component). On the vertical and east components the coherence remains sufficiently high to

comment at frequencies exceeding the upper end of the desired passband of 40 Hz for a number of sensors.

3.1.5 Tilt

Test Description: Each Nanometrics OBS was placed on the granite pier with case North oriented approximately straight down, then a leveling command was initiated. After a report from the command and control software that the sensor platform had leveled, the sensor was carefully placed, while under power, on a tilt jig and rotated upon the North and East axes. Another leveling command was initiated and upon report of success with regard to leveling, the sensor was returned to the pier to its original orientation for a final leveling prior to further testing and calibration necessary to characterize the sensor.

Results and Discussion: All Nanometrics OBS sensors passed the tilt test. The ease with which the sensors passed varied though; comments related to any anomalies or test difficulties are provided in the table below. In at least one case it is believed (sensor 3128), the behavior noted during tilt testing was consistent with behavior noted by Nanometrics in other units, leading to a subsequent firmware update made available to Nanometrics customers after testing had been completed.

Note in all cases, except sensor 3136, a failure of a sensor leveling attempt is based upon:

1. The fact the sensor did not report a status of the leveling attempt (e.g. success or failure) after waiting at least 15 minutes after initiation, the maximum expected duration of any leveling sequence according to the *Nanometrics Trillium OBS Users Guide*.
2. SOH review of the sensor accelerometer and mass position values after power cycling to re-initiate communications after a failure as described in point 1.

Table 10 Nanometrics OBS Tilt Test Notes

Sensor	Firmware	Date	Comments
3125	2.2.4	10/13/15	-
3126	2.2.4	10/13/15	-
3127	2.2.4	10/13/15, 3/14/16	Failed multiple leveling attempts, returned to NMX for evaluation. Nanometrics determined no action required. Retested and passed on 3/14/16.
3128	2.2.4	4/21/15	Sensor failed first attempt, upon power-cycling to re-establish comm, SOH data are reviewed and sensor is found to be reasonably level; mass positions, U = 0.14V, V = 0.461 V and W = -0.434 V; sensor accelerometers, X = -0.0028, Y = -0.0085 and Z = 0.995.
3129	2.2.4	12/7/15	Failed multiple leveling attempts. Laptop was inadvertently running on battery and went to sleep during 1st leveling attempt. Sensor was power-cycled to re-establish comm and subsequently re-levelled on 3rd attempt.
3130	2.2.4	11/19/15	-
3131		10/13/15	-
3132	2.2.4	11/19/15	-
3133	2.2.4	3/14/16	-
3134	2.2.4	11/2/15	-
3135	2.2.4	3/14/16	-
3136	2.2.4	12/7/15 - 12/8/15	Upon final leveling on granite pier, lost comm and power cycled. Subsequent leveling failed. Last leveling attempt evaluated the following day. Leveling command output indicated leveling failed, referencing error code 5. However, upon further inspection of the sensor SOHs, mass positions and sensor accelerometers indicated sensor was reasonably level. Mass positions U = 0.011 V, V = 0.476 V and W = -0.368 V. Sensor platform accelerometers: X = -0.0017 V, Y = -0.0054 V and Z = 0.9939 V.
3137	2.2.4	11/2/15	-
3138	2.2.4	11/2/15	-
3139	2.2.4	11/19/15	-
3140	2.2.4	4/21/15	Sensor failed two leveling attempts. Moved sensor to another break-out box (includes the use of a different cable). Subsequent leveling failed. Could hear leveling motor(s) running essentially continuously. Reseated connector on sensor and rotated sensor about case "East" axis, rotated case by East axis ~10° (CW looking East) and sensor leveled shortly after initiating the level command.
3141	2.1.0	12/7/15, 3/14/16, 4/21/16	Failed multiple leveling attempts. Leveling motor(s) could be heard running essentially continuously during failed leveling attempts. Sensor was removed from the pier. Sensor retested on 3/14/16. During March 14 testing the sensor did not level; essentially continuous operation of the level motor(s) was noted during the leveling attempt. Returned to Navy for discussion and further diagnosis/troubleshooting with Nanometrics. Subsequently retested on same breakout box and cable as testing on 12/7/15 and sensor passed on 4/21/16.
3142	2.1.0	12/7/15	-

3.1.6 Calibration

Test Description: The Nanometrics sensor has the means to accept calibration signals from an external source. A 10 Hz sinusoid of one minute duration was sent to the sensor via the Q330 internal sine calibrator; the Q330 recorded the calibration input signal internally while the signal was injected into the calibration input line of the sensor. The sensor's calibration lines were enabled via the web page interface of the sensor, individually for each U, V and W element and also simultaneously to each element, essentially simulating a calibration on the vertical axis. The sensor recorded the individual and simultaneous calibrations while recording in "UVW" mode and a simultaneous calibration while recording in "XYZ" mode. The sensor remained in 120 second mode for all calibrations. A period of 1 minute of settling time before and after the calibration signal was set for each calibration and selected amplitudes varied between a nominal value of 0.625 V_p and 1.25 V_p as input to the calibration line of the sensor.

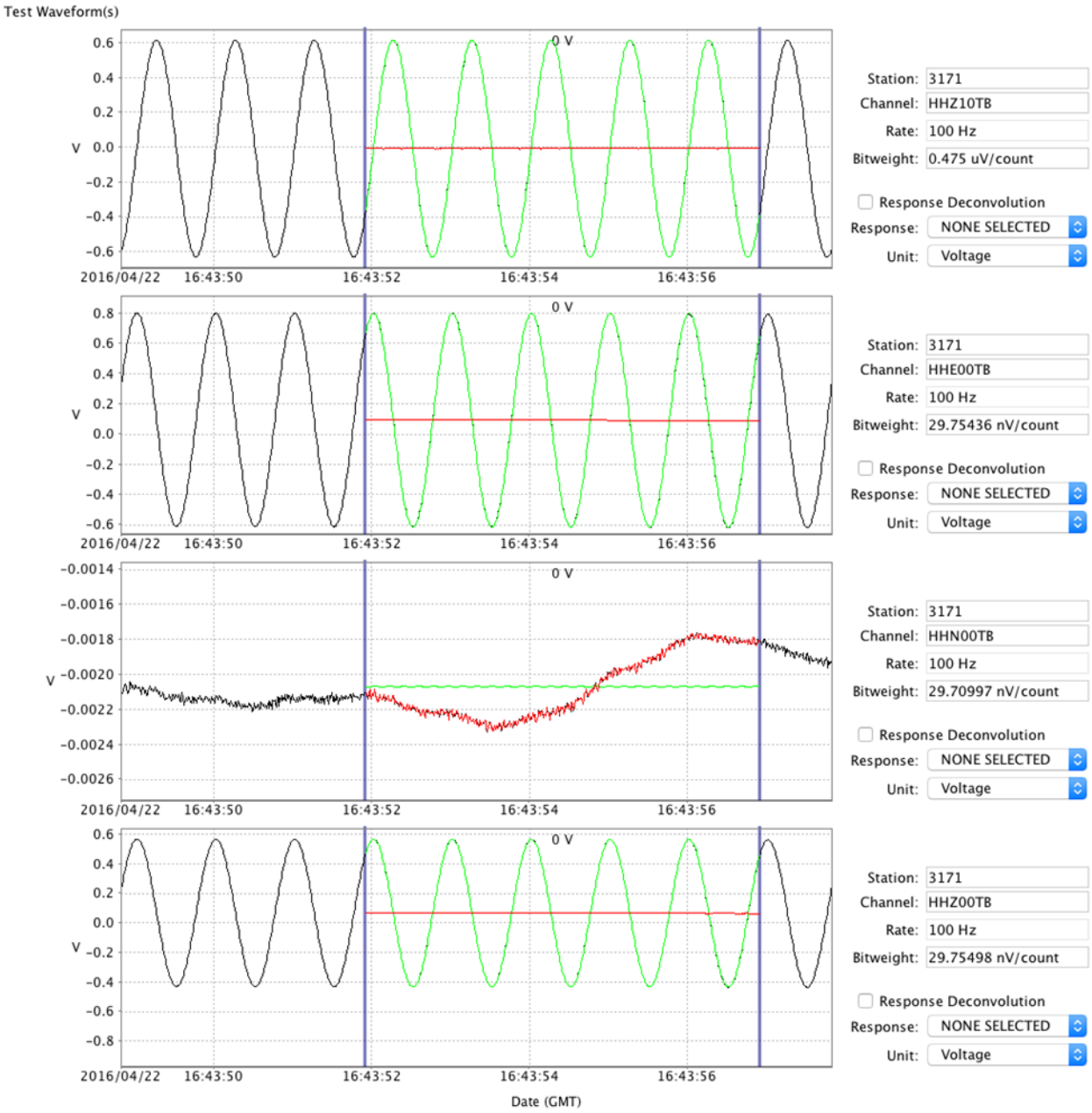

Figure 77 Example of Calibration Input (top plot) and Output (bottom 3 plots), Sensor 3128, U element cal.

Figure 77 serves as an example of a calibration measurement. The time series between the blue vertical lines serves as the source to which sinusoids are fit for measurement purposes. In this case, the U element of the Nanometrics sensor is sent a 1.25 V_{peak} calibration signal by its Q330 while simultaneously recording the calibration signal on channel 4 of the Q330 (HHZ10TB). The tri-axial design and orientation of the U axis provide, when transformed to X, Y and Z, ground motion on the Vertical and East axes only. See Appendix C for the transformation matrix and resulting equations.

Revised calibration constants were prepared following the relationships defined in Appendix C. The revised constants for each element of the Nanometrics Trillium 120 OBS are provided in the following table.

Table 11 Revised Calibration Constants for the Nanometrics Trillium 120 OBS

	U element		V element		W element	
Sensor	Constant ($m/(V\ s^2)$)	Difference from Nominal	Constant ($m/(V\ s^2)$)	Difference from Nominal	Constant ($m/(V\ s^2)$)	Difference from Nominal
3125	-0.01150	-4.55 %	-0.01184	-7.64 %	-0.01154	-4.91 %
3126	-0.01182	-7.45 %	-0.01187	-7.91 %	-0.01173	-6.64 %
3127	-0.01159	-5.36 %	-0.01158	-5.27 %	-0.01160	-5.45 %
3128	-0.01164	-5.82 %	-0.01173	-6.64 %	-0.01168	-6.18 %
3129	-0.01165	-5.91 %	-0.01170	-6.36 %	-0.01159	-5.36 %
3130	-0.01162	-5.64 %	-0.01166	-6.00 %	-0.01155	-5.00 %
3131	-0.01154	-4.91 %	-0.01146	-4.18 %	-0.01153	-4.82 %
3132	-0.01184	-7.64 %	-0.01189	-8.09 %	-0.01170	-6.36 %
3133	-0.01157	-5.18 %	-0.01170	-6.36 %	-0.01176	-6.91 %
3134	-0.01159	-5.36 %	-0.01172	-6.55 %	-0.01152	-4.73 %
3135	-0.01170	-6.36 %	-0.01170	-6.36 %	-0.01169	-6.27 %
3136	-0.01179	-7.18 %	-0.01192	-8.36 %	-0.01174	-6.73 %
3137	-0.01171	-6.45 %	-0.01171	-6.45 %	-0.01173	-6.64 %
3138	-0.01155	-5.00 %	-0.01154	-4.91 %	-0.01155	-5.00 %
3139	-0.01175	-6.82 %	-0.01165	-5.91 %	-0.01165	-5.91 %
3140	-0.01181	-7.36 %	-0.01173	-6.64 %	-0.01166	-6.00 %
3141	-0.01152	-4.73 %	-0.01120	-1.82 %	-0.01122	-2.00 %
3142	-0.01164	-5.82 %	-0.01160	-5.45 %	-0.01159	-5.36 %

Revised calibrator constants deviated from the nominal calibrator constant of 0.011 $m/(V*s^2)$ from as little as -1.82% to as much as -8.36%.

4 SUMMARY

Self-Noise – Nanometrics OBS: the self-noise estimates (0.02 Hz to 40 Hz) of the Nanometrics sensors were lowest for the verticals with an average estimate 5.378 nm/s rms; the east components rank second, with an average self-noise estimate of 9.73 nm/s rms; and the north components have the highest calculated self noise averageing 20.7 nm/s rms.

Self-noise – Navy OBS: estimates (1 Hz to 40 Hz) of the passive Navy OBS were, not surprisingly, better than those of the active broadband sensors (Nanometrics OBS). The north component self-noise average was the lowest, at 0.878 nm/s rms; The east component follows with an average self-noise is 0.924 nm/s rms; finally the vertical component average self-noise was the noisiest at 1.104 nm/s rms

Dynamic Range – Nanometrics OBS: while the average dynamic range (20 V_{peak}) for the vertical components meets the requirement of 130 dB, 6 individual sensors do not meet the criteria. While the dynamic ranges of 4 sensors' east components meet the 130 dB criterion; their average does not. None of the North component (20 V_{peak}) meet the 130 dB criterion.

Dynamic Range – Navy OBS: the Navy OBS' component-specific average 20 V_{peak} full scale dynamic range exceeds the requirement of 130 dB in the band of interest, 1 Hz -40 Hz: 142.1 dB, 143.8 dB and 143.8 dB, for the vertical, north and east components, respectively.

Sensitivity – Nanometrics OBS: the sensors remained tightly clustered around the nominal sensitivity of 750 V*s/m, varying no more than 1.3%.

Sensitivity – Navy OBS: the sensitivities of the Navy OBS varied, as much as 16% from the nominal value of 1050 V*s/m.

Magnitude/Phase Response and Passband – Nanometrics OBS: the Nanometrics sensors remained relatively flat over the passband in amplitude; however only in the lower frequency bands did the sensors meet the objective of being flat to within 0.1 dB. In phase though, the units regularly maintained phase within 5° of the nominal response over most of the passband. In both amplitude and phase, limits in coherence often limited comment at the lowest and highest frequencies of the passband.

Magnitude/Phase Response and Passband – Navy OBS: the Navy sensors did not remain as flat in the passband in amplitude as the Nanometrics units and do not meet the objective of being flat to 0.1 dB across the passband. Phase response varied appreciably and did not meet the objective of remaining within 5° of the nominal phase response over the passband. In both amplitude and phase, limits in coherence often limited comment at the lowest and highest frequencies of the passband.

Tilt: all Nanometrics sensors passed the tilt evaluation, though it must be noted, a number of sensors did not level on the first attempt and required additional effort to level.

Calibration: Revised calibrator constants deviated from the nominal calibrator constant of 0.011 $m/(V*s^2)$ from as little as -1.82% to as much as -8.36%.

5 REFERENCES

1. Holcomb, Gary L., A Direct Method for calculating Instrument Noise Levels in Side-by-Side Seismometer Evaluations, DOI USGS Open-File Report 89-214,1989.

2. IEEE Standard for Digitizing Waveform Recorders, IEEE Std. 1057-1994.

3. IEEE Standard for Analog to Digital Converters, IEEE Std. 1241-2001.

4. McDonald, Timothy S., Modified Noise Power Ratio Testing of High Resolution Digitizers, SAND94-0221, 1994.

5. Merchant, B. John, and Darren M. Hart (2011), *Component Evaluation Testing and Analysis Algorithms*, SAND2011-8265, 2011.

6. Nanometrics, Inc., Nanometrics Trillium Compact OBS Users Guide, 2011.

7. Sleeman, R., Wettum, A., Trampert, J. (2006), *Three-Channel Correlation Analysis: A New Technique to Measure Instrumental Noise of Digitizers and Seismic Sensors*, Bulletin of the Seismological Society of America, Vol. 96, No. 1, pp. 258-271, February 2006.

8. Wyatt, F., Date Unknown, *Cecil and Ida Green Piñon Flat Observatory (PFO)* , Retrieved from: http://pfostrain.ucsd.edu/pfo/#Development%20of%20the%20Observatory

9. Wyatt, F., Date Unknown, *PFO Facility Attributes*, Retrieved from http://pfostrain.ucsd.edu/pfo/pfoback.html

APPENDICES

Appendix A: Reference Sensors

Reference sensors utilized in this study include a Nanometrics Trillium OBS 120, serial number 2100, and a set of three Geotech GS13 short period seismometers, serial numbers 878, 877 and 879, respectively, to provide Vertical, North and East sensitivity.

The GS13 sensitivities came from their respective calibration sheets from the manufacturer and free periods of each sensor were adjusted to ensure a 1.000 +/- 0.001 second free period on site at Pinon Flats Geophysical Observatory prior to testing.

The sensitivities of the Nanometrics reference sensor were calculated at 10 Hz by RPKromer Consulting, by way of evaluation of the sensor against the GS-13 reference sensors.

Geotech GS13

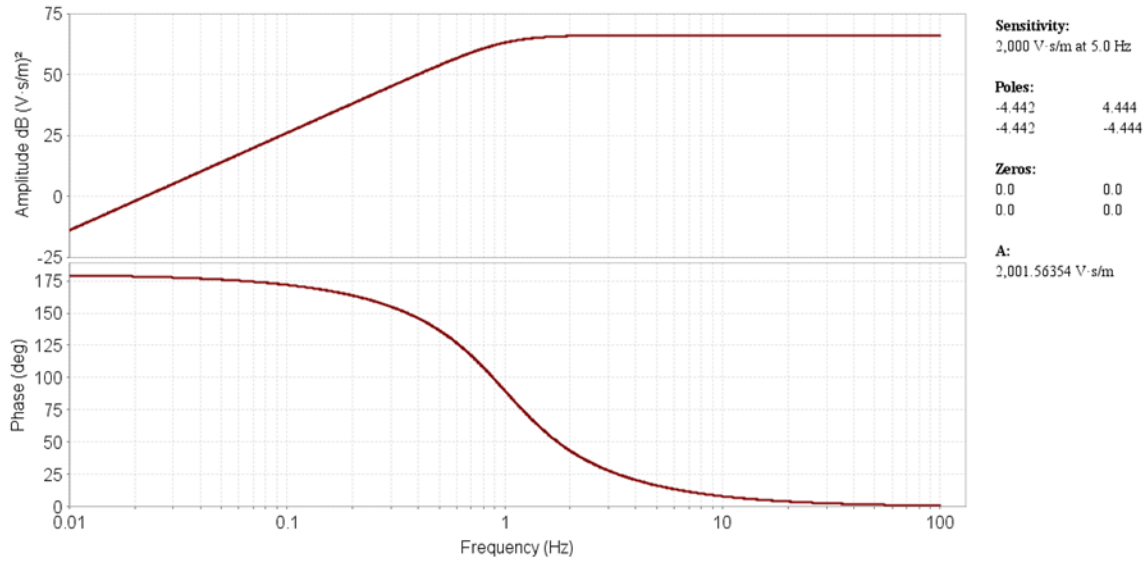

Nanometrics Trillium OBS

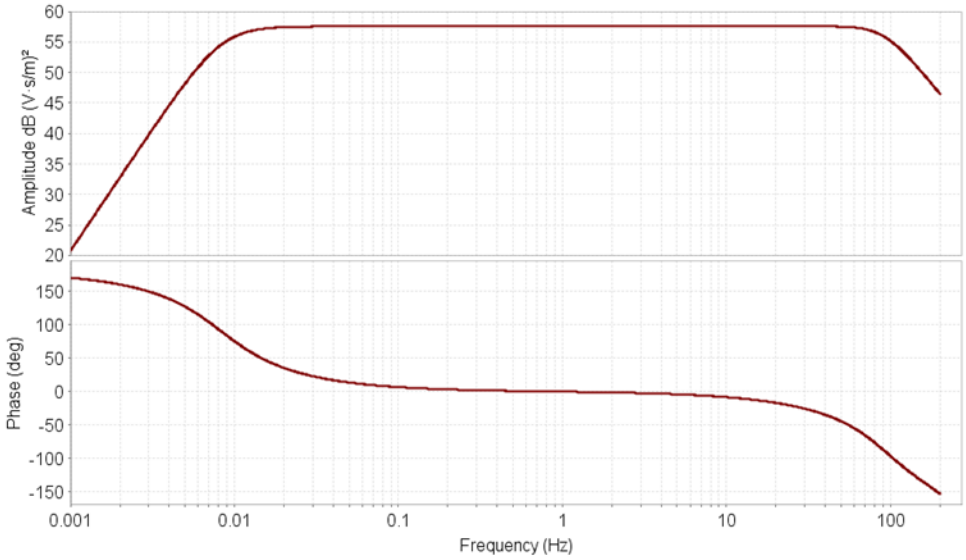

Sensitivity:
754.3 V·s/m at 1.0 Hz

Poles:

-15000.0	0.0
-6900.0	0.0
-4900.0	4700.0
-4900.0	-4700.0
-836.0	1522.0
-836.0	-1522.0
-370.0	467.0
-370.0	-467.0
-343.0	0.0
-0.03691	0.03702
-0.03691	-0.03702

Zeros:

-1960.0	0.0
-1490.0	1740.0
-1490.0	-1740.0
-392.0	0.0
0.0	0.0
0.0	0.0

A:
327.73793E12 MV·s/m

Appendix B: Earthquakes

While southern California has a wealth of regularly occurring small magnitude earthquakes, specific events were chosen for the evaluation of the sensors, following the magnitude and distance criteria of Test Plan, Section A.3.b. The table below summarizes these events and their use in the evaluation.

Table 12. Local Earthquakes Utilized in the Analysis

Origin Time (UTC)	Magnitude	Distance/ Bearing to Event/ Depth	Sensors Tested Utilizing this earthquake
October 17, 2015, 02:31:59	3.31	71 km/NNW/7.2 km	3125, 3126,3131
November 18, 2015, 04:41:48	3.39	110 km/NW/10.6 km	3134, 3137, 3138, 82, 88, 89
November 27, 2015, 01:21:28	3.01	39 km/NE/6.6 km	3130, 3132, 3139, 86, 92, 93
January 6, 2016, 14:42:34	4.39	50 km/NW/16.7 km	3126, 3136, 3142
January 9, 2016, 11:43:10	3.3	22 km/NNW/13.6 km	84, 91, 94
April 13, 2016	2.0	13 km/SE/	81, 87, 90
April 20, 2016, 11:41:45	2.91	26 km/NW/13.6 km	3127, 3133, 3135
May 2, 2016, 17:16:19	2.85	43 km/S/12.6 km	3128, 3140, 3141, 85, 95, 96
June 7, 2016, 00:13:01	2.87	15 km/SW/10.2 km	83, 97, 98

Data from a selection of teleseisms were utilized to provide a more robust evaluation of the Nanometrics broadband sensors at the lower frequencies of interest, specifically below 0.5 Hz. The table below summarizes these events and their use in the evaluation.

Table 13. Tele-seismic Earthquakes Utilized in the Analysis

Origin Time (UTC)	Magnitude	Geographic location, Coordinates and Depth	Sensors Tested Utilizing this Earthquake
October 26, 09:09:42	7.5	Afghanistan 36.524°N 70.368°E 231 km	3125, 3126,3131
November 11, 2015, 01:54:38 November 11, 2015, 02:46:19	6.9 6.9	Chile 29.507°S 72.007°W 12 km Chile 29.510°S 72.058°W 10 km	3134, 3137, 3138
November 24, 2015, 22:45:38 November 24, 2015, 22:45:38	7.6 7.6	Peru 10.573°S 70.944°W/606.2 km Brazil 10.060°S 71.018°W 620.6 km	3030, 3032, 3039
January 24, 2016, 10:30:30	7.1	Alaska 59.636°N 153.405°W 129.0 km	3026, 3036, 3042
April 24, 2016, 23:58:36	7.8	Ecuador 0.382°N 79.922°W 20.6 km	3127, 3133, 3135
May 28, 2016, 05:38:50 May 28, 2016 09:46:59	6.9 7.2	Fiji 21.972°S 178.204°W 405.7 km South Sandwich Islands 56.241°S 26.935°W 405.7 km	3128, 3140, 3141

Appendix C: Procedure for Calculation of Nanometrics OBS Calibration Constants

Procedure for Calculation of Calibration Constants

A. Obtain revised sensitivities by comparing reference NMX sensor against the test Nanometrics sensor via a Sine-Amp Response test in TALENT.
B. Obtain zero-to-peak amplitude of calibrations of test NMX sensor via a Sine Amp Response test in TALENT.
    a. All single element cals must have been recorded in the XYZ mode. Cals of all elements simultaneously should have been run twice, once while recording in XYZ mode and again in UVW mode.
    b. Recall the cal input signal is in acceleration.
    c. Note the polarity of each channel record in the Sine-Amp Response test. The zero-to-peak amplitude calculation does not take into account the polarity, nor the phase shift, from acceleration to velocity, which occurs during the cal operation.
C. For each element, convert the cal signal recorded in XYZ to the respective element's acceleration equivalent. Utilizing the transformation provided by Nanometrics:

$$\begin{bmatrix} U \\ V \\ W \end{bmatrix} = \frac{1}{\sqrt{6}} \begin{bmatrix} 2 & 0 & \sqrt{2} \\ -1 & \sqrt{3} & \sqrt{2} \\ -1 & -\sqrt{3} & \sqrt{2} \end{bmatrix} \cdot \begin{bmatrix} E \\ N \\ Z \end{bmatrix}$$

and the relationship between acceleration and velocity:

$$Acceleration = 2\pi * Frequency * Velocity$$

a. The U element,

$$U = \frac{1}{\sqrt{6}}(2E + \sqrt{2}\,Z)$$

simplified, and expressed in acceleration (at 1 Hz), with input in voltage and sensitivity in V*s/m:

$$U_{acc} = \frac{2\pi f}{\sqrt{6}} * (2E * \frac{1}{Sens_E} + \sqrt{2}Z * \frac{1}{Sens_Z})$$

b. The V element,

$$V = \frac{1}{\sqrt{6}}(-E + \sqrt{3}N + \sqrt{2}Z)$$

simplified, and expressed in acceleration (at 1 Hz), with input in voltage and sensitivity in V*s/m:

$$V_{acc} = \frac{2\pi f}{\sqrt{6}} * (-E * \frac{1}{Sens_E} + \sqrt{3}N * \frac{1}{Sens_N} + \sqrt{2}Z * \frac{1}{Sens_Z})$$

c.The W element,

$$W = \frac{1}{\sqrt{6}}(-E - \sqrt{3}N + \sqrt{2}Z)$$

simplified, and expressed in acceleration (at 1 Hz), with input in voltage and sensitivity in V*s/m:

$$W_{acc} = \frac{2\pi f}{\sqrt{6}} * (-E * \frac{1}{Sens_E} - \sqrt{3}N * \frac{1}{Sens_N} + \sqrt{2}Z * \frac{1}{Sens_Z})$$

D. Calculate the cal constant, in m/(V*s^2), for each element (U, V, W), based on the acceleration measured and the zero-to-peak cal input voltage.

$$Cal\_constant_{element} = \frac{Acceleration_{element}}{Cal_{in}}$$

As a sanity check, one may calculate the expected velocity of the 1 Hz sinusoid cal input signal, on the vertical component, based on the cal input voltage and the calculated cal constants, as shown below, and then compare it against the actual vertical component velocity recorded by the sensor in XYZ mode while the same cal is run.

$$Z_{vel_{expected}} = \frac{Cal_{in}}{2\pi f\sqrt{3}}(Cal\_constant_U + Cal\_constant_V + Cal\_constant_W)$$

E. Finally, calibrations run in the future may be compared with these initial calibrations to assess the sensor calibration and velocity output circuits. If assumptions are made, e.g. that the calibration circuitry remains stable and the input cal sinusoid is well constrained, then any change noted in the velocity output of calibrations run in the "All" mode may be attributed to a change in vertical component sensitivity and hence the vertical component sensitivity may be adjusted to reflect this change.

F. Alternatively, a cal constant may be calculated, for the vertical component, if making the same assumptions as made in section E, based on the vertical velocity output of the sensor while recording, in XYZ mode, using a 1 Hz sinusoid as the cal input.

$$Cal\_constant_Z = 2\pi f * \frac{Z_{vel}}{Cal_{in}}$$

Note, revised sensitivities (or cal constants) for the North and East components cannot be calculated as the calibration circuitry does not support sending the cal input signal as necessary to emulate North or East ground motion.

Appendix D: Navy OBS Ticket number - Serial Number Reference

Ticket Number	Serial Number/ End Cap Notes
81	10
82	8
83	14
84	13
85	6
86	End Cap 9
87	12
88	4
89	9
90	15
91	18
92	17
93	5
94	16
95	LRIP2
96	LRIP1
97	11903
98	End Cap 7

Serial Number/ End Cap Notes	Ticket Number
4	88
5	93
6	85
8	82
9	89
10	81
12	87
13	84
14	83
15	90
16	94
17	92
18	91
11903	97
End Cap 7	98
End Cap 9	86
LRIP1	96
LRIP2	95

6 DISTRIBUTION

1 Leslie Casey
U.S. Department of Energy/NNSA
Office of Nuclear Nonproliferation Research and Development (NA-222)
1000 Independence Avenue SW
Washington, DC 20585

1 Brett Moeller
Air Force Technical Applications Center/TTG
1030 S. Highway A1A
Patrick AFB, FL 32925-3002

1 James Neely
Air Force Technical Applications Center/TTG
1030 S. Highway A1A
Patrick AFB, FL 32925-3002

1	MS0404	George Slad	06911
1	MS0404	B. John Merchant	05752
1	MS0404	Randy K. Rembold	05752
1	MS0404	Neill P. Symons	05752
1	MS0899	Technical Library	9536 (electronic copy)


Sandia National Laboratories